DESIGN AND EVOLUTION OF BEACH NOURISHMENT IN ALANYA

by
İrem Bilgün
B.S., Civil Engineering, Boğaziçi University, 2020

Submitted to the Institute for Graduate Studies in
Science and Engineering in partial fulfillment of
the requirements for the degree of
Master of Science

Graduate Program in Coastal and Hydraulics Engineering
Boğaziçi University
2023

ACKNOWLEDGEMENTS

I would like to express my sincere gratitude to my thesis advisor Prof. Emre Otay for his guidance and support throughout my research. I would also like to thank him for introducing me to the field of coastal engineering and help me acquire new skills and knowledge through different projects during my master's studies. I am truly grateful for his mentorship, motivation and inspiration.

I would like to thank Muhammed Aslan and Ogan Sevim for their guidance through my work and my thesis. Thank you for introducing me to this project, giving a chance to work together and especially teaching me the practical knowledge on coastal engineering during our studies together.

I am grateful for my dear friends Sofi Farazande and Pelin Uzun for their support and friendship throughout my classes and research.

I would like to thank Onur Akagündüz for his assistance and friendship during the field measurements and laboratory works, and Selin Bardak for her help.

I would like to thank to my family for their endless love and support, especially my mother for being a role model for me to pursue a degree in engineering and a master's degree, thank you for having faith in me and always encouraging me.

I would like to thank Dr. Sarıkaya for her help and guidance when I needed the most during my thesis studies.

Finally, I would like to express my gratitude to my dear soulmate and best friend Sercan Demirkılıç, thank you for your love, support and patience even through the hardest times during these three years.

ABSTRACT

DESIGN AND EVOLUTION OF BEACH NOURISHMENT IN ALANYA

This thesis explores the causes and effects of beach erosion, as well as potential solutions for mitigating its impact. The resulting loss of beach ecosystems has significant implications for both the environment and local economies. Through a combination of field research and analysis of existing literature, the study aims to find the causes of beach erosion in Alanya and suggest a proposal through an environmentally and economically sustainable way. Overall, the study highlights the need for increased awareness of the importance of beach ecosystems and the urgent need to address the issue of beach erosion. Beach nourishment is a widely used method of restraining coastal erosion and maintaining the recreational and protective functions of coastal areas. The effectiveness of beach nourishment as a coastal management strategy through a comprehensive review of existing literature and the study of the suggested beach nourishment project in Alanya is investigated. The results of this study suggest that beach nourishment can be an effective approach to coastal management, but its effectiveness depends on a variety of factors, including the characteristics of the beach and the surrounding environment, the design and implementation of the project, and the social and economic context of the area. Extensive coastal and topographic survey is done by BUCEL in August 2022 in demand of Municipality of Alanya and with the data collected from surveys, wind and wave regime, analyses of the current coastal environment are done. A beach nourishment of 1km is designed according to the geometry of the shore. The planform and profile evolution of the nourishment is modeled to test the sustainability and reliability of the beach nourishment. Primitive equations and empirical relationships of wave mechanics are used to apply the methods of coastal evolution onto a crenulate bay example. As a result, a combination of analytical solutions of the evolution of crenulate bays, beach nourishments and river deltas are used to demonstrate the mitigation of beach erosion through environmentally friendly solutions like beach nourishments.

ÖZET

ALANYA KIYI BESLEMESİ TASARIM VE GELİŞİMİ

Bu tezde, sahil erozyonunun nedenleri, etkileri ve erozyona bağlı etkileri azaltmak için olası çözümler araştırılmıştır. Plaj ekosistemlerinde ortaya çıkan sediman kaybının hem çevre hem de yerel ekonomiler için önemli etkileri vardır. Bu çalışma, saha araştırması ve mevcut literatür analizinin birleşimi yoluyla, Alanya'daki plaj erozyonunun nedenlerini bulmayı ve çevresel ve ekonomik olarak sürdürülebilir bir şekilde bir öneri sunmayı amaçlamaktadır. Ayrıca, plaj ekosistemlerinin önemi konusunda farkındalığı arttırmayı ve sahil erozyonu sorununu acilen ele alma ihtiyacını vurgulamaktadır. Kıyı beslemesi, kıyı erozyonunu sınırlamak ve kıyı alanlarının ekonomik ve koruyucu işlevlerini sürdürmek için yaygın olarak kullanılan bir yöntemdir. Mevcut literatürün kapsamlı bir şekilde gözden geçirilmesi ve Alanya'da önerilen sahil besleme projesinin incelenmesi yoluyla bir kıyı yönetim stratejisi olarak sahil beslemesinin etkinliği araştırılmıştır. Bu çalışmanın sonuçları, sahil beslemesinin kıyı yönetimine etkili bir yaklaşım olabileceğini, ancak etkinliğinin sahilin ve çevredeki ortamın özellikleri, projenin tasarımı, uygulanması, sosyal çevre ve bölgenin ekonomik durumu gibi çeşitli faktörlere bağlı olduğunu göstermektedir. Alanya Belediyesi'nin talebi üzerine Ağustos 2022'de BUCEL tarafından, kapsamlı bir kıyı ve topografik etüt yapılmıştır. Ölçümlerden elde edilen veriler ile rüzgar ve dalga rejimlerinin verileri sayesinde mevcut kıyı sisteminin analizleri yapılmıştır. Kıyı geometrisine ve özelliklerine uygun bir kumsal beslemesi tasarlanmıştır. Beslemenin kuşbakışı ve profil değişimleri, beslemenin sürdürülebilirliğini ve güvenilirliğini test etmek için modellenmiştir. Koy tipi kıyılardaki sahil beslemelerinin gelişimi, dalga mekaniğinin basitleştirilmiş denklemleri ve deneye bağlı ilişkileri kullanılarak modellenmiştir. Sonuç olarak, tek çizgili model ve koy şeklinde kıyıların değişimine ilişkin analitik çözümün bir birleşimi, sahil beslemeleri gibi çevre dostu çözümler yoluyla sahil erozyonunun önüne geçilebildiğini göstermek için modellenmiştir.

TABLE OF CONTENTS

LIST OF FIGURES

LIST OF TABLES

LIST OF SYMBOLS

B	Berm height
D_{50}	Medium diameter of particle size distribution
G	Longshore diffusivity constant
g	Gravitational acceleration
H_b	Breaking wave height
H_s	Significant wave height
h_*	Depth of closure
i	Coordinate step
j	Time step
K	Longshore transport coefficient
N	Number of data points
p	Porosity of sediment
s	Specific gravity of sediment
T	Wave period
t	Time
x	Shore-parallel direction for the diffusivity model
y	Shore-normal position for the diffusivity model
κ	Spilling breaker

LIST OF ACRONYMS

BUCEL	Boğaziçi University Coastal Engineering Laboratory
CAD	Computer Aided Design
CFSR	Climate Forecast System Reanalysis
CTD	Conductivity, Temperature, and Depth
DHI	Danish Hydraulic Institute
EBP	Equilibrium Beach Profile
GPS	Global Positioning System
ITRF96	International Terrestrial Reference System 1996
RTK	Real Time Kinematic
S	South
Se	South extreme
SSE	South-Southeast
SSEe	South-Southeast extreme
SSW	South-Southwest
SSWe	South-Southwest extreme
SW	Southwest
SWAN	Simulating Waves Nearshore
SWe	Southwest extreme
TUDES	Turkey National Sea Level Monitoring System
TUDKA-99	Turkish National Vertical Control Network 1999
W	West
We	West extreme
WSW	West-Southwest
WSWe	West-Southwest extreme

1. INTRODUCTION

Beach erosion and sediment migration is a highly encountered problem in many beaches around the world. Although there are different ways to restrain shoreline recession, the solution is exclusive for each area where the problem is encountered. Building protective structures with hard materials can only help at some extend but its main aim is to protect upland, so generally it does not protect the natural harmony of the beach, in some cases it aggravates it. Shoreline evolution can be defined in three time scales;

(i) Century long evolutions from geological movements,
(ii) Yearly or decadely long-term evolution,
(iii) Seasonal or storm induced evolution in short-term.

Water waves or wave-generated currents are the main factors of long-term evolution. Three ways waves act on long-term evolution are;

(i) beach material erosion by short period waves and accretion by long period swells,
(ii) effect of level changes on erosion,
(iii) effect of hard coastal structures.

Replenishing the beach by beach nourishment aims to maintain a beach for social, economic and recreational factors by also protecting the beach’s natural characteristics. In this thesis, the erosion of the Alanya beach and its beach nourishment project is studied.

Even though erosion of bays of this type are encountered in various places around the world, this is especially an interesting study to exemplify upcoming beach replenishment projects in Turkey coastlines using soft structures. Previous work done to prevent beach erosion in Turkey coasts were mostly hard structures, mainly groins and detached breakwaters which are especially common in the Black Sea region. Attempts of beach nourishment in areas where tourism is an important economic factor are done at small extends regularly before tourism seasons. But these nourishments have no or little scientific background and monitoring of the nourishments are not done, so they require repeated application every few years or sometimes every year, evidentially resulting in higher cost in the long run.

Alanya is a district of Antalya with main economic factor of tourism year-round. As a result of the natural characteristics of the beach and dominant wave direction, beach erosion is an expected problem in this region. For the last couple decades, this problem became more observable, mostly affecting tourism. With increased erosion, leaving smaller space at the beach and rocks being exposed at the wading depth, the decrease of touristic activity is a concerning problem for Alanya's economy.

The study's area is a crenulate bay with a length of approximately 7 km's starting from the Alanya Castle to Kestel region. The beach extends from north-west to south-east, where the dominant wave direction is from south-west, making the beach vulnerable to beach erosion. The bay side of the beach is at the north-west end, curbed by a headland. Although the fetch distance of the Mediterranean Sea from the north of Africa to Turkey is long, the natural land shape of the southwest Antalya provides a shelter from extreme wave heights resulting in a milder wave climate. The orientation of the beach in Alanya and its geographical position in the Mediterranean Sea is shown in Figure 1.1.

A breakwater for the Alanya Pier was built and in time, with natural characteristic of crenulate bays, beach and river sediment were accumulated in the pier causing bathymetry decrease which is a trouble for ships to sail. A concrete groin as a secondary breakwater was built to protect the pier from sand accumulating as shown in Figure 1.2. The area studied in this project has four rivers with varying discharges that bring small diameter sediments. The biggest river, Dim River, is at the south-east end of the beach. A dam on the Dim River was built, in 2004, decreasing the amount of sediment arriving to the beach enhancing the erosion problem.

The aim of this thesis is to determine the erosion problem in Alanya, investigate the mechanisms that cause erosion, design a beach nourishment that is suitable for the natural characteristics of the beach and reclaim land for touristic activities, and finally test its economical and engineering sustainability.

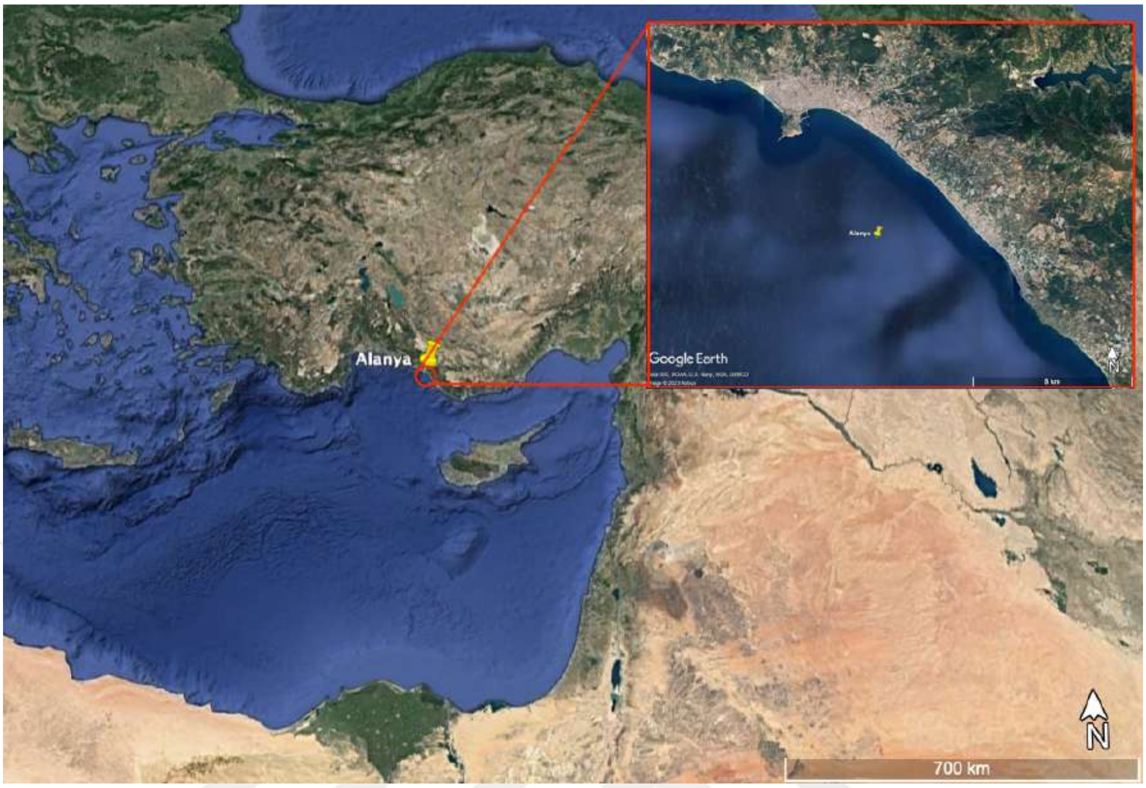

Figure 1.1. Alanya map shown on a bigger scale map of the Mediterranean Sea.

Figure 1.2. Concrete groin and sand accumulation.

To apply a beach nourishment project successfully, a material to nourish the coast is needed, that is called the fill material. This material can either be supplied offshore through dredging or it can also be supplied from a quarry to fit certain specifics. A fill material that is convenient for the residents, business owners and tourists is important while it has to be economically feasible for the Municipality of Alanya to afford the project. A trial of the nourishment is requested to see the outcomes of the project and to invest in larger nourishments in future in the area. A fill of 1 km width is found adequate for such trial that is in the mid-range of the beach with the most damage from erosion.

To understand the geometry and bathymetry of the area and to use it in analyses and models, field measurements were done in Alanya by BUCEL, in August 2022, to develop a project for beach nourishment requested by Alanya Municipality. First site works for the project are done between 6 August 2022 and 11 August 2022. The measurements included GPS survey, wading profile survey which is done by leveling instrument, boat survey with a single beam echo sounder and GPS, CTD measurements, sediment sample collection from the beach, and offshore for possible sand sources, water level measurements. The extent of the measurement area is given in Figure 1.3.

With the initial data collected, a report for the first impressions were presented to Alanya Municipality. First measurements presented the beach contours, bathymetry of the bay, cross-shore profiles, and the sediment distribution of the area. Later on, wind and wave data were collected from Copernicus and MetOcean for wind and wave analysis to be used in the model. To simulate the waves in the nearshore area, SWAN model is used, which is a model developed by University of Delft. Bathymetric grids to be used in the model were compiled by PDS2000 software with using all the data points collected in the site including wading measurements and boat survey. Extreme conditions were selected depending on the wind and wave roses of the data mentioned above. The SWAN model outputs were used to compute breaking waves in the surf zone, wave setup along the shoreline, longshore sediment transport rate, and shoreline change using a one-line model.

One-line model is used to predict the shoreline evolution of the nourished beach. The model uses primitive equations in a staggered grid to accurately forecast future evolution. One-line model is combined with the crenulate bay analytic model to predict the evolution of the nourished planform and profiles in this thesis. One 2nd order and two 1st order differential equations are used and the cross-shore evolution is determined with equilibrium beach profile theory to predict post-nourishment profiles.

Figure 1.3. Area covered in measurements.

In light of these analyses, an initial fill of 1 km with a net shoreline advancement of 20m's was proposed and designed by BUCEL. In the following chapter, a brief literature review of the sediment transport and characteristics of such shoreline formations are mentioned.

The hypothesis is that longshore sediment transport mechanisms, varying river discharges and a dam being built on the largest river that diminish the supply of sediments to the bay, enhances the erosion problem. Typically, in crenulate bays, there are areas of accumulation and erosion, and we aim to find the areas of accumulation and erosion through time history analysis of the shoreline. Also, the field measurements help us find sudden bathymetric changes and currents, except longshore currents, if they exist and contribute to erosion. By designing and building a beach nourishment suitable for the wave climate and beach characteristics, the erosion problem is targeted to be mitigated.

2. BEACH EROSION AND PROPOSED SOLUTION

Beach erosion can be caused by a variety of factors, including natural processes like waves, tides, and storms. Human activities like construction, dredging, and beach nourishment can also contribute to erosion as they can alter the natural sediment transport processes and cause the beach to become destabilized. Climate change is another factor that can lead to beach erosion, as rising sea levels and more frequent and severe storms can increase the intensity of wave action and cause more erosion.

Most of the earlier harbors were settled near natural headlands that act as breakwaters. As population and industry grows, more shelter will be needed for ships, so artificial structures like breakwaters and jetties are built. This causes beach erosion in the bay due to interception of littoral drift. Also, by transport of particles finer than sand may cause siltation in the harbor, reducing the depth in the port area.

Crenulate bays are characterized by a series of small headlands and bays, which can be particularly susceptible to erosion. In these types of bays, beach erosion is often caused by wave refraction, which can concentrate wave energy on the headlands and cause them to erode more quickly than the adjacent bays. Additionally, the narrowness of the bays can cause the waves to become more focused, which can increase their destructive force.

Similar beach erosion problems are encountered around the world mainly in beaches downcoast of harbors since the crenulate bay shape is associated with a harbor near the headland that forms the crenulate bay (Hsu, 1993). Port Orford, Oregon and Durban, South Africa (Hsu, 1997) are very similar examples to the problem faced in Alanya.

2.1. Causes of Erosion in Crenulate Bays

The main reason for beach erosion is the sediment transport process which can either happen as bedload transport or suspended transport. Sediment transport occurs along two directions: longshore transport and cross-shore transport. These transport processes are results of the longshore and cross-shore currents.

By the conservation of mass, there should be a back flow to the mass transport induced by the waves since the beach is a no flow boundary. This back flow separates into longshore and cross-shore currents. Longshore currents can occur in two alongshore directions depending on the incident wave angle. The cross-shore currents are results of undertow.

Obliquely incident waves and wave-breaking is the main generator of longshore currents. In the case of Alanya, three main contributors of longshore transport are given below sorted from more effective to less,

(i) Oblique waves that act as primary transport in longshore direction,
(ii) Wave setup gradient that acts as secondary transport in longshore direction,
(iii) Changes in river discharges.

The primary transport in the surf zone is due to obliquely incident waves to shoreline. Oblique waves result in longshore currents alongshore in both directions. In the case of crenulate bays, from the dominant wave vector towards the headland is called the shadow zone and is most likely similar to the diffraction zone of the crenulate bay. This shadow zone starts on the shore where the net longshore current zero. The longshore current towards the shadow zone is smaller than the longshore current opposite the shadow zone.

Wave setup is the difference in the water level elevation caused by breaking waves. The wave energy is proportional to wave momentum flux and as waves break, the momentum flux decreases. Momentum flux change is balanced by slope in the water level. As water moves from the higher elevation to lower, secondary currents caused by wave breaking occurs. The secondary longshore transport is towards the shadow zone, as the effects of shadow zone decreases and the incident wave to shoreline are relatively similar, water level elevation difference decreases so as the currents from wave setup.

River discharges are also a factor in sediment transport. Not only rivers can act as a source for sediments, they can trigger beach erosion depending on the discharge and location. Out of four rivers in Alanya, Gümüş River and Hacet River has small significance in the coastal zone. Oba River is larger than first two, it’s apparent effect on the beach is in source condition. Dim River on the other hand is the largest river in the area with varying discharge. As observed during the field measurements, the river can have a great extent when the discharge is increased from the dam. It has a radial coverage with greatest velocities in the shore normal, which can cause movement of the sediments in the offshore. Its sediment capacity already decreased when the dam was built and from sediment characteristics analysis in the whole bay indicates that the Dim River causes sediment drift in a radial way offshore.

Statically equilibrated bay shape responds to persistent swell wave action and its shape remains unchanged. Hsu and Evans (1989) equated the planform equilibrium of a beach by a second order polynomial. Static equilibrium bay shape equation was used for coastal protection applications in Thailand (Weesakul, 1999), Spain (Gonzalez and Medina, 2001), Taiwan (Hsu et al., 2006) and other locations. Most analytical solutions available for beach planform change are proposed for straight shorelines. Only a few of these solutions are used to simulate a bay planform.

2.2. Proposed Solution of Beach Nourishment

As attempted in many beaches around the world, the beach erosion in Alanya was also tried to restrained by construction of a groin or groin system. However, since Alanya is an area where touristic activity is an important contributor to economy year-round, a beach nourishment is a better solution. Alanya beaches has small diameter median particle size with average diameter of 0.87mm so, with a possible fill material with sediment size of 2.47mm, a stable beach nourishment can be done. An initial fill of 1km length is proposed and to predict its future performance, an analytical model is developed. Both the planform and profile evolutions are predicted for the nourished beach. The beach nourishment is designed in a way that the net shoreline advancement in equilibrium will be 20m. A fill sediment sample sent from the quarry is found adequate after analysis and comparison with the native sediment samples. The nourishment of length and width mentioned is within the budget of Municipality of Alanya with the fill sediment selected from the quarry.

2.3. Planform Evolution of Beach Nourishment

Main components that govern longshore evolution of a beach are wave-induced currents, sediment characteristics and the boundary conditions of the beach. Longshore currents are essential for composition of equilibrium planform of beaches, since they have an important potential of sediment transport.

In 1956, Pelnard-Considere linearized and applied equations for longshore evolution. He introduced the one-line theory and affirmed its applicability with experiments by taking shoreline change at a groin as an example. This was a simple model that contours the beach planform change around coastal structures. The model describes the time history and shoreline position along the shoreline combining the sediment transport equation and continuity equation. Shoreline change at groins with and without sand bypassing were discussed by LeMahaute&Brebner(1961).

In the one-line model, Pelnard-Considere assumed that the cross-shore profile down to depth of closure is controlled by the equilibrium beach profile and remains similar to initial profile, no longshore transport is assumed seaward of the depth of closure. This assumption allows him to solve the planform evolution problem with one contour line.

The angle between the incident wave direction and the shoreline is assumed to be small and constant. Lastly, the longshore sediment transport and the incidence angle is linearly related. The mass conservation principle is always applied.

2.3.1. One-line Model for Crenulate Bays

Weesakul and Rasmeemasmuang (2002) use a numerical model that combines polar and cartesian coordinates to simulate longshore evolution of crenulate beaches. The model uses polar coordinates for the diffraction zone where the bay has a parabolic geometry, and cartesian coordinates for the refraction zone. The crenulate bay shape of Alanya does not have a significantly diffraction zone, so the use of polar coordinates is not necessary in this model.

2.3.2. Sediment Transport Model

To form the sediment transport model, primitive equations are used in a staggered grid. A control volume over a width Δx and a fixed depth is taken and the sediment discharge input and output are directional alongshore. Schematic diagram for the control volume is shown in Figure 2.1 where D = h_*+B.

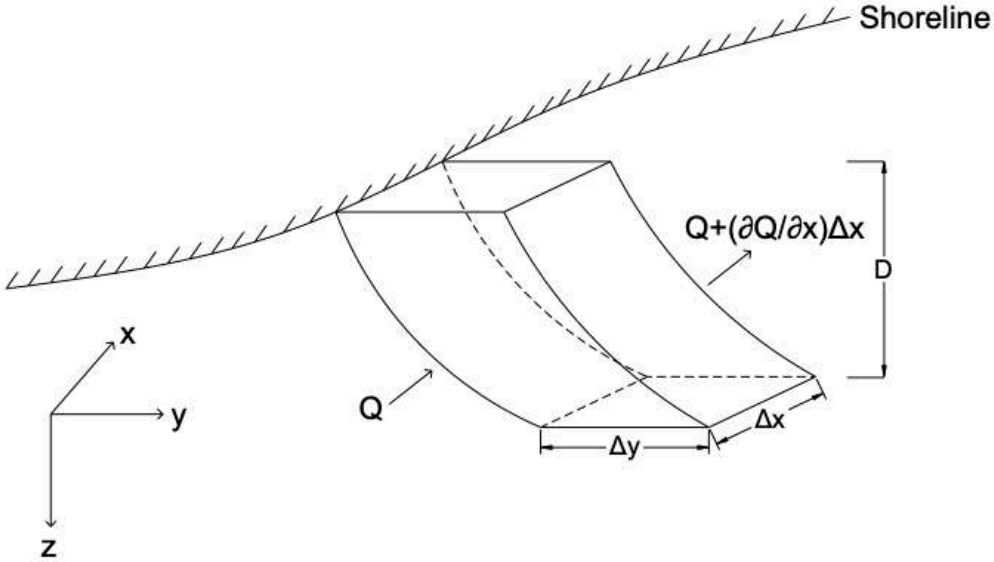

Figure 2.1. Schematic illustration of a hypothetical equilibrium beach profile with sediment transport rates over a control volume.

The continuity equation becomes

$$\frac{\partial Q}{\partial x}\Delta x = \frac{\partial y}{\partial t}\Delta x(h_* + B)\,. \tag{2.1}$$

The original transport equation for one-line is

$$Q = Q_0 - G(h_* + B)\frac{\partial y}{\partial x}, \tag{2.2}$$

where

$$Q_0 = c_Q' \sin 2(\delta_b - \gamma), \tag{2.3}$$

$$G = \frac{K H_b^{\frac{5}{2}}\sqrt{g/\kappa}}{8(1-p)(s-1)(h_* + B)}\;. \tag{2.4}$$

So Q_{ls} becomes,

$$Q_{ls} = \frac{KH_{s,b}^2\sqrt{g/\kappa}\sin 2(\delta_b - \gamma)}{16(s-1)(1-p)}, \tag{2.5}$$

where breaking index $K \cong 0.78$ for Komar and $\kappa \cong 0.35$ for Rosati. $H_{s,b}$ is the breaking significant wave height, δ_b is the angle of the incident wave, γ is the angle of beach planform normal, s being sand specific gravity and p is the porosity of the sediment. Using θ_b for the angle between the shore normal and incident wave, Q_{ls} can also be written as,

$$Q_{ls} = c'H_b^{5/2}\sin 2(\theta_b), \tag{2.6}$$

where θ_b is the angle between incident wave angle and shore normal and constant c' is

$$c' = \frac{K\sqrt{g/\kappa}}{16(s-1)(1-p)}. \tag{2.7}$$

2.4. Profile Evolution of Beach Nourishment

Sediment transport alongshore is driven mainly by wave-induced longshore currents, while the cross-shore transport is driven by wave mechanics and undertow. The relation between sediment transport and hydrodynamics is not well defined, but there are several methods to compute cross-shore evolution by using empirical equations. Increased wave heights and frequency of storms in the winter is considered to be the main reason of seasonal shoreline changes. Seaward sediment transport results in storage of sand in the nearshore bars. These bar features are generally associated with undertow resulting from wave breaking, with no precise understanding. As wave height increases, the bar formations take place farther from the shoreline and with increased depth, the volume of sediment required also increases with result of erosion of the beach affecting the beach planform.

Beaches around the world have similar characteristics such as shape and elements. A cross section perpendicular to the shore of the beach is the beach profile and is given in Figure 2.2. This profile consists four sections: the coast, also called upland, the beach, the nearshore zone and the offshore. The foreshore or beach face are also called the swash zone, where the waves swash up and down, and this zone generally has a steeper profile. Berms are created by larger waves or storms in the backshore area. Nearshore zone is where waves steepen and break, the depth of closure and wave breaking depth are in this zone.

In the following sections, various models used to compute cross-shore transport are mentioned.

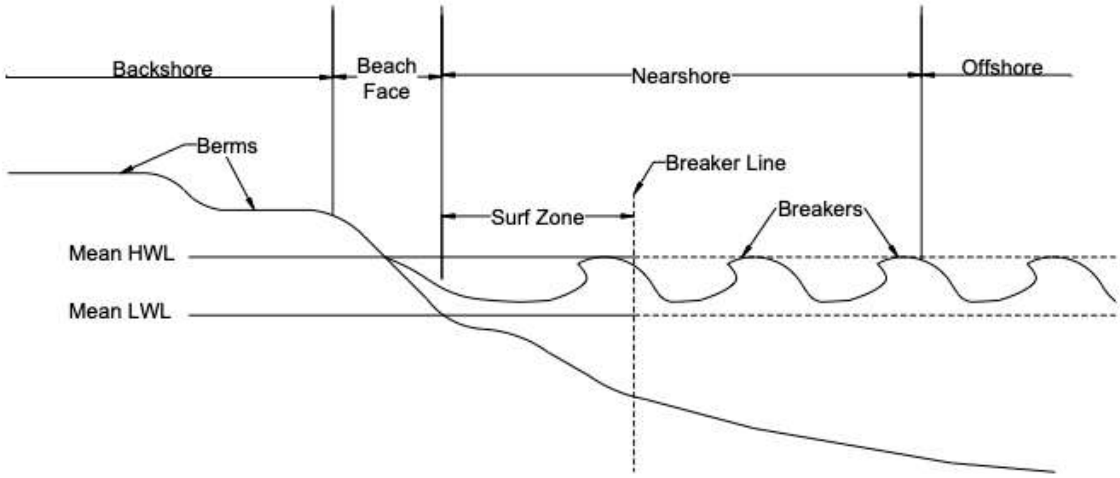

Figure 2.2. Beach profile terminology.

2.4.1. Simple Cross-shore Transport Model

Moore first (1982) proposed this model, Kriebel (1982), Kriebel and Dean (1982) later modified it. The principle of the model is, for uniform sediment size along the profile of equilibrium beach, the energy dissipation rate per unit volume is constant and is controlled by $Ay^{2/3}$ profile. If the equilibrium profile is disturbed, the energy dissipation rate will differ from its value in the surf zone. So, this concludes that the sediment amount that is moved is related to the difference between the energy dissipation rates.

2.4.2. Energetics Model

Stive (1986) and Roelvink and Stive (1989) studied Bailard's sediment transport relationship for cross-shore transport. To model the beach profile evolution, the Bailard equation coupled with a sediment conservation equation was studied by Roelvink and Stive. A random wave-breaking model (Battjes and Janssen, 1978) was used and wave nonlinearity, wave grouping, undertow, and wave-induced turbulence was included. It was concluded that the wave hydrodynamics were predicted well by the new model and Bailard equation was insufficient for areas outside the surf zone.

2.4.3. Equilibrium Beach Profile Theory

There are three different methods to derive the equilibrium of a beach profile: kinematic, dynamic and empirical. The approach with most success to provide a solution to coastal problems is the dynamic one, so the following sections will concentrate on dynamic solution. This equilibrium profile is formed by constructive and destructive forces that act on the beach. If the balance between these forces is disturbed, the beach will evolve and form a new equilibrium profile until the forces are even again. One of the most important factor that alters the equilibrium beach profile is the sea level changes, this theory was first proposed by Bruun in 1962. The Bruun Rule does not give us an exact solution of the equilibrium profile but will give a mean slope of the active profile.

Beach profiles are affected by various different destructive and constructive forces but not all of these forces are identifiable with current knowledge. Empirical relationships are proposed to demonstrate the effect of these non-identifiable and non-quantifiable forces on the equilibrium profiles.

2.4.4. Destructive Forces and Constructive Forces

The most important destructive force is gravity. Gravity will act in a way to make the beach profile more horizontal. Secondly, turbulent water from braking waves in the surf zone is a significant destructive force. With highly turbulent water, sand particles are dislocated, carried and with the gravity force acting on them, they move towards offshore direction and settle. In equilibrium, a beach profile with smaller slope will have lower turbulence since the wave breaking occurs over a greater surf zone and is distributed. Whereas a beach profile with steeper slope will have higher turbulence that reaches deeper due to energy dissipation of breaking waves over a smaller surf zone. This is the reason mildly sloped beaches are associated with smaller sediment particles and steep slope is associated with coarse particles.

Asymmetric shallow water will produce net shear stress at the bottom towards beach. Although the net velocity is zero at the bottom, the second-degree equation of the bottom shear stress gives us the result that there is a mean shear stress towards onshore. Streaming velocities at the bottom are another force. Energy dissipation and momentum transfer at the bottom result in these velocities. This theory was studied by Bagnold in 1947 and improved by Longuet-Higgins in 1953.

Last force is generated wave-induced crest velocities that are shoreward and result in suspension and selective transport of the sediments. If the turbulence created by wave breaking is great, a sediment particle can be transported. This force is also discussed by Dean(1973) as mentioned above in the Fall Time Model section. Effects of cross-shore transport in the beach profile is presented with the equilibrium beach profile theory in the problem. In the following section, the model to predict the evolution of the beach profile in the surf zone will be explained. Linear wave theory for shallow water will be used and some necessary equations to develop the model are as,

$$E=\frac{1}{8}\rho g H^2, \tag{2.8}$$

$$\mathcal{F} = E C_g , \tag{2.9}$$

$$C_g = \sqrt{gh} , \tag{2.10}$$

$$H = \kappa h \ , \tag{2.11}$$

where E is wave energy per unit surface area, $\mathcal{F}$ is energy flux, C_g is shallow water group velocity and κ is the breaking index. Spilling breaker assumption in the surf zone is shown in Equation 2.11. A right-handed coordinate system is used where the alongshore direction is on the x-axis.

The general equation for equilibrium beach profiles are derived from uniform energy dissipation of unit volume principle. In this theory, the greatest destructive force is turbulence in surf zone caused by wave breaking. Energy dissipated per unit volume is represented as the amount of turbulence caused by breaking waves. The constructive forces acting on the beach will not be quantified in this theory. Uniform energy dissipation per unit volume is $D_*(d)$ and is a function of the sediment size d. The energy conservation can be written as

$$-D_*(d) = \frac{1}{h}\frac{d\mathcal{F}}{dy'} \tag{2.12}$$

where y’ is the shore normal coordinate. According to this equation, a change in energy flux over a distance and depth is equal to energy dissipation per unit volume of a stable sediment particle. Using the relationships mentioned above, taking its derivative and simplifying, the equation becomes,

$$h(y) = \left(\frac{24D_*(d)}{5\rho g\sqrt{g}\kappa^2}\right)^{\frac{2}{3}} y^{2/3} = A(d)y^{\frac{2}{3}} \tag{2.13}$$

where A is the profile scale factor and is dimensionless.

2.4.5. Depth of Closure

Depth of closure is the depth where the waves starts to affect the seabed. Seaward of this depth, sediment movement is possible but not in a way that the beach profile is affected significantly, the net sediment transport from this depth offshore is considered zero. Hallermeier (1978) experimented the closure depth of EBP on planar beaches by using wave tanks. He proposed that the most sediment transport is caused by largest waves so he came up with an empirical equation that use the extreme wave height H_e, which is the wave height that is exceeded 12 hours a year and similarly the extreme wave period T_e. With this equation annual wave statistics could be utilized. By assuming that $(\rho_s - \rho)/\rho = 1.65$, the equation for closure depth is

$$h_c = 2.28H_e - 68.5\left(\frac{H_e^2}{gT_e^2}\right). \tag{2.14}$$

Extreme wave height and wave period values are calculated from the wave and wind datasets where $H_e = 3.13m$ and $T_e = 7.66s$. Using Equation 2.14 with these values, the depth of closure for Alanya is h_c=5.97m. This closure depth is the average of the whole bay and varies throughout the beach, but it is in accordance with the sediment characteristics analyses which will be covered in the later chapters.

2.5. Alanya in Literature

There are a couple studies done in Alanya region for beach erosion however these studies lack coastal geography and topography. Reliable measurements of wind, wave and water level is not done in Alanya. The nearest water level measurement gages are in Antalya and Bozyazı, measured by TUDES. So, to acquire more knowledge on the area, measurements to establish bathymetric surveys and analysis of wind and wave are done.

The most detailed prior study done to research the beach erosion problem and a solution proposal was done by Aksel and Dikici (2019). The proposed solution was a set of T-groins built at the right end side of the secondary breakwater, one being right at the mouth river of Hacet river. The river discharges and sediments transported by the rivers to the bay were taken from this study. River discharges were computed using the river basin area, river length, bottom slope and precipitation rates obtained from Meteorological Station of Alanya. Bishop et al., Lauresen, and sediment discharge calculation through river basin methods are used for the sediment discharge calculations of the Hacet, Oba and, Dim Rivers. Gümüş River appears to be the river with least effect on the sediment budget on the bay, so its discharge is neglected on calculations of the sand budget. In Table 2.1, river discharges and sediment discharges calculated by Aksel and Dikici (2019) with three different methods are given for the three rivers.

Table 2.1. River and sediment discharges of rivers.

Rivers	River Discharges(m^3/s)		Sediment Discharges(m^3/year)		
	Mean	Max	Bishop et al.	Lauresen	River basin method
Hacet	52.16	165.98	32004.63	35801.87	13739.35
Oba	64.14	205.26	25603.70	15575.32	26276.91
Dim	81.44	302.50	32004.63	32071.33	15591.47

To acknowledge beach erosion in Alanya, a time history analysis is done using Google Earth images of previous 20 years. Shorelines are traced on the images and compared with each other as well as the measurements done by BUCEL. All the previous shorelines are drawn using the images of summer months for similarity to current situation where wave heights are smaller and water level due to tides are similar. Five years of historical images are shown in Figure 2.3. and Figure 2.4. It is certain that there is sediment transport through the bay and it can be seen clearly when shorelines near hard structures are compared, like the breakwaters or small headlands. The diffraction zone of the bay has significant sand accumulation near the second breakwater.

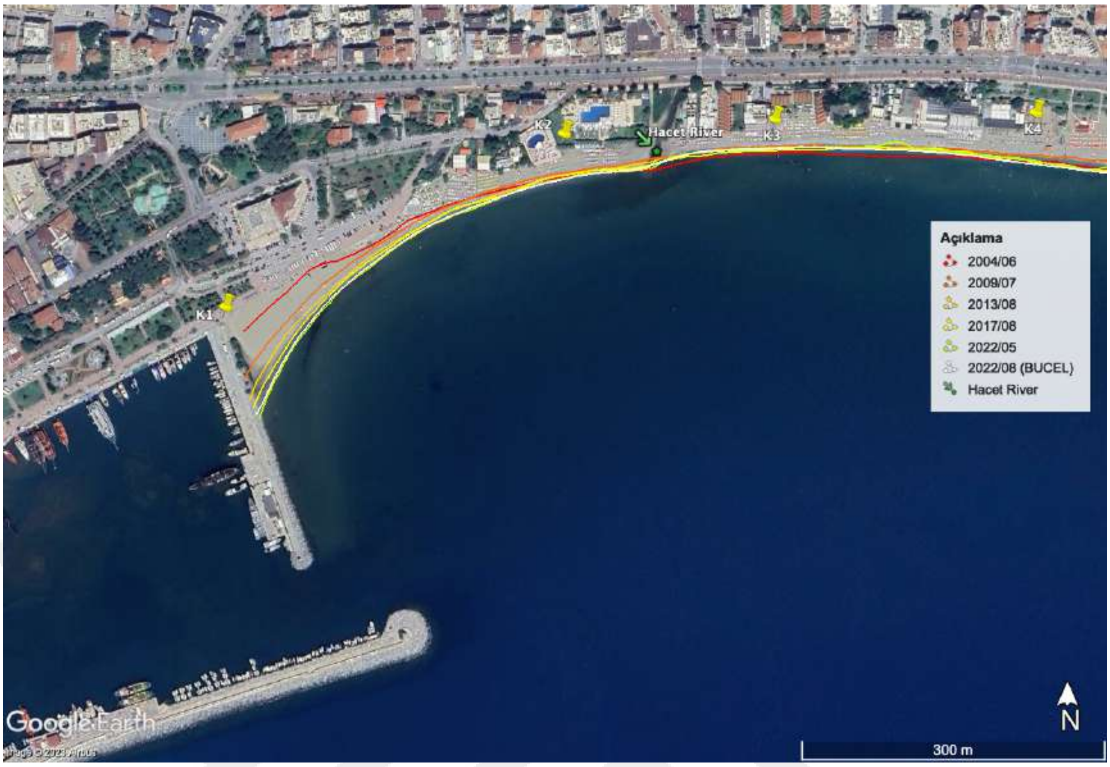

Figure 2.3. Time history of shoreline near the secondary breakwater.

Figure 2.4. Time history of shoreline between the Oba River and Dim River.

3. METHODOLOGY

In this chapter, the methodologies followed to back up the hypothesis on beach erosion problem and its possible solution are covered. Hypothesis states that the main drivers of beach erosion in Alanya, primary and secondary longshore currents and varying river discharges. The primary longshore currents are induced by oblique waves, so to be able to calculate these currents, most important two parameters are the shoreline direction and incident wave angle. Secondary longshore currents are caused by wave setup gradient in the bay. Wave heights acting onto shore and shoreline geometry is needed for secondary current calculations. Lastly, river discharges are varying in Alanya and their flow rates are not well measured and monitored, so to predict their effect water quality measurements are done. In this particular thesis, water quality is not directly necessary but it helps us detect significant changes in parameters in water column which can indicate river currents.

3.1. Field Measurements

A comprehensive hydrographic survey of the project area is required to calculate the amount of beach fill that is required for the nourishment, to act as a baseline for future monitoring and performance checks of the project, to use as an input for the sand transport and shoreline evolution models. They help to analyze the current situation and identify the problem. The field data is essential for geometric mapping and to be able to propose an adequate design for the area. Measurements also act as a datum for future monitoring and evaluation of the models. The detailed survey is done by BUCEL in August 2022, the following chapter contains the descriptions and results of the survey. Bathymetric map of the area and cross-shore profiles were established with the data collected in field.

3.1.1. Bathymetry and Topography

3.1.1.1. GPS Measurements. GPS surveying is done approximately 7 km's along the shoreline starting from the breakwater. 5 benchmark locations were set prior to measurements by Alanya Municipality to be used as GPS bases. TOPCON RTK GPS devices are used, the base point of the GPS remained same during measurements at a secure location shown in Figure 3.1 so that it is not disturbed during the measurements. Points were collected with the GPS rover by stop-and-go method at +1m, 0m, -0.5m and -1m contours with 20m intervals. 31 points were selected as benchmarks on the starting points of the beach that are approximately 200 m apart and were marked by Alanya Municipality beforehand. Cross section measurements were taken with GPS devices instead of leveling instruments where the boat survey covered within the wading depth. The coordinate system for the GPS measurements are in ITRF96 system.

Figure 3.1. GPS base station.

3.1.1.2. Wading Profiles. Wading profiles were taken where the boat couldn't cover wading depth and the method is shown in Figure 3.2. 14 profiles are measured by rod and leveling device and 3 GPS points were taken for adjustment purposes at the base point, berm and sea level since leveling rod can be used in water unlike GPS rover, a more precise profile is obtained with this method. The wading profiles covered from the benchmark point up to 2.5m of depth of water. The coordinates of the benchmark points used for profiling is given in Table 3.1. All of the measurements taken and survey cross sections are shown in Figure 3.3.

Figure 3.2. Measurement of wading profiles with leveling device.

Figure 3.3. Profile sections and survey area shown on map.

3.2. Model Shoreline

A shoreline of 16.3 km starting from the secondary breakwater to 16 km east of Alanya. The shoreline to be used for the sediment transport model is selected wider so that the model will develop better results when the location step is in the project domain. The reason to selecting the boundary edge at 16.3km is a no flow boundary condition exist at a rocky peninsula, so it is for sure known that no sediment far from that point will transport. The extended shoreline is shown on map in Figure 3.4. The existing shoreline data measured by GPS devices cover a 7 km area so to extend the shoreline, Google Earth images. Shoreline coordinates are according to TUDKA-99 datum.

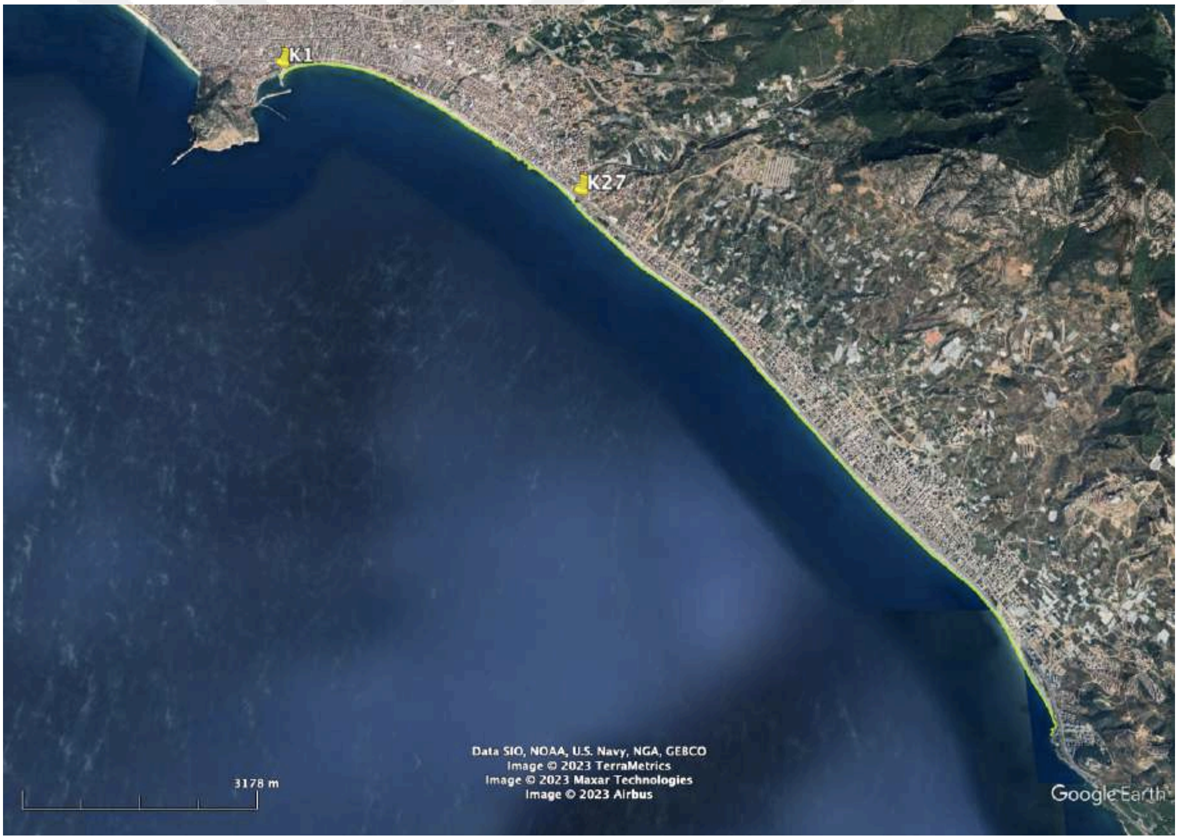

Figure 3.4. Extended shoreline for the model.

In the project zone, which is approximately 7 kms long, the TUDKA-99 0 elevation is calculated by triangle geometry of measured GPS points, one from above 0 level and one from below, since the GPS device is already set to TUDKA-99 coordinates. Then, to match the rest of the shoreline, where no measurements are taken, to TUDKA-99 shoreline, a line starting from the secondary breakwater to a no flow boundary point 16 km far from the first point is drawn in Google Earth by precisely following the shoreline image taken in May 22th of 2022. The two lines are then compared and best fitted in AutoCAD at the last point of measured beach. The first half of the Google Earth image up to measurement boundary is deleted. Merging to shoreline, the 16.3 km long shoreline at TUDKA-99 0 elevation is formed. Last tuning is made with the help of rock map and the final TUDKA-99 shoreline is created to be used in the one-line model.

To run the model with the nourished shoreline, the nourished shoreline points are added to the planform. Between the K4 and K9 profiles, an initial shoreline advancement of approximately 23m is built and run in the model. The H_b values are translated from SWAN boundaries to model boundaries since the effect of H_b variations are negligible in this case.

Table 3.1. Benchmark points for beach profiles.

Point Name	**Definition**	**GPS Measurements**		
		X(m)	Y(m)	Z-TUDKA(m)
K1	Benchmark	410680.25	4046109.94	1.472
K2	Benchmark	411014.68	4046272.64	2.669
K3	Benchmark	411218.75	4046284.96	2.048
K4	Benchmark	411470.78	4046290.43	2.578
K5	Benchmark	411684.05	4046251.93	2.354
K6	Benchmark	411859.28	4046238.06	4.349
K7	Benchmark	412109.71	4046164.84	3.592
K8	Benchmark	412296.58	4046059.90	3.140
K9	Benchmark	412479.59	4045995.72	3.703
K10	Benchmark	412646.23	4045873.50	3.399

Table 3.1. Benchmark points for beach profiles. (cont.)

K11	Benchmark	412796.96	4045755.33	3.132
K12	Benchmark	413012.62	4045712.42	2.980
K13	Benchmark	413209.32	4045560.57	3.061
K14	Benchmark	413372.90	4045449.11	3.309
K15	Benchmark	413534.27	4045317.31	3.403
K16	Benchmark	413675.69	4045205.41	2.851
K17	Benchmark	413833.67	4045086.29	3.342
K18	Benchmark	414011.55	4044948.77	4.376
K19	Benchmark	414168.69	4044818.93	3.017
K20	Benchmark	414326.38	4044708.49	3.584
K21	Benchmark	414459.63	4044597.60	3.560
K22	Benchmark	414620.28	4044474.98	2.186
K23	Benchmark	414764.97	4044367.24	3.079
K24	Benchmark	414947.93	4044220.35	3.439
K25	Benchmark	415071.11	4044120.63	3.861
K26	Benchmark	415230.94	4043988.87	3.091
K27	Benchmark	415337.39	4043821.62	1.804
K28	Benchmark	415423.86	4043670.35	2.732
K29	Benchmark	415542.74	4043541.43	2.917
K30	Benchmark	415719.34	4043377.50	4.009
K31	Benchmark	415858.24	4043219.11	2.850

3.3. Boat Survey

Boat survey is done for the project area up to 20m depth in the bay from 2.5m depth contour. The GPS device and a single beam echo sounder were connected and the data collected from both devices combined by using a software called Kordil. The device setup on the boat is shown in Figures 3.6 and 3.7. Sailing with approximately 1.5 m/s speed, the area was covered in profiles. Two rounds of profile were done for each section to eliminate the effects of waves on single beam echo sounder. Otherwise the profile of the bathymetry would be in the shape of sinusoidal waves since the day of the survey the sea was quite heavy. Bathymetry is calculated for each section with the average of the both profiles taken with boat survey for more accuracy. The single beam echo sounder propagated 8 signals per second and notes were taken to eliminate any errors while taking samples or when the boat reduced speed, so that the bad data could be taken out of the dataset.

3.3.1. Sediment Characteristics

The median sediment size is one of the most important parameters to determine the equilibrium beach profile, therefore effecting the design process. In order to find the median diameter size of the sand throughout the beach, a total of 80 sediment samples were taken both from the beach and the sea bed and were send to the Boğaziçi University Geotechnical Laboratory. Samples were taken from +2m, +1m, 0m, -1m and -2 meters from the beach and while the boat survey was done, samples from -5m, -10m were collected with the Van Veen grab as shown in Figure 3.5. Also, a group of divers took samples from outside the project zone, northwest side of the Alanya Castle, for potential sand sources, ranging from -10m to -20m. Sand samples collected at -10m or below were washed to prevent aggregation and to eliminate small particles like clay and silt. All the samples were kept in the oven for 24 hours at 220 degrees for the water to evaporate. Sieve analysis is done for each sample separately. The sieve sizes that are used during the analyses are shown in Table 3.2.

Figure 3.5. Van Veen grab.

Figure 3.6. Single beam echo sounder device attached to GPS rover.

Figure 3.7. Set-up for the single beam echo sounder and GPS measurements.

Table 3.2. Sieve sizes used for sediment characteristics analysis.

Sieve No	Sieve Size [mm]
-	16
-	9.5
-	8
4	4.75
6	3.35
10	2
16	1.18
20	0.841
30	0.59
40	0.425
60	0.25
70	0.212
120	0.125
140	0.106
200	0.075
Pan	0

3.3.2. Water Quality

CTD measurements were taken from the boat at -5, -10, -20m depths at 6 different section that are almost equally distanced and in line with rivers. Also, 2 sections of measurements are done at the Alanya Castle area, one from the Dock and the other from the Cape and all of the CTD points can be seen in Figure 3.8. CTD device is set to measure temperature, salinity, density and sound velocity for this thesis. Measurement of sound velocity is especially important because it alters the single beam echo sounder waves' velocity, thus the depth measured by the single beam echo sounder. The rest of the parameters help us detect any currents in those points.

Figure 3.8. Points where CTD measurements are taken.

3.3.3. Water Level Variations

Water level measurements are done to convert section surveying data to TUDKA-99 system. A piezometer tube is installed in the pier where waves do not affect the measurements, the value on the tube is noted every hour on the days of the measurements. The top point of the tube is also measured with the GPS device to check if it moved, so that the data is consistent.

Also, water level measurements with the TUDKA-99 datum are collected from TUDES (Turkey National Sea Level Monitoring System). Since there is no measurement station in Alanya, two of the near most stations in Antalya and Bozyazı are used which are 134 km’s and 92 km’s far from Alanya relatively. So, the water level data collected at a sheltered point by BUCEL in Alanya is different from the stations that are kilometers away from the study area, yet, it can be seen that the peaks and lows of the data are in accordance with the TUDES stations’ data. The water level data with the TUDKA-99 datum for both stations and BUCEL measurements are shown in a graph given in Figure 3.9.

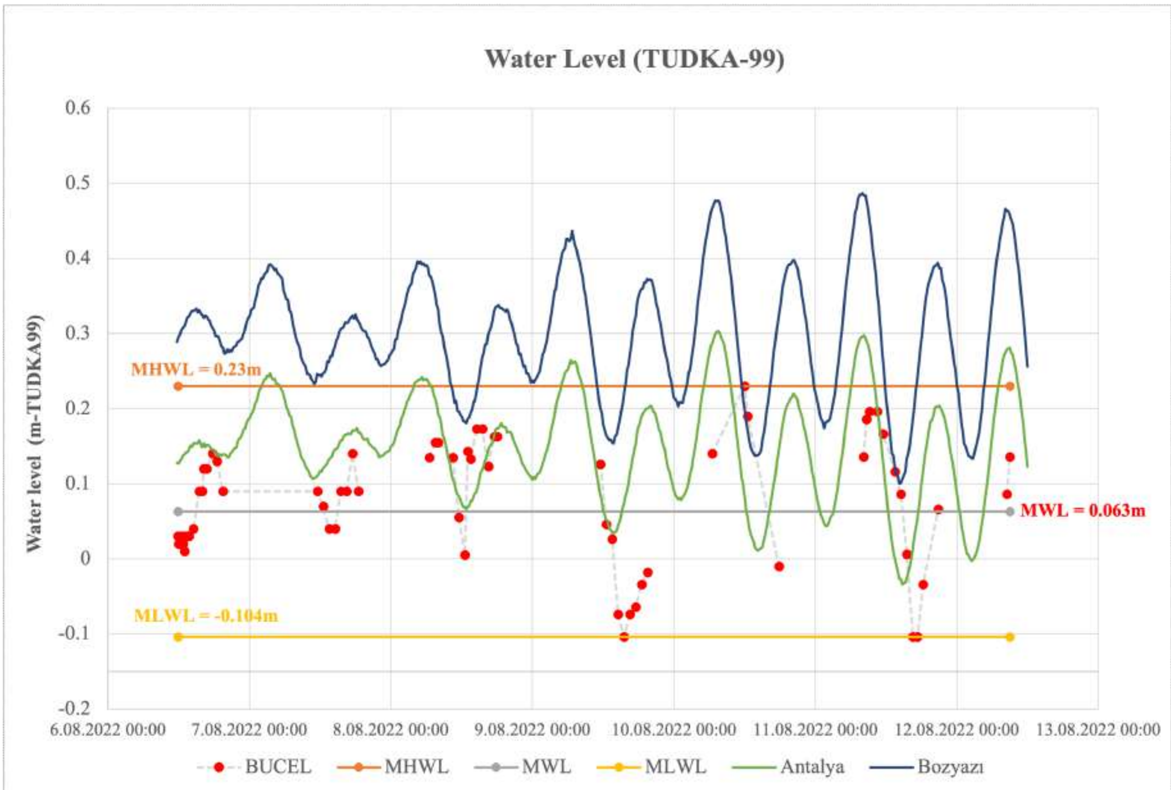

Figure 3.9. Change of water level change throughout measurements.

3.4. Meteorology and Oceanography

Wind and wave data are taken from more than one database. The data are collected at the point nearest to the nourishment area and is at the center of the shoreline. The data collection point is shown in Figure 3.10. Climate Forecast System Reanalysis (CFSR) dataset for wind is taken from Danish Hydraulic Institute (DHI) and reanalyzed wave forecast dataset is taken from European Union Marine Services (Copernicus). Both datasets cover a 29-year span starting from January 1993 to end of June 2021. Data from the datasets are shown in Table 3.3.

Table 3.3. Datasets used in the analyses.

Data Name	Description	Timeline	Data Location	Measured Parameters
Copernicus	Reanalyzed wave forecast dataset	1993-2021 (29 years)	36,479°N 32,042°E	Hourly wave height, period and direction
DHI	Climate Forecast System Reanalysis (CFSR) dataset	1993-2021 (29 years)	36,479 °N 32,042°E	Hourly average wind speed and direction

Hourly offshore wind data of 29 years from 1993 to 2021 from DHI database is analyzed to create a wind rose, wind speed histogram and wind direction histogram.

3.4.1. Winds and Waves

Although wind is the main reason for waves, currents and transport, most important parameter effecting the shoreline change processes is waves propagating to the beach. From Offshore water dataset taken from Copernicus of 29-years is analyzed for the wave rose, wave height histogram and wave period histogram.

SWAN is a third-generation wave model, developed at Delft University of Technology, that computes random, short-crested wind-generated waves in coastal regions and inland waters. It is a widely used model throughout the world in coastal and offshore engineering practices. SWAN models the physical processes like wind generated waves, shoaling, refraction, diffraction, reflection, bottom friction and breaking. Model uses deep water wave conditions, bathymetry, wind regime, currents and water level data as inputs to calculate spectral wave distribution in the model domain.

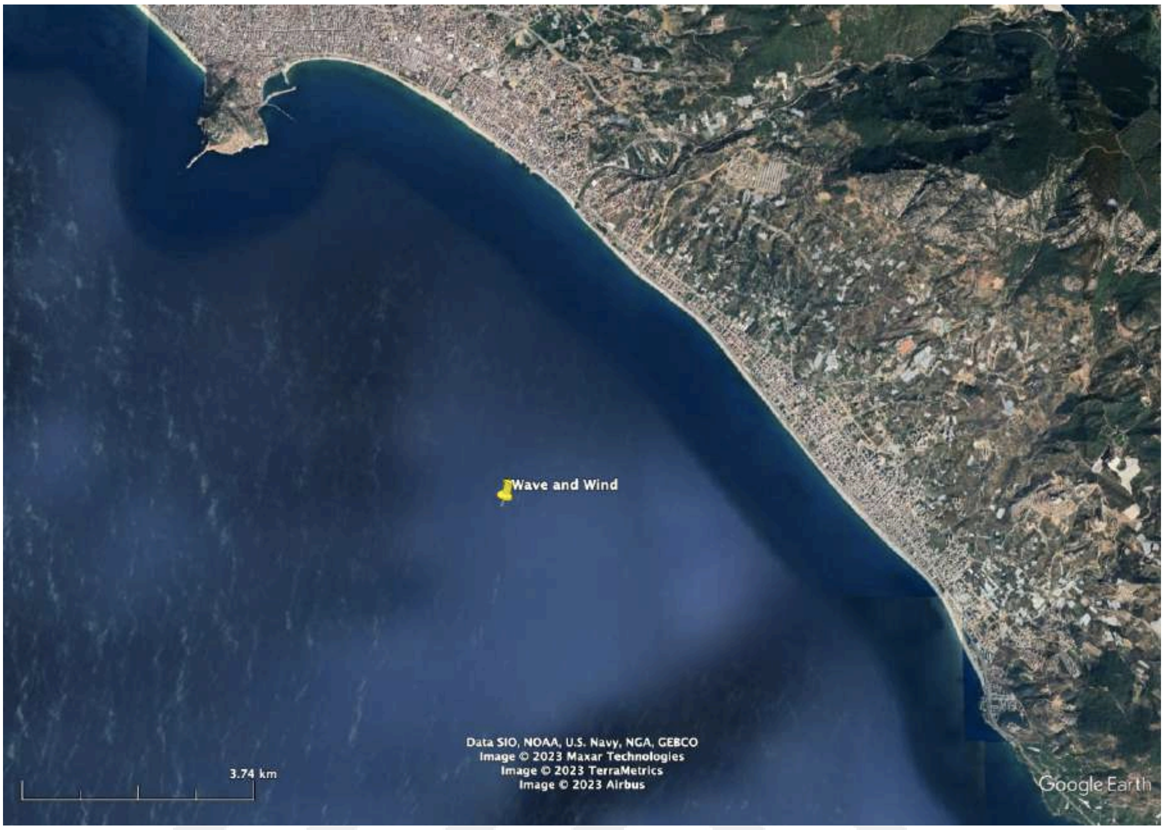

Figure 3.10. Data point for wind and wave from Copernicus and DHI.

The model uses conservation of wave energy to numerically solve wave energy spectrum for two dimensional domains. Generation and transport of the wave energy are important for the calculation of engineering parameters such as wave height and wave direction. Important parameters for this project are significant wave height (H_s), average wave period (T_{m02}), wave peak period (T_p), average wave direction (θ_m), wave breaking direction (θ_b), wave breaking ratio (Q_b) and wave setup at the beach (η_s), although SWAN can compute more extensive outcomes.

For the design of the shore structures, the wave that are recorded from the data station are translated to shoreline with the wave transformation model. A wider model domain starting from west side of the Alanya Castle peninsula to east of the Dim River is selected for better results at every point in the project area as shown in Figure 3.11, the dimensions of the x and y axes are 9500m and 4250m respectively. 20 different scenarios are run for the simulation regarding the variety of direction and intensity of offshore wave and wind climate. For every scenario, waves are individually modelled from deep water to shore throughout the domain. Wave parameters are calculated at critical points where shore structures exist. Model grid is in west-east orientation with a grid size of 20m x 20m in both axes. To utilize the model area efficiently, the +y axis of the model area is rotated 38 degrees counter-clockwise.

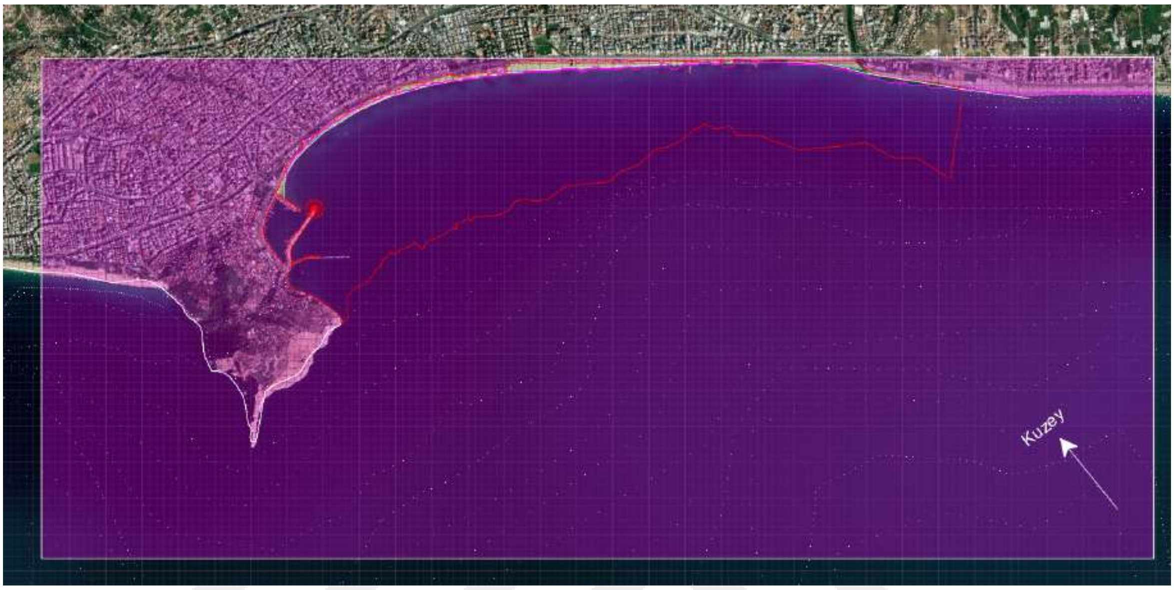

Figure 3.11. Wave model domain.

To reflect the current wind and wave climate for the simulation, 29-year datasets are distributed in 20 different groups. The scenario matrix of is shown in Table 3.4 in different wave and wind groups and directions.

Winds and waves coming from different directions are grouped in accordance with their intensity and frequency, average values for each group are calculated. These values are shown in Table 3.4 with their probability in all the data.

3.5. Modelling

The planform evolution of the beach nourishment cannot be done by a numerical one-line model because the numerical models assumes the shore as a long, straight line with parallel contours, but instead we have a crenulate bay. The one-line numerical model would try to straighten the beach by erosion in the diffraction zone and deposition in the east end side, which we know that the real case is as the opposite. Instead, a combination of analytical models is used.

Table 3.4. Scenario matrix according to wave and wind directions.

Direction \ Group	1	2	3	4	5	e
W	W1	-	-	-	-	We
WSW	WSW1	WSW2	WSW3	-	-	WSWe
SW	SW1	SW2	SW3	SW4	SW5	SWe
SSW	SSW1	SSW2	-	-	-	SSWe
S	S1	S2	-	-	-	Se
SSE	SSE1	-	-	-	-	SSEe

Since the governing equation of the problem, which is the diffusivity equation, is a linear differential equation, individual solutions can be superposed. The static equilibrium of the crenulate bay, the analytical solution of a rectangular beach fill and point discharge to represent the three biggest rivers in the area. For the end result of the evolution of the bay, all advancements and erosion values were combined and fitted to the shoreline coordinates. The boundary conditions of the model were selected at the headland specifically to provide no flow boundaries as it is assumed that no sediment transport occurs from these boundaries.

3.5.1. Crenulate Bays

The analytical modelling of crenulate bays are a challenge due to their geometry. In reality, the geometry of the beaches not always fit the analytical shape function in the literature. Wind (1994) has described the analytical model for crenulate bay shapes depending on their spirality. With unknown empirical parameters of the current case, it is decided to use Hsu&Evans (1989) static equilibrium bay shape to best fit the measurement of the area.

3.5.2. Beach Nourishment

For the initial beach fill design, two alternatives of 1 km length were considered. One in the shadow zone where residential use was more common and one where touristic use was more common. The first option was designed between sections K4 and K9, where it is less subject to higher wave heights and the cross-sections of the area are mildly sloped. The second fill option was between Oba River and Dim River between section K17 and K22. Here, the slopes are steeper and most of the beach is eroded with large rocks exposed at water level. Although this area is in more need of a beach fill, the beach is more subject to higher wave heights and the cost of a beach fill over an uneven rocky beach is greater.

The net shoreline advancement after reaching equilibrium profile is aimed to be 20m, so a fill width of approximately 25m with a length of 1000m is designed. Total volume of the fill is calculated as 73.000m^3 that corresponds to 73 m^2/m which is within the budget of Alanya Municipality when the cost per m^3 of sand is assumed to be \$25.

The cross-shore evolution of the beach fill is calculated with EBP theory and it is considered that the equilibrium profile would be reached within 2-3 weeks. For planform evolution, the analytical model of rectangular beach fill is used for 3 months, 6 months, 1 year, 2 years, 5 years and 10 years are compared. Analytical solution for a rectangular finite beach by Magnus and Larson (1987) is

$$y(x,t) = \frac{1}{2} y_0 \left[erf\left(\frac{a-x}{2\sqrt{Gt}}\right) + erf\left(\frac{a+x}{2\sqrt{Gt}}\right)\right], \tag{3.1}$$

for $t > 0$ and $-\infty < x < \infty$, where 2a is the length of the beach fill and G is the longshore diffusivity.

3.5.3. Rivers

With the sediment discharge data taken from previous literature, analytical models of the rivers were done as sand discharge from a river acting as a point source. The source coordinates were given as the real mean coordinates of the rivers, since they may change seasonally or depending on the discharge. The analytical solution from Magnus and Larson (1987) is

$$y(x,t) = \frac{V}{2D\sqrt{\pi G(t-ts)}}\, e^{-(x-xs)^2/4G(t-ts)}\,, \qquad (3.2)$$

where t > ts and -∞ < x < ∞, ts and xs are the point source release time and coordinate respectively. V is the instantaneous volume discharge and $D = h+B$.

3.6. Coordinate Convention

Coordinate convention used in the one-line model is shown in Figure 3.13, and a definition sketch for the one-line model with the compass directions is shown in Figure 3.12 and by using these sketches, a combined convention is formed.

SWAN model uses a different convention than shoreline models. Wave angle in SWAN uses a cartesian convention counter clockwise, measured from $+\vec{x}$ axis to the wave vector. So, to match the angles from the outputs of SWAN to Matlab codes, the conversions below are done as shown in Figure 3.14. N is the vector that indicates the North in compass directions, $\vec{k}$ is the wave vector, these two vectors are the same in both conventions since they are real vectors of North and the waves. And $\vec{n}$ is the shoreline normal.

The angles shown in Figure 3.14 and their rotations directions from the vectors or axes are as follows,

(i) The angle β_{SWAN} is clockwise from vector N to vector $\overrightarrow{y_{SWAN}}$,
(ii) The angle α_{SWAN} is counter-clockwise from $\vec{x}$ axis to vector $\vec{k}$,
(iii) The angle α_{b} is clockwise from vector N to vector $\vec{k}$,
(iv) The angle δ is counter-clockwise from vector $\vec{y}$ to vector $-\vec{k}$,
(v) The angle β_0 is clockwise from vector N to vector $\vec{y}$,
(vi) The angle β is clockwise from vector N to normal $\vec{n}$,
(vii) The angle Δβ is counter-clockwise from vector $\vec{y}$ to normal $\vec{n}$.

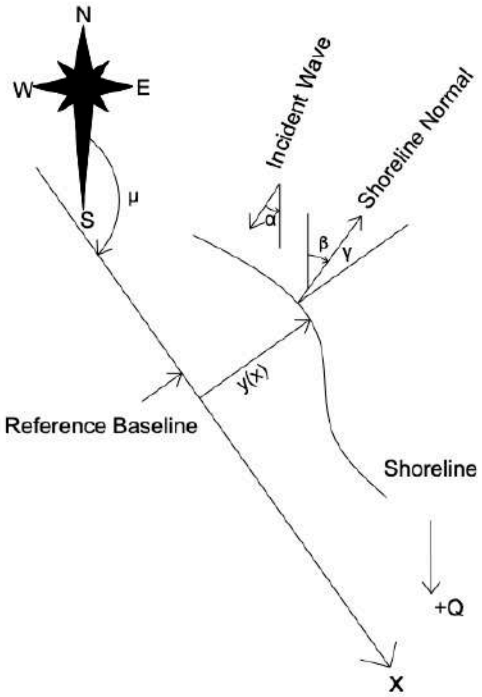

Figure 3.12. Definition sketch for the one-line model utilizing compass directions.

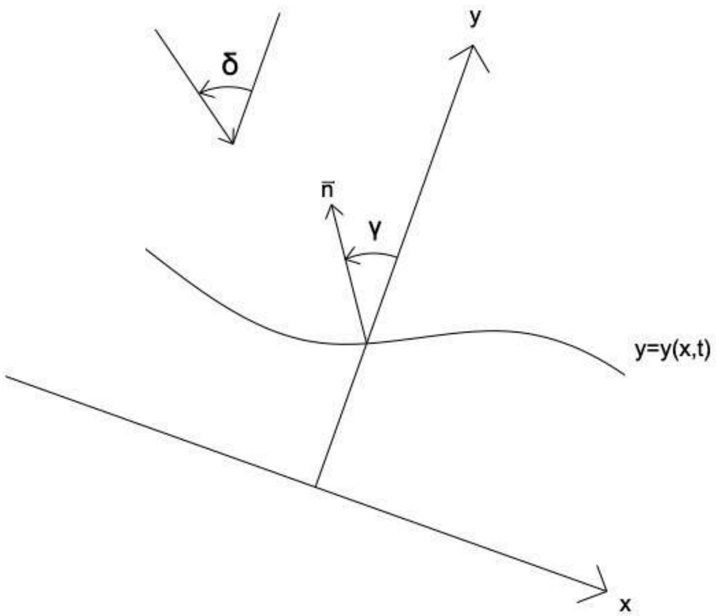

Figure 3.13. Coordinate diagram for the one-line model.

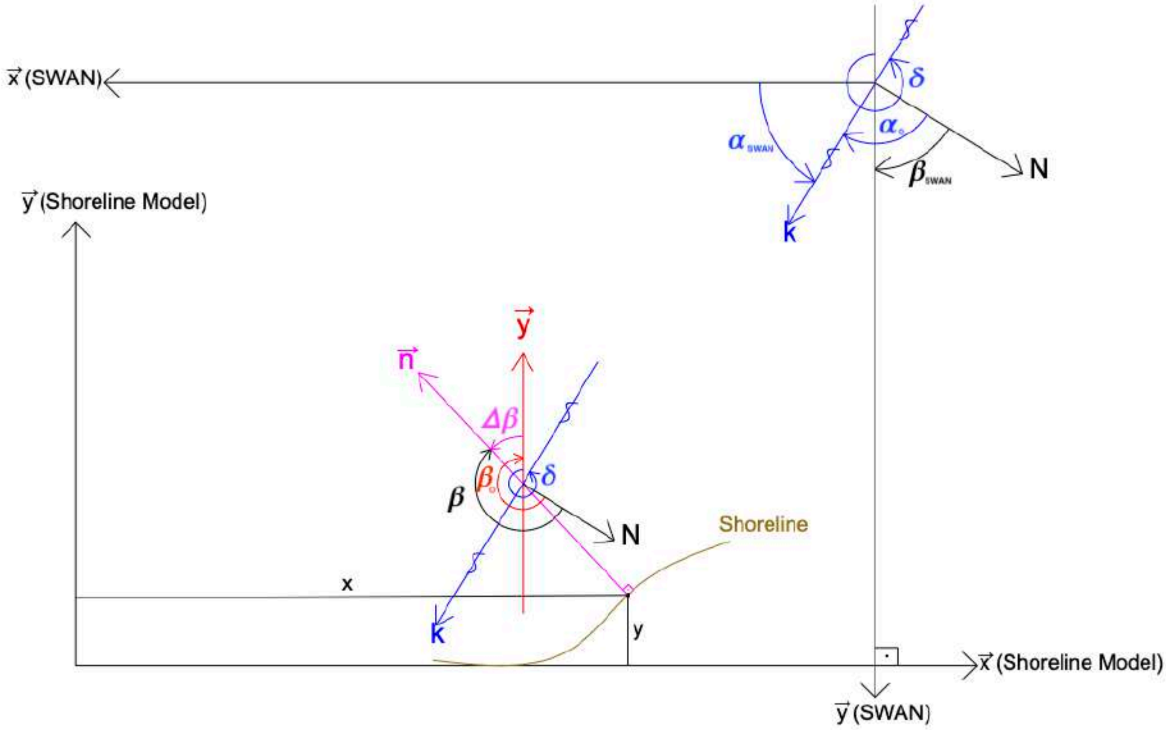

Figure 3.14. Coordinate convention used for the shoreline model.

α_{SWAN} is the wave angle in SWAN convention and δ is the wave angle in Matlab convention. β_{SWAN} is a fixed angle and β_{SWAN}=38°, this angle is the determined after the model area is selected. To simplify the calculations of SWAN, contour grids of the area are given after rotating 38°. Two necessary angles to equate the rest of the angles are β_{SWAN}, which is a constant angle and α_{SWAN} that is computed by SWAN.

4. RESULTS

4.1. Analyzed Bathymetric Data

The data collected from boat survey, leveling profiles, GPS measurements of the shoreline and the beach are combined to use for the bathymetry map. PDS2000 software is used for bathymetric mapping of the project area. Before the bathymetric data is used, the data is corrected with the sound velocity measured with the CTD device for boat survey and water level measurements are also added to calculation. Interpolation is done from the start of the beach at +2m to 20m depth, using point coordinates of XYZ. Trajectory of the boat survey is shown in Figure 4.1 and topographic survey and its analyzed results are shown in Figure 4.4.

Figure 4.1. Boat survey trajectory.

With the data collected from field surveys the coastal geometry and topography is developed. By using the boat survey and the survey data collected, a bathymetric map of the area is created. The bathymetric map shows that the area where the beach is subject to harsh wave climate has steeper slope whereas the area protected by the headland by wave diffraction has milder slope as seen in Figure

PDS2000 also interpolates and computes the profiles starting at each priory fixed benchmark point to end of domain. The profiles generated by PDS are exported to AutoCAD and compared with the GPS profiles and levelling profiles which are given in Figure 4.2 and Figure 4.3 for nourishment sections K4 and K9 respectively.

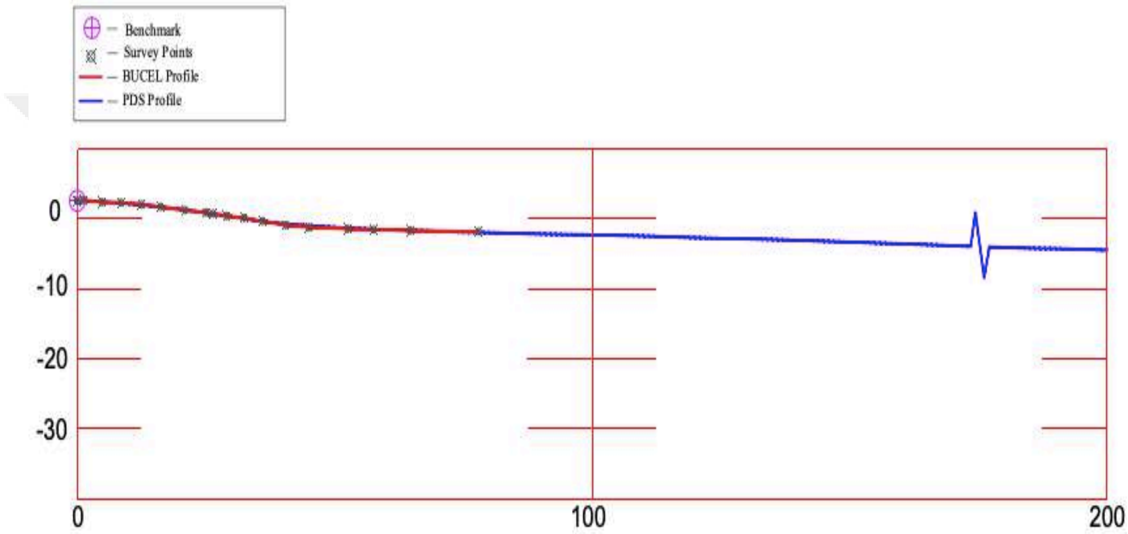

Figure 4.2. Measured and compiled beach profile of K4.

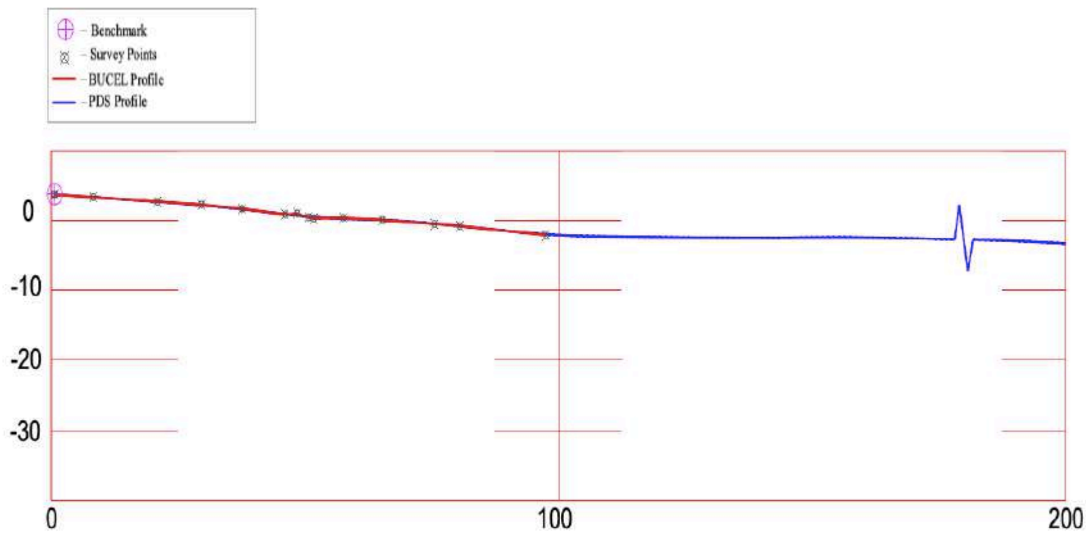

Figure 4.3. Measured and compiled beach profile of K9.

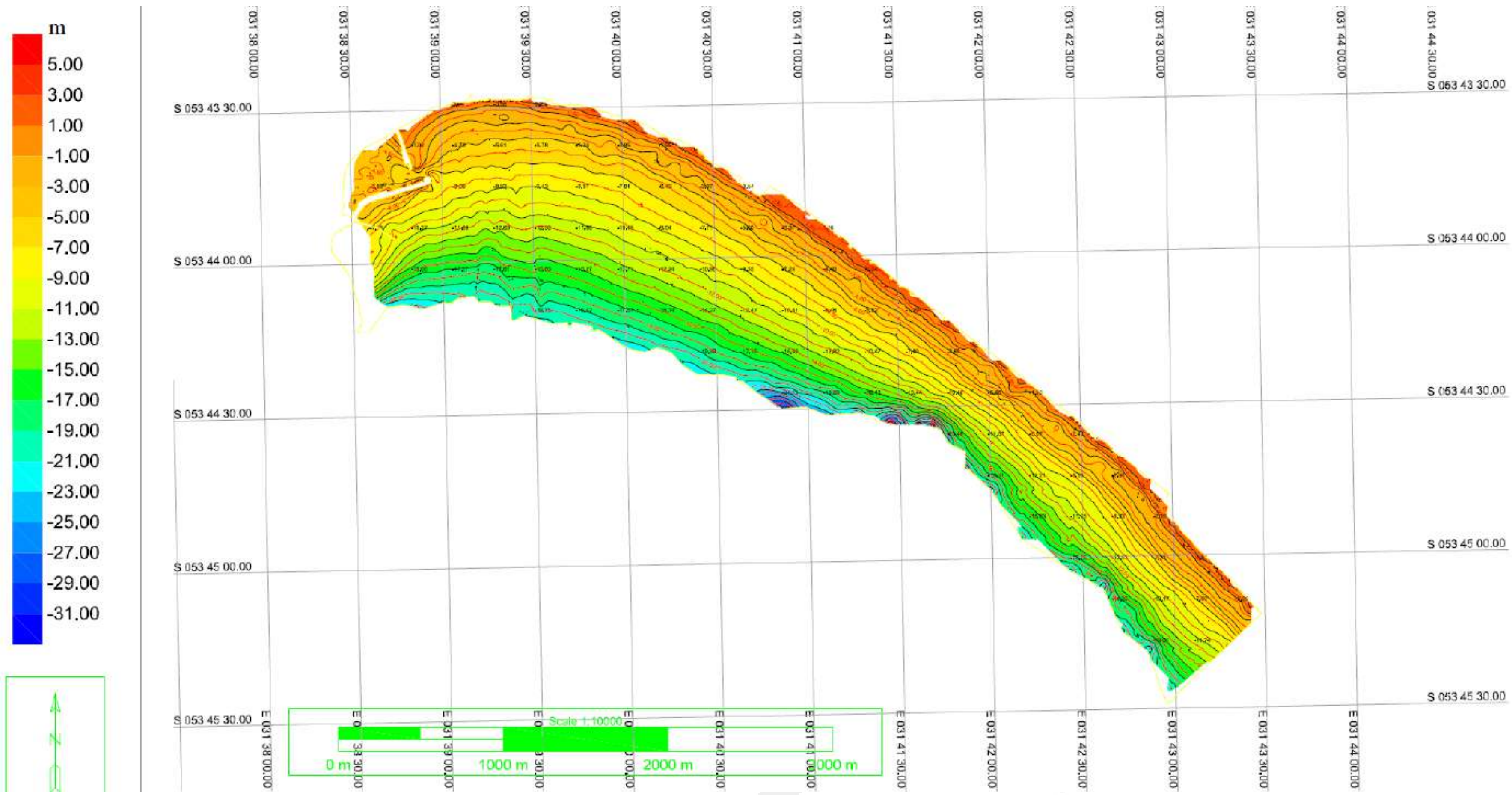

Figure 4.4. Bathymetric map compiled from PDS2000.

The large rocky part of the shoreline is marked to further elaborate the TUDKA-99 shoreline and to mark as a no flow boundary for the sediment transport model. Alanya Municipality provided drone footages of the beach on still water and Google Earth images are also used. The rocks are marked on the AutoCAD shoreline and then used for detailing. The rock map created by using the drone shots is shown in Figure 4.5 and the model shoreline is tuned using the rock map for more accuracy. The rocks exposed from beach erosion are highly visible with these footages as shown in Figure 4.6. In some areas these rocks are exploded to make space for touristic activities such as beach expansion and water sports.

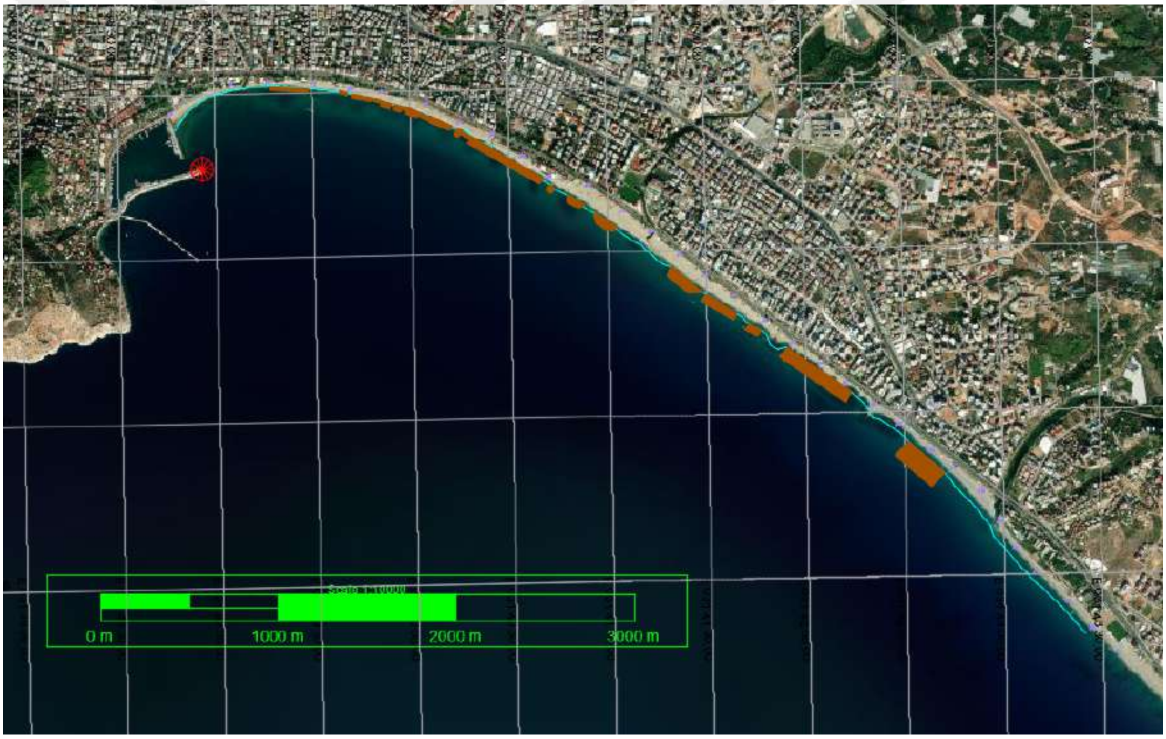

Figure 4.5. Rock map drawn using drone footages.

These artificially broken or exploded rocks not only increases the amount of fill sediment to cover the area for a beach fill, it also aggravates the erosion of the remaining beach between the broken rocks creating cusps along the shoreline. In a larger project, these gaps between the rocks can be filled with other rocks or small concrete blocks where human height allows, so that these rocks can be utilized as underwater breakwaters.

Figure 4.6. Image of exposed beach rocks from air.

4.2. Winds and Waves Analyses Results

Long term average of hourly wind speed is 3.3 m/s and the maximum value recorded is 20.3 m/s as shown in Table 4.1. The wind rose summarizes the wind analysis with colors as wind speeds at 10m height and occurrence probability as radial distance from the center. Dominant wind direction is from Northeast (NE) and secondary wind direction is from Southwest (SW) which is in accordance with Turkey's dominant wind orientation. Winds with most speed come from Southwest (SW) direction as shown in in Figure 4.7.

The analysis indicates that the dominant wave direction is from Southwest (SW), secondary wave direction is from West-Southwest (WSW) as given in Figure 4.8. Significant wave height (H_s) and mean wave period (T_{m02}) are 0.54m and 4.0 cm respectively. Wave recorded at the greatest storm has a significant height of 6.26m, direction of 215 ^{o}N (SW) and a period of 8.7 seconds as shown in Table 4.2. Wind and wave roses have different distributions as expected because of the location of the beach as shown in Figure 4.9 and Figure 4.10, the wind and wave roses are shown on the point where their data is collected from.

Table 4.1. Long term offshore wind statistics (Data from DHI).

Primary/Secondary Wind Directions	Average Wind Speed	Maximum Wind Speed	Data timeline
Northeast/Southwest	3.3 m/s	20.3 m/s	1993-2021

Table 4.2. Long term offshore wave statistics (Data from Copernicus).

Dominant Wave Direction	Average Significant Deep-Water Wave Height	Average Wave Period	Maximum Significant Wave Height	Maximum Wave Angle and Direction	Maximum Wave Period
215 °N (SW)	0.54 m	4.0 s	6.26 m	215 °N (SW)	8.7 s

Since beach erosion is highly sensitive to wave climate and especially wave direction, these data are carefully procured and analyzed. The results of the analyses are used in the wave models. Yearly extreme values with 1.37% possibility to exceed the 29-year hourly average wind speed and significant wave height are calculated to be used for the design of the shore structures. These are the winds and waves which only exceed 12 hours a year. The extreme wave height is the approximate wave height of the greatest storm of the year. After the extreme wave height (H_e) is calculated, extreme wave period corresponding to this wave is calculated from the wave with the extreme wave height. Extreme wave and wind values from different directions are shown in Table 4.3. Average wave period (T_{m02}) is the average value of the hourly recorded wave spectrum and the wave peak period (T_p) is the wave period of highest energy within the wave spectrum, for this reason, there is a difference of 50% between the two period values. In the following sections, these two wave period values will be used in a variety of analyses.

Table 4.3. Extreme conditions calculated for wind and wave with probability of exceedance of 1.37%.

Incoming Direction	H_s (m)	T_{m02} (s)	T_p (s)	Wind Speed (m/s)
We	1.21	5.0	8.5	7.9
WSWe	1.95	6.9	9.9	7.3
SWe	3.39	7.6	9.9	8.8
SSWe	3.65	7.7	10.2	13.1
Se	2.14	5.9	8.7	12.6
SSDe	1.69	4.8	7.5	14.5

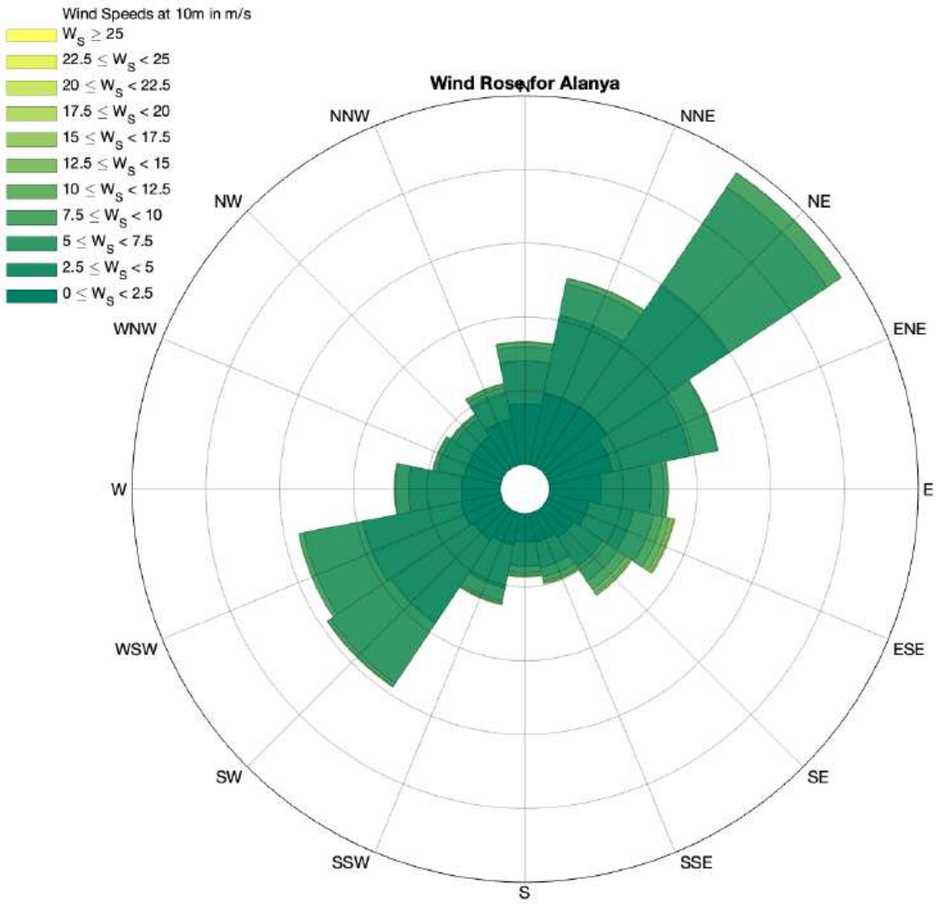

Figure 4.7. Wind rose of the Alanya bay.

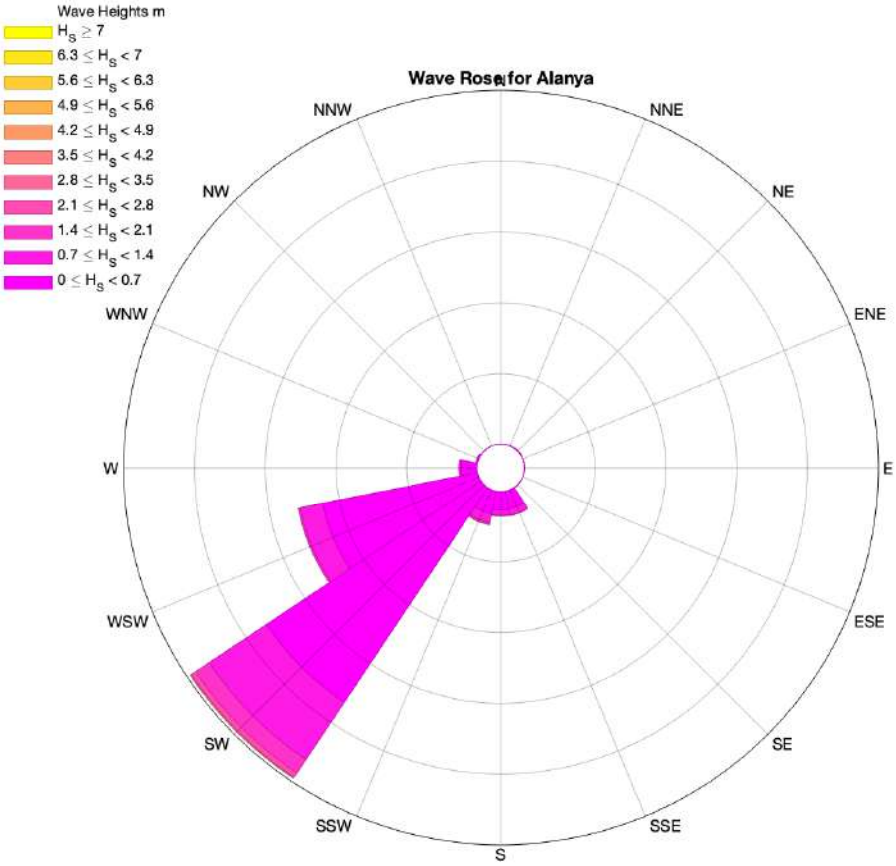

Figure 4.8. Wave rose for Alanya bay.

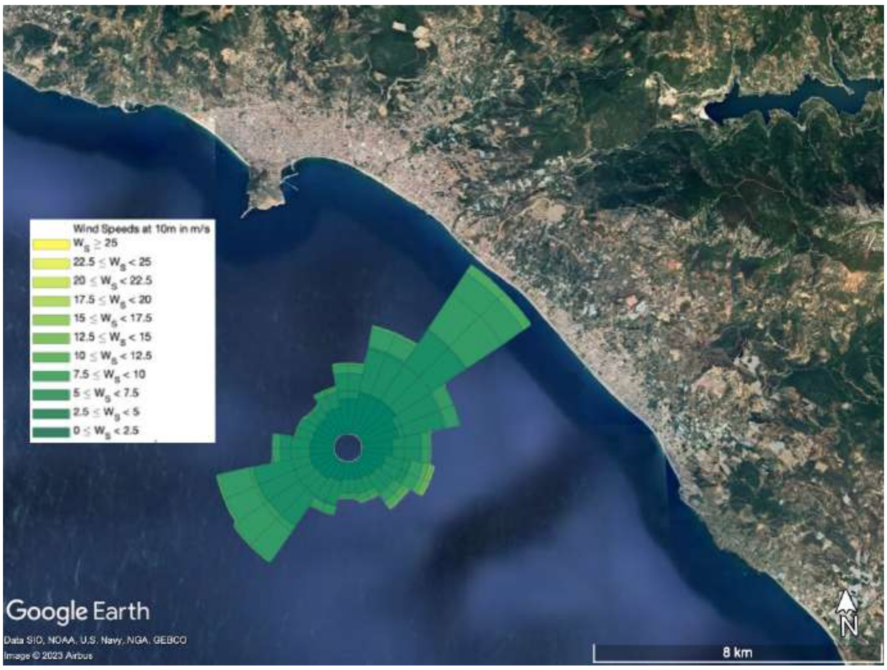

Figure 4.9. Wind rose of Alanya shown on map.

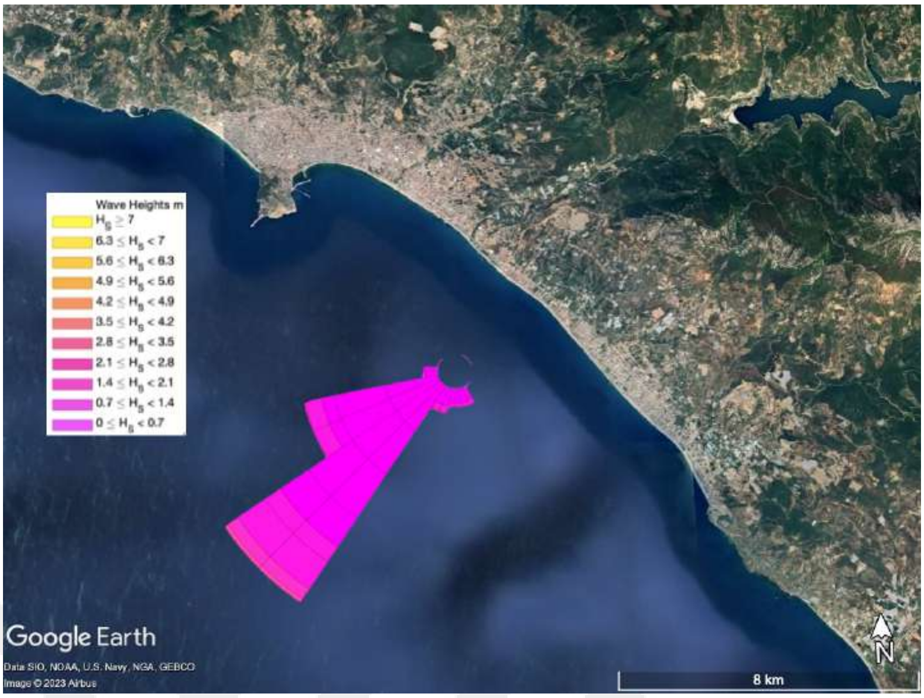

Figure 4.10. Wave rose of Alanya shown on map.

4.2.1. Wave Model

By using the wave model, offshore waves and winds are translated to shoreline. The wave model is run for 20 different scenarios as shown in Table 4.4, significant wave height (H_s), mean wave period (T_{m02}), peak wave period (T_p), mean wave direction (θ_m), wave breaking ratio (Q_b) and wave setup (η_s) are calculated in the model grid. The wave breaking line is shown in Figure 4.11, wave height and directions are shown in Figure 4.12 as vectors. In the shoreline and profile models, the extreme scenario of dominant wave direction of Southwest is used, since the beach is subjected to these waves most of the year and the most damage to beach nourishment can happen from this direction’s extreme conditions.

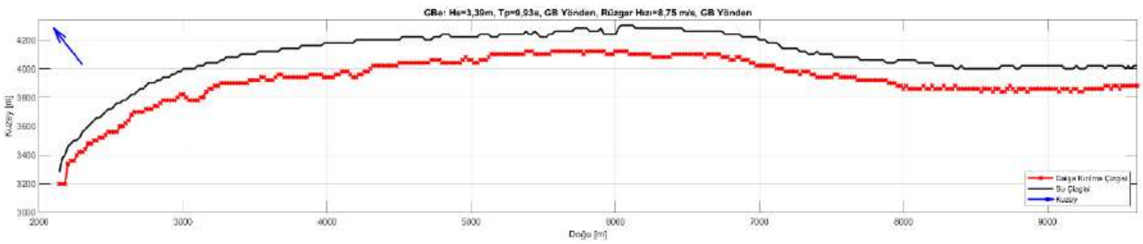

Figure 4.11. Shoreline and wave breaking line (SWe).

Table 4.4. Wind and wave scenarios grouped according to directions.

		1	2	3	4	5	e
Direction	Parameter		Scenario Average Value				
W	Probability	3%	-	-	-	-	0.14%
	Hs (m)	0.42	-	-	-	-	1.21
	Tm02 (s)	3.45	-	-	-	-	5.04
	Tp (s)	5.63	-	-	-	-	8.46
	Wind Speed (m/s)	2.89	-	-	-	-	7.92
WSW	Probability	10%	10%	10%	-	-	0.14%
	Hs (m)	0.22	0.39	0.73	-	-	1.95
	Tm02 (s)	3.06	3.72	4.77	-	-	6.87
	Tp (s)	5.01	5.7	7.06	-	-	9.9
	Wind Speed (m/s)	2	3.75	5.31	-	-	7.32
SW	Probability	11%	11%	11%	11%	11%	0.14%
	Hs (m)	0.22	0.35	0.47	0.66	1.34	3.39
	Tm02 (s)	3.06	3.48	3.89	4.51	5.8	7.6
	Tp (s)	4.88	5.26	5.79	6.44	7.77	9.93
	Wind Speed (m/s)	1.69	3.14	4.06	4.81	5.88	8.75
SSW	Probability	3%	3%	-	-	-	0.14%
	Hs (m)	0.26	0.92	-	-	-	3.65
	Tm02 (s)	3.11	4.58	-	-	-	7.7
	Tp (s)	5.42	6.86	-	-	-	10.18
	Wind Speed (m/s)	1.9	4.65	-	-	-	13.1
S	Probability	2%	2%	-	-	-	0.14%
	Hs (m)	0.24	0.7	-	-	-	2.14
	Tm02 (s)	2.93	3.88	-	-	-	5.9
	Tp (s)	4.76	6.06	-	-	-	8.75
	Wind Speed (m/s)	1.66	4.53				12.64
SSE	Probability	3%	-	-	-	-	0.14%
	Hs (m)	0.52	-	-	-	-	1.69
	Tm02 (s)	3.56	-	-	-	-	4.84
	Tp (s)	5.8	-	-	-	-	7.52
	Wind Speed (m/s)	3.24	-	-	-	-	14.53

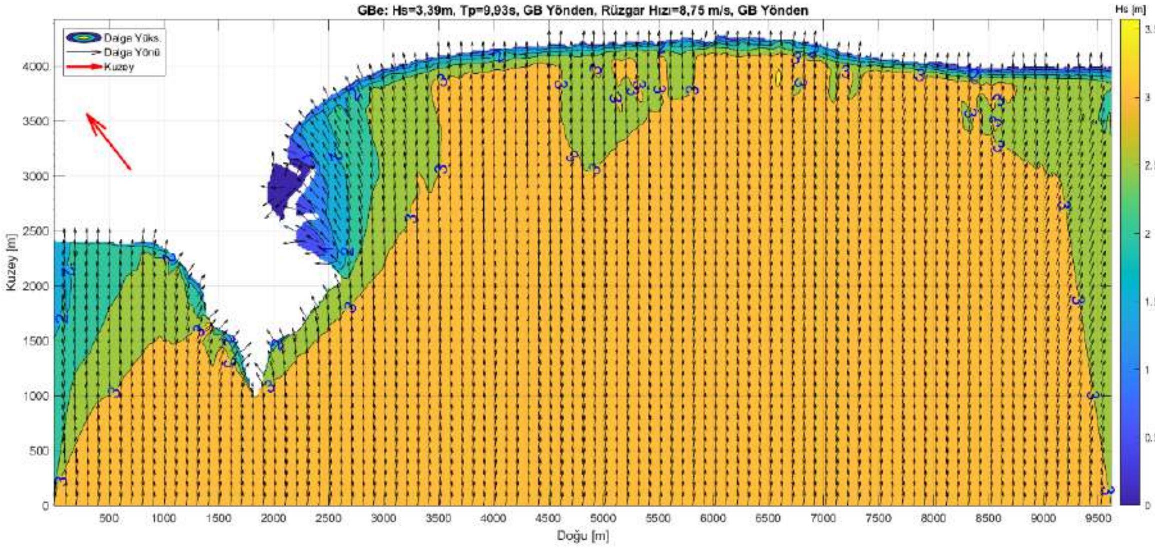

Figure 4.12. Wave model result for significant wave height for SWe.

4.3. Transport Mechanisms of Longshore Currents

As told in the previous chapters, the hypothesis suggests that there are three main drivers to the shoreline change in Alanya: primary transport, secondary transport and river discharges. The longshore transport induced by the breaking of oblique waves is the primary transport in this region. The dominant wave direction in Alanya is from Southwest and although the angle between the shoreline and the waves are small most of the year, even small obliquity creates a long short transport along the shore. The longshore transport is calculated using the transport equation where the main drivers are significant weight height and the angle between the incident waves and the shoreline.

By the natural characteristics of the crenulate bays, the headland of the western side of the bay provides a shelter. The headland and the port create a shadow zone where the waves are subject to diffraction and the wave heights are decreased significantly in this zone. In Figure 4.13, the waves approaching shore and diffraction from the headland can be seen clearly. The difference in the wave height between the shadow zone and the shoreline open to the waves create a secondary longshore transport due to wave set up gradient.

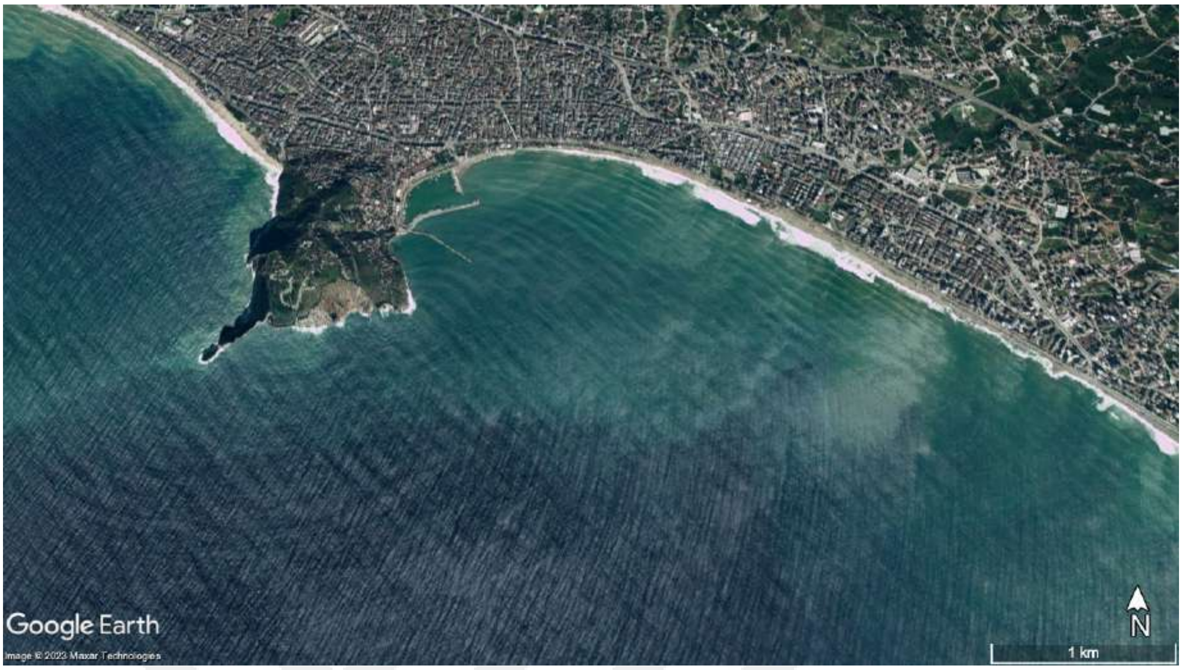

Figure 4.13. Diffraction patterns seen on project site (Google Earth Historic Image).

The rivers act as a third driver to the erosion problem, although the rivers bring sediments to the bay, it is observed during the measurements and it can also be seen in the satellite images that the rivers have irregular discharges, not only in different seasons but they can even vary daily. Significantly, the Dim River has a dam and its discharge can be controlled by the dam. Sudden increase of the river discharge might create strong stream currents in all direction at the river mouth that can transport fine sediments offshore. It is seen in both the bathymetric map that the bottom slope near the Dim River is the steepest in the area which is associated with larger sediment particles. Moreover, the sediment analyses show that the mean sediment diameter near the Dim River is significantly larger than the rest of the bay.

From calculation of the longshore transport vectors using transport equation and wave setup gradient shown in Figure 4.15a and 4.15b, longshore currents are sketched In Figure 4.16. The primary longshore vectors that are induced by breaking of oblique waves are shown closer to the breaker line since the lateral mixing causes these currents to occur in a position farther from the shoreline and for the secondary longshore currents that are induced by wave setup gradients, they occur closer to the shoreline as wave setup increases significantly as waves approach the shore, so the transport is closer to shoreline than of primary transport. The position the longshore currents occur is directly related to the ratio of the eddy viscosity to bottom friction, so as this ratio decreases, the longshore currents take place closer to the breaker line.

By combining the transport Equation 4.1 and continuity Equation 4.2, we get the shoreline change rate in two terms in Equation 4.3. The magnitude is not important since this value will be changing along the shoreline and in time. But the ratio between these terms is a more stationary measure of transport mechanisms, therefore a measure of relative importance of primary vs secondary transport. Figure 4.14 shows the ratio between the primary and secondary transport and it is clear that the dominant transport driver in the bay is the longshore transport induced by oblique waves.

The primary and secondary transport rates from the continuity and transport equation can be derived from Dean and Yoo (1992).

The transport equation is,

$$Q_x = \frac{KH_b^{5/2}\sqrt{g/\kappa}}{8(s-1)(1-p)} \sin\alpha_b \cos\alpha_b \tag{4.1}$$

and can be simplified as,

$$Q_x = G(h_* + B)\sin\alpha_b \cos\alpha_b \tag{4.2}$$

where, G is the longshore diffusivity and is,

$$G = \frac{KH_b^{5/2}\sqrt{g/\kappa}}{8(s-1)(1-p)(h_* + B)}. \tag{4.3}$$

Rewriting Equation (4.1) as a function of a new constant G_0 excluding parameters that may vary in the longshore direction including H_b, h_* and B,

$$G = G_0 \frac{H_b^{5/2}}{(h_* + B)}. \tag{4.4}$$

We can derive a new transport equation in the longshore direction as the following,

$$Q_x = G_0\, H_b^{5/2}\ \sin\alpha_b \cos\alpha_b \tag{4.5}$$

where,

$$G_0 = \frac{K\sqrt{g/\kappa}}{8(s-1)(1-p)}. \tag{4.6}$$

The second governing equation is derived from the conservation of the sediment mass,

$$\frac{\partial y}{\partial t} + \frac{1}{h_* + B}\frac{\partial Q_x}{\partial x} = 0\,. \tag{4.7}$$

To find the longshore gradient of the longshore sediment transport rate, take the derivative of Equation (4.5) with respect to x,

$$\frac{\partial Q_x}{\partial x} = G_0\left(H_b^{\frac{5}{2}}\cos 2\alpha_b\frac{\partial \alpha_b}{\partial x} + \sin 2\alpha_b\frac{5}{4}H_b^{\frac{3}{2}}\frac{\partial H_b}{\partial x}\right). \tag{4.8}$$

Now inserting Equation (4.8) into Equation (4.7), we obtain the rate of shoreline change as,

$$\frac{\partial y}{\partial t} = -\frac{G_0}{h_* + B}\left(H_b^{\frac{5}{2}}\cos 2\alpha_b\frac{\partial \alpha_b}{\partial x} + \sin 2\alpha_b\frac{5}{4}H_b^{\frac{3}{2}}\frac{\partial H_b}{\partial x}\right). \tag{4.9}$$

Now we can write the shoreline change rates as a summation of two terms V_1 and V_2, which are due to primary and secondary transports, respectively,

$$\frac{\partial y}{\partial t} = V_1 + V_2 \tag{4.10}$$

where,

$$V_1 = -\frac{G_0}{h_* + B}H_b^{\frac{5}{2}}\cos 2\alpha_b\frac{\partial \alpha_b}{\partial x}\,, \tag{4.11}$$

$$V_2 = -\frac{G_0}{h_* + B}\sin 2\alpha_b\frac{5}{4}H_b^{\frac{3}{2}}\frac{\partial H_b}{\partial x}\,. \tag{4.12}$$

4.4. Sediment Characteristics and Water Quality Analysis

Sediment samples collected are analyzed in laboratory and their grading curves, median particle diameter and percent fine rates are computed. It is concluded that the median particle diameter D_{50} is 2.92mm and the average fine particle percent of the samples that are collected in the nearshore area is 2.28%. The analysis shows that the zone protected from the waves by the headland has significantly smaller sand particles and the area that is subjected to higher wave heights has larger sediment sizes which is consistent with the bathymetric map since milder slopes are associated with smaller sand size and steep slopes are associated with larger particle sizes. Greatest percent of fine particles in the samples are collected from deeper water. Most probably the fine sediments accumulate where the sea bed is not affected by the waves, in this case deeper than 6m. a summary of the particle size and percent fine rates are shown in Figure 4.18 and Table 4.6.

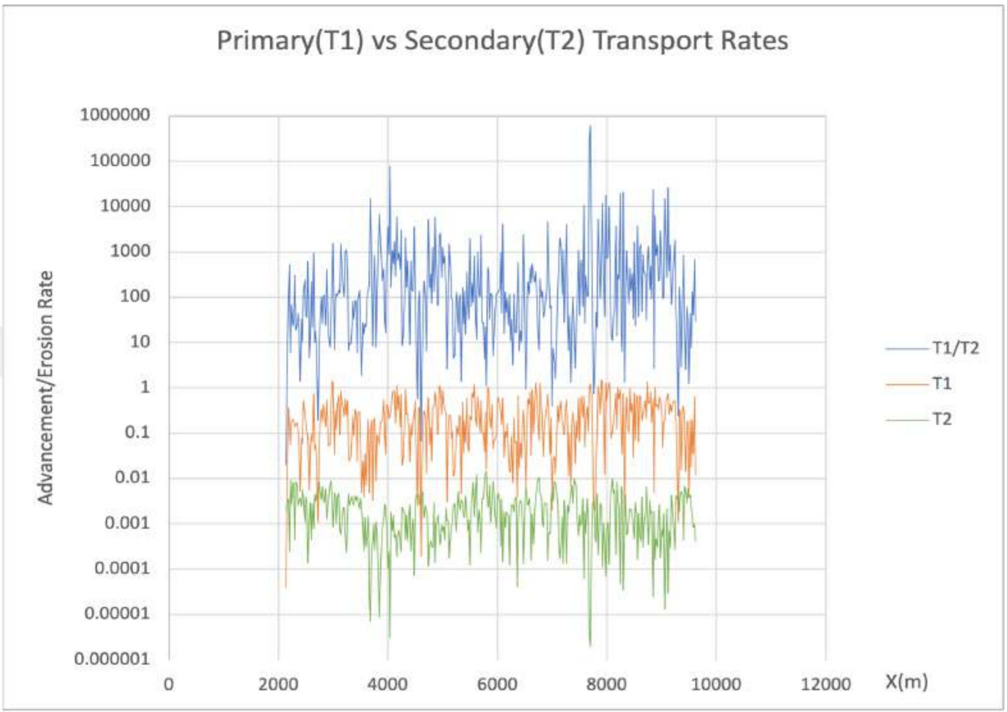

Figure 4.14. Primary and secondary transport rates.

Sediment samples outside the study area are also collected by divers for the analyses of possible barrow materials. However, the D_{50} and percent fine rates of these samples were not suitable for a project in Alanya. Detailed information about the possible borrow material samples are in Appendix A, market as Diver Sample. So, for the fill material a medium sand sample sand from the quarry is examined and found adequate for the project. Discussion on sediment analysis are listed below:

(i) The largest D50 is at the shoreline.
(ii) Sediment size decreases from 0 contour to seaward side.
(iii) The rivers on the project area bring sediments to the bay.
(iv) Largest river-Dim River- creates longshore currents to both sides, since there are large sediments in both S20 and S31 sections at -2m depth with D_{50}'s ranging from 0.18mm to 48.49mm.
(v) Smallest sediment particles with D_{50}=0.15mm accumulate inside the jetty.

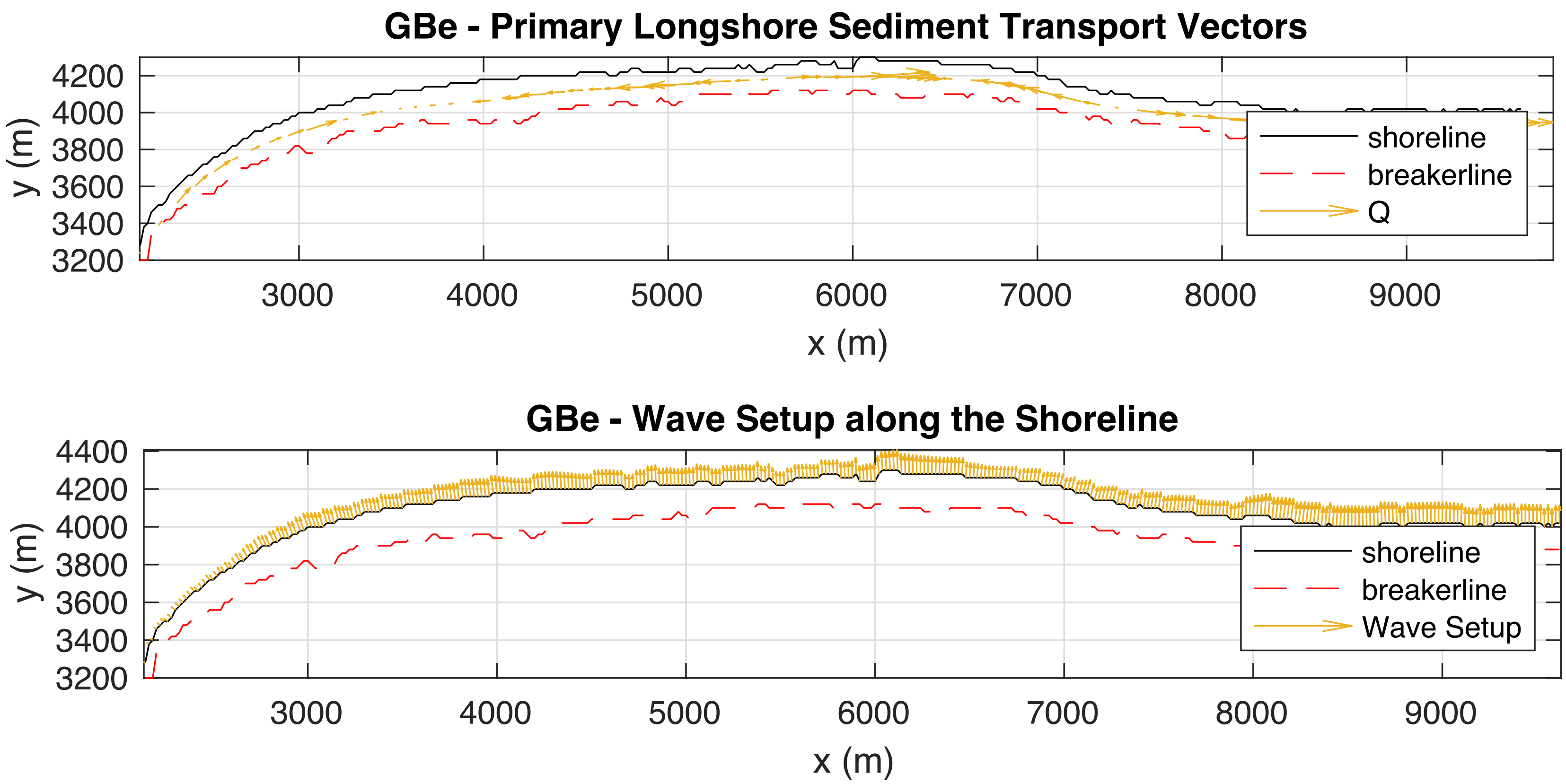

Figure 4.15. Longshore transport vectors(a), wave setup(b) (SWe).

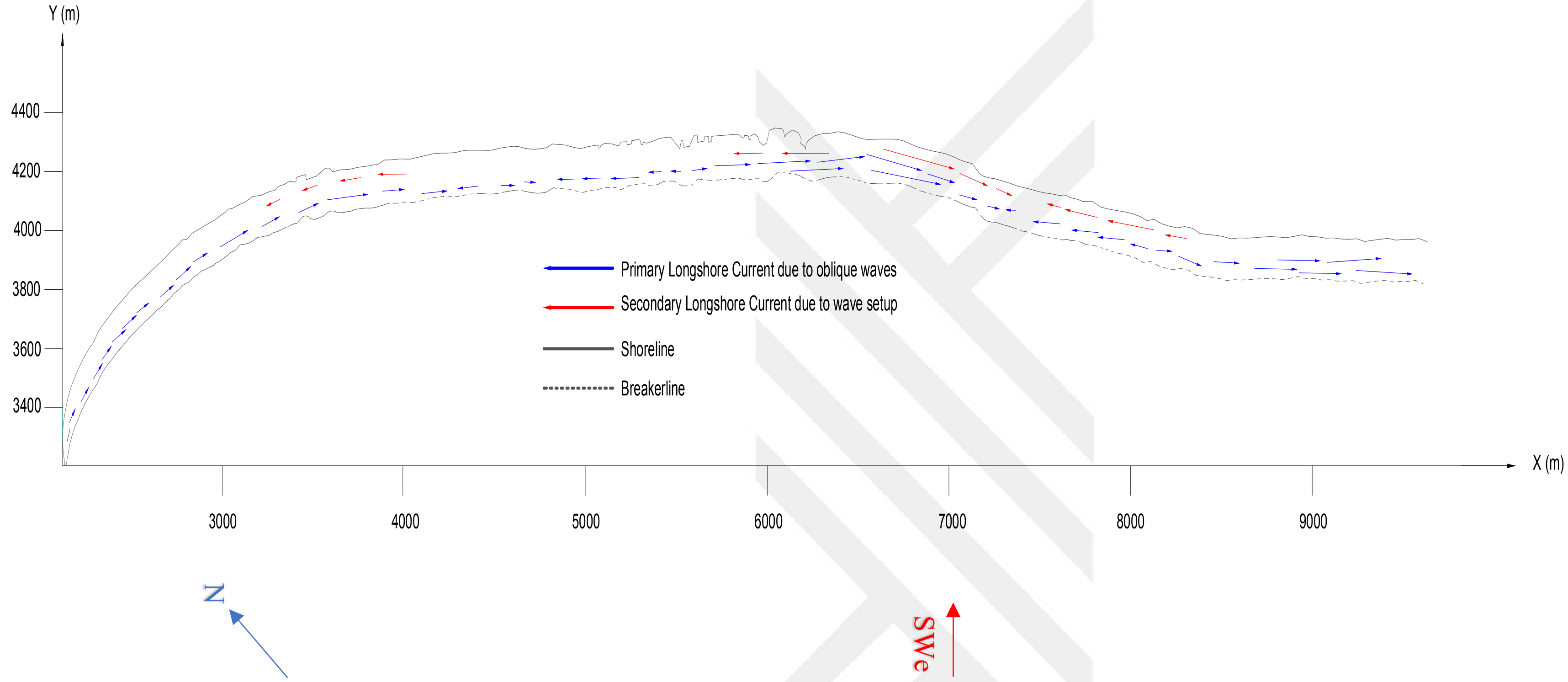

Figure 4.16. Primary and secondary transport vector along the surf zone.

CTD measurements are normally done to measure water quality but in this thesis water quality is not necessary for their direct use but they are indirectly used to determine the effects of river discharges on the longshore sediment transport. The results of the CTD analyses for the measurements taken near the river mouths show that that small rivers which are Hacet River, Gümüş River and Oba River has minor effects on longshore currents. However, the Dim River has a slight effect on the water column of the first 2m depth on the day of the measurements. The minimum and maximum values of CTD measurements are given in Table 4.5 and an example of the measurements over depth are shown in Figure 4.17.

Table 4.5. Minimum and maximum values of CTD measurements.

	Minimum Value	Maximum Value
Salinity (PSu)	36.87	39.33
Temperature (°C)	23.00	30.00
Density (kg/m^3)	1025.06	1027.16
Sound Velocity (m/s)	1532.22	1548.50

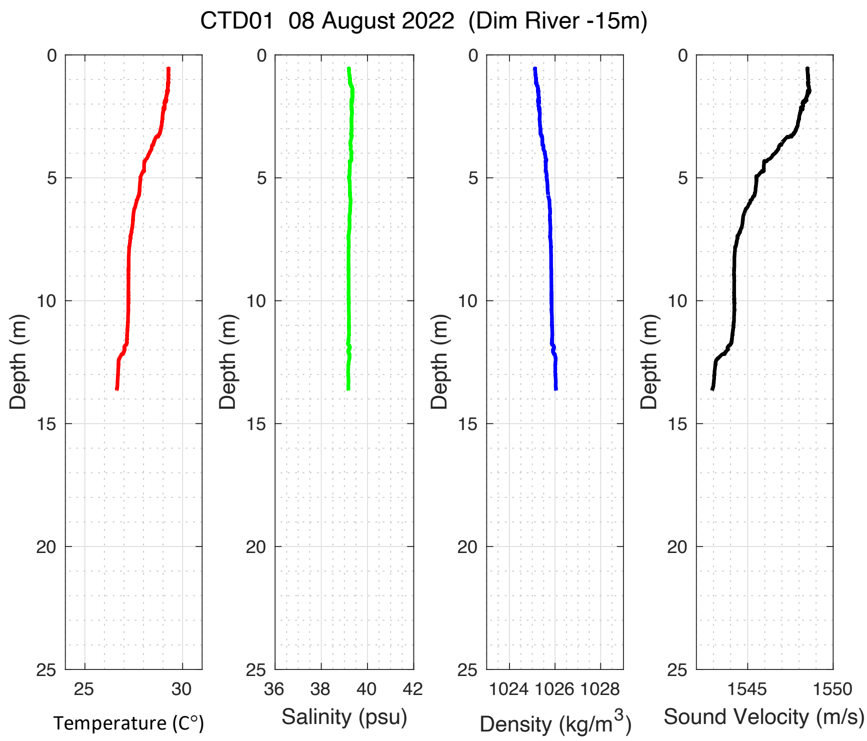

Figure 4.17. CTD measurement near Dim River.

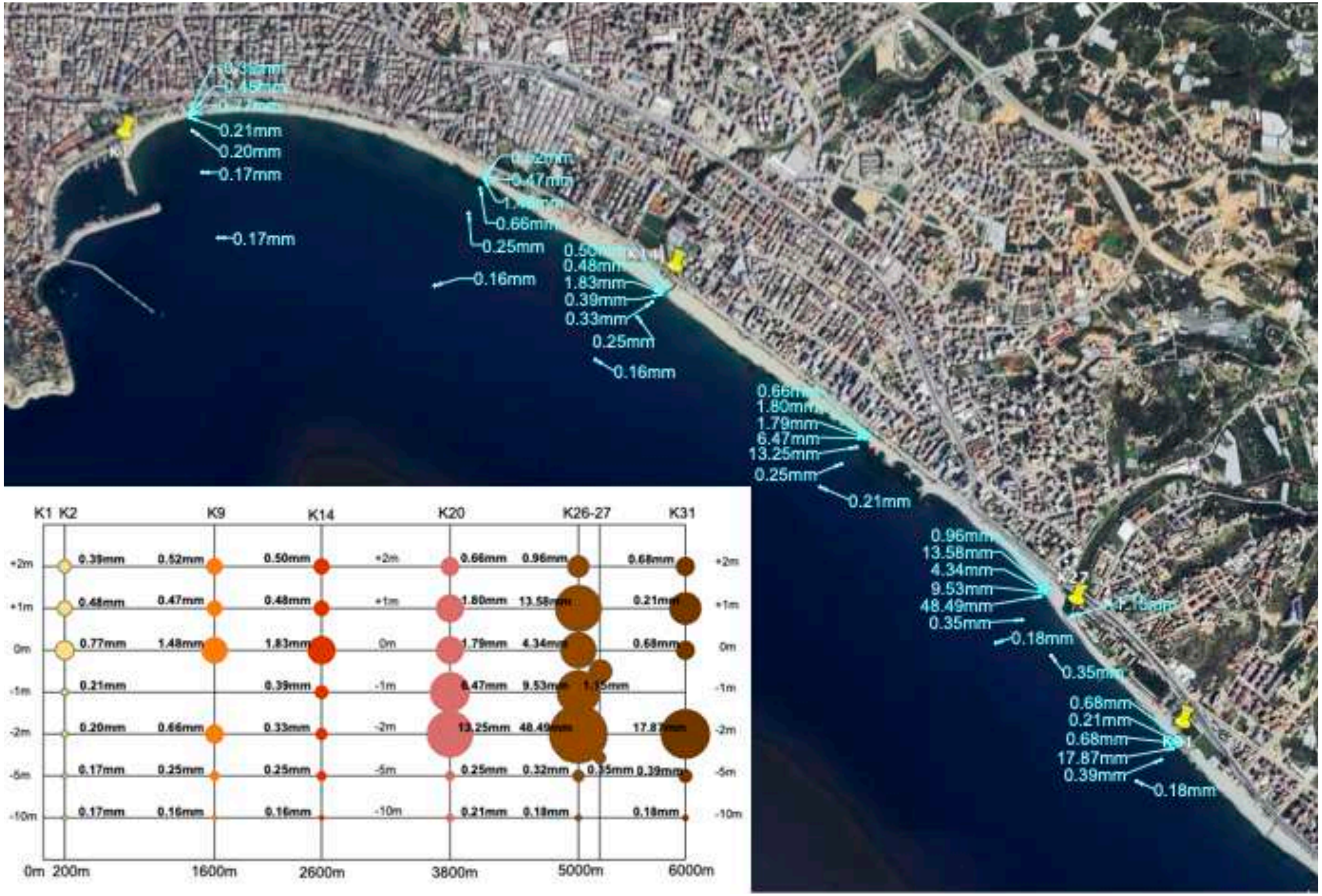

Figure 4.18. Results of the sediment analysis showed on map.

Table 4.6. Sediment sizes and types of collected samples.

Sample No.	Description	Depth	Sediment Type	D50	F%
N1	K02+2m	+2m	Medium Sand	0.39	0.41%
N2	K02+1m	+1m	Medium Sand	0.48	0.59%
N3	K02-0m	0m	Coarse Sand	0.77	0.00%
N4	K02-1m	-1m	Fine Sand	0.21	0.63%
N5	K02-2m	-2m	Fine Sand	0.20	0.69%
N6	K02-5m	-5m	Fine Sand	0.17	4.64%
N7	K02-5m(HR)	-5m	Fine Sand	0.16	6.06%
N8	K02-10m	-10m	Fine Sand	0.17	28.51%
N9	K09+2m	+2m	Sand+Pebble	0.52	0.95%
N10	K09+1m	+1m	Sand+Pebble	0.47	0.11%
N11	K09-0m	0m	Fine Pebble	1.48	0.00%
N12	K09-2m	-2m	Coarse Sand	0.66	0.00%
N13	K09-5m	-5m	Fine Sand	0.25	0.56%
N14	K09-5m(GR)	-5m	Fine Sand	0.26	0.98%
N15	K09-10m	-10m	Fine Sand	0.16	15.76%
N16	K14+2m	+2m	Medium Sand	0.50	0.38%
N17	K14+1m	+1m	Medium Sand	0.48	0.04%
N18	K14-0m	0m	Coarse Sand+Pebble	1.83	0.00%
N19	K14-1m	-1m	Medium Sand	0.39	0.18%
N20	K14-2m	-2m	Medium Sand	0.33	0.00%
N21	K14-5m	-5m	Medium Sand	0.20	2.90%
N22	K14-5m(Oba)	-5m	Medium Sand	0.31	1.60%
N23	K14-10m	-10m	Fine Sand	0.16	5.65%

Table 4.6. Sediment sizes and types of collected samples. (cont.)

N24	K20+2m	+2m	Medium Sand	0.66	0.33%
N25	K20+1m	+1m	Fine Pebble	1.80	0.00%
N26	K20B-0m	0m	Fine Pebble	1.79	0.00%
N27	K20-1m	-1m	Pebble	6.47	0.00%
N28	K20B-2m	-2m	Pebble	13.25	0.10%
N29	K20-5m	-5m	Fine Sand	0.25	0.73%
N30	K20-10m	-10m	Fine Sand	0.21	13.24%
N31	K26+2m	+2m	Coarse Sand	0.96	0.12%
N32	K26+1m	+1m	Pebble	13.58	0.00%
N33	K26-0m	0m	Pebble	4.34	0.00%
N34	K26-1m	-1m	Coarse Pebble	9.53	0.05%
N35	K26-2m	-2m	Coarse Pebble+Rock	48.49	0.00%
N36	K26-5m	-5m	Fine Sand	0.30	1.33%
N37	K26-5m(Dim)	-5m	Fine Sand	0.35	0.85%
N38	K26-10m	-10m	Fine Sand	0.18	8.41%
N39	Dim-0.5m	-0.5m	Coarse Sand+Pebble	1.15	0.04%
N40	Dim-3.5m	-3.5m	Sand	0.35	0.23%
N41	K31+2m	+2m	Coarse Sand	0.68	0.09%
N42	K31+1m	+1m	Pebble	0.21	0.00%
N43	K31-0m	0m	Coarse Sand	0.68	0.00%
N44	K31-2m	-2m	Pebble	17.87	0.03%
N45	K31-5m	-5m	Sand	0.39	0.21%
N46	K31-10m	-10m	Sand	0.18	8.29%

4.5. Beach Nourishment and Profile Evolution

One of the most important parameters for the beach nourishment is the profile scale factor A and it is a function of energy dissipation and the factor is unitless. The sediment size of the beach indirectly affects this factor. For the native beach sand, the area between sections K4 and K9 has an average particle size of 0.87mm which corresponds to an A of 0.2. The fill material chosen adequate from the quarry has median particle size of 2.47mm which corresponds to an A=0.29 as shown in Table 4.7. Since the equilibrium profile that will form will affect the fill sediments, the scale parameter of the fill material is used for the calculation of the EBP. The profile scale factor is taken according to adapted graph of Dean (1987).

Beach nourishment design for this thesis is done according to the profile evolution of the nourished beach as shown in Figure 4.19. For the profile evolution, the EBP theory of Dean's (1977) profile formula is used. The net shoreline advancement is designed as 20m from the shoreline. The $Ay^{3/2}$ profile is started from 20m offshore of the shoreline normal, then a berm height of 1m is continued with a slope of 1:2 which is the angle of repose of the fill material, so the equilibrium profile of the nourished profile is developed. The initial nourishment profile is constructed upon this EBP as shown in Figure 4.22. The areas A are equal as EBP suggests. The evolution of the beach profiles after construction are given in Figures 4.23a and 4.23b for section K4 and K9 respectively.

Table 4.7. Sediment parameters for nourishment.

	Native Material	Fill Material
D50	0.87mm	2.47mm
A	0.20	0.29

For the volume calculation of the nourishment, average areas of the nourished profiles of section K4 and K9 is multiplied by the nourishment length of 1000m. The area of nourished profile of K4 and K9 are $68m^2$ and $78m^2$ respectively as shown in. So, the average volume of the nourishment is calculated as $73000m^3$. With the cost of fill material and construction costs combined as $25 per $1m^3$ of sand, the total cost of the fill is $1.825.000, which is within the budget of Municipality of Alanya of $2M.

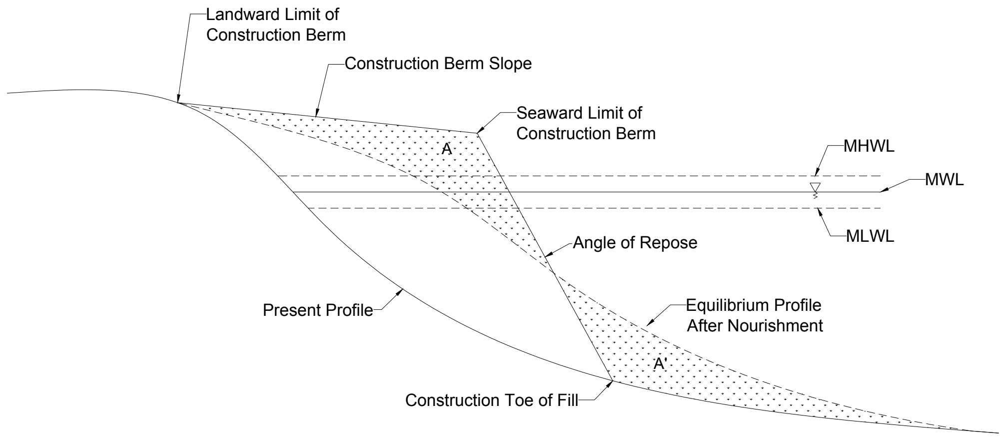

Figure 4.19. Beach nourishment terminology.

The planform design of the 1 km long beach nourishment is shown in Figure 4.24. For the analyses of planform evolution, Hsu and Evans (1989) spiral equation is used. The comparison of the measured shoreline with the one created with the coefficients can be seen in Figure 4.20. The spiral equation used is

$$R = R_0\left(C_0 + C_1\left(\frac{\beta}{\theta}\right) + C_2\left(\frac{\beta}{\theta}\right)^2\right), \tag{4.13}$$

where R_0 is the control line, drawn from the diffraction point to beach end. Constants C_0, C_1 and C_2 are empirical constants. β is the angle between the wave crest and R_0, and θ is the angle increment.

The point applications of the rivers with each of their yearly sediment capacities are computed and added to the equilibrium shoreline as well as the nourished profile shown in Figure 4.21. Six different time steps were shown other than the initial condition: 3 months, 6 months, 1 year, 2 years, 5 years and 10 years. Since the spiral shape does not fit perfectly to the real shoreline, the same analytical models of the rivers and the nourishment is also demonstrated on the measured shoreline given in Figures 4.25 and 4.26. In the first three months, the nourishment loses nearly 90% of its initial width with a maximum advancement of 1.6m after 3 months of construction.

The reason of the rapid recession of the nourished profile is due to the scale of the nourishment. It is known for small scale nourishments in the open sea are less feasible to larger scale ones. To demonstrate it better, analytical model for the same time steps of a rectangular beach nourishment is shown in Figure 4.28. and 4.29. Figure 4.28 shows the current nourishment of 1000m’s and Figure 4.29 shows the nourishment of 10000m’s. The last Figure 4.30 is each time step shown on planform for the larger scale nourishment project.

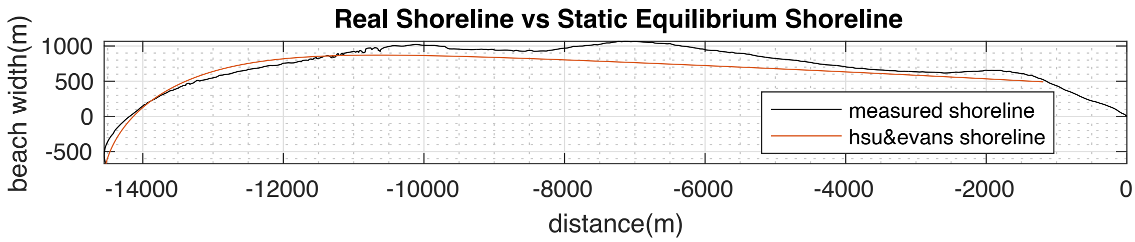

Figure 4.20. Measured shoreline compared with Hsu&Evans spiral bay.

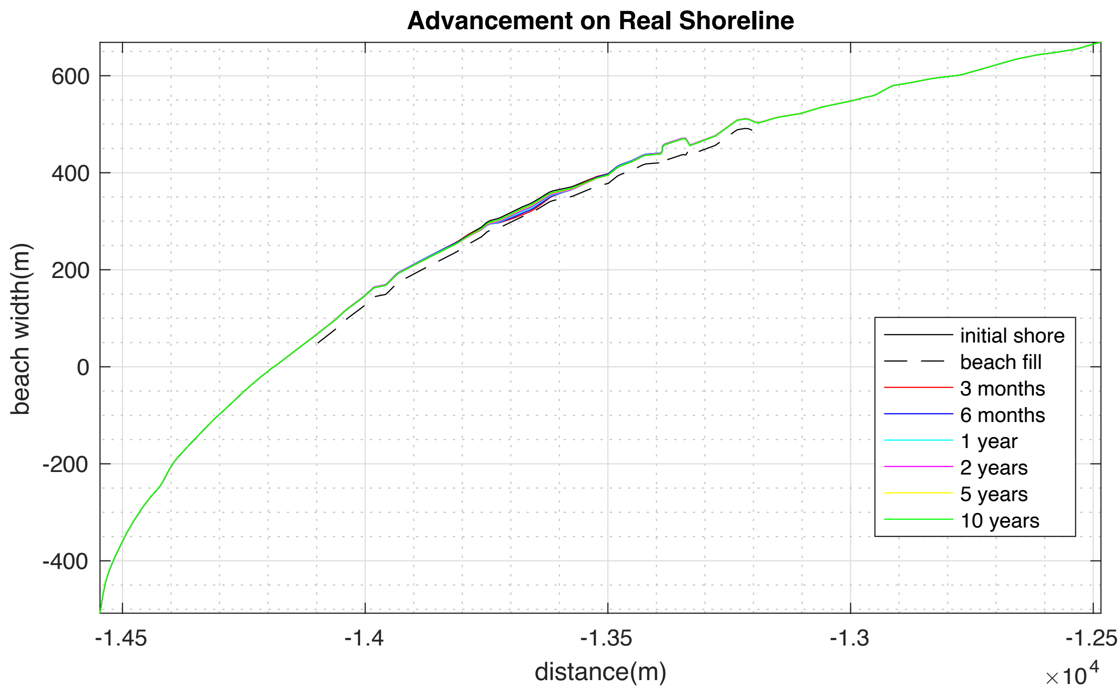

Figure 4.21. Beach nourishment evolution with river effects on measured shoreline.

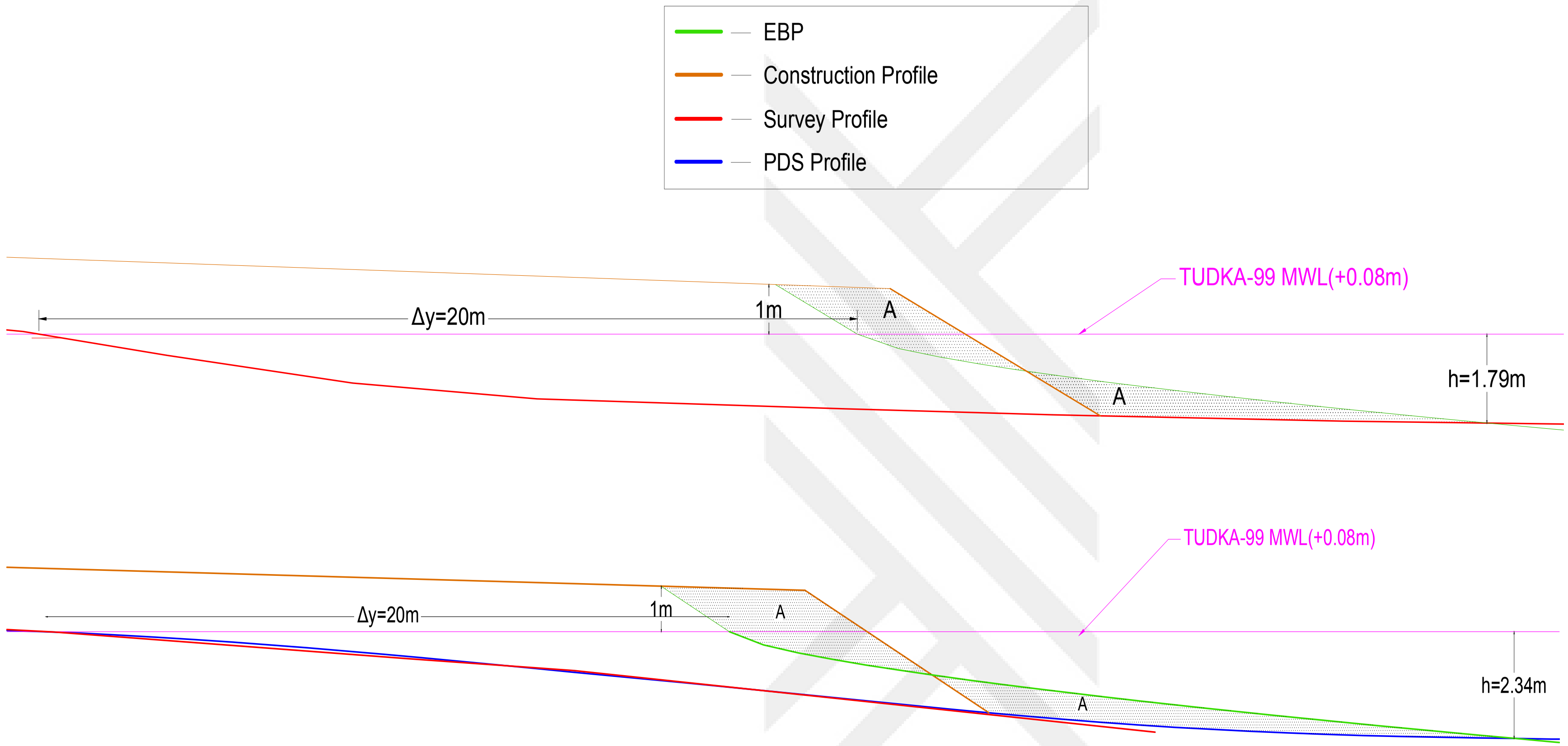

Figure 4.22. EBP and design of the construction profiles for section K4(a), and K9(b).

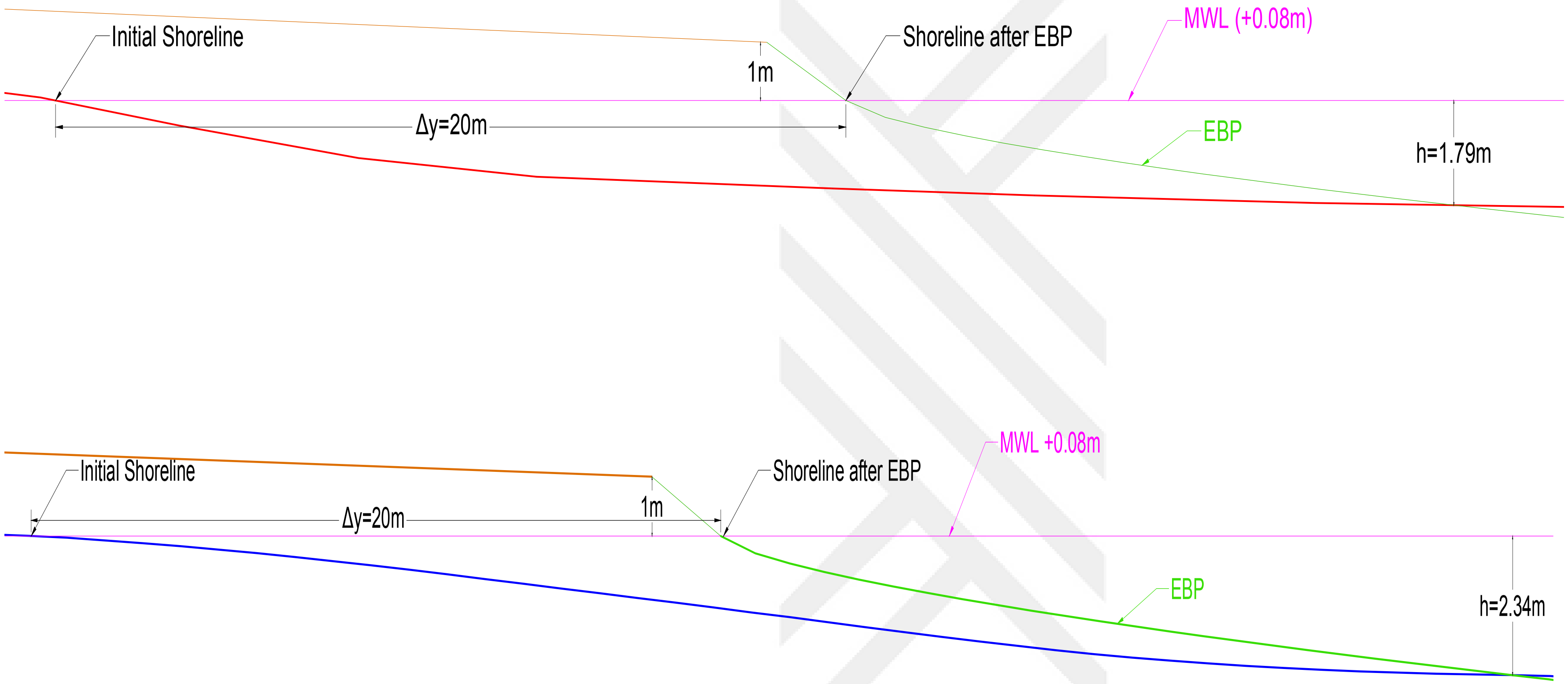

Figure 4.23. Equilibrium beach profiles of (a) section K4, (b) section K9.

Figure 4.24. Nourishment design between section K4 and K9 shown on map.

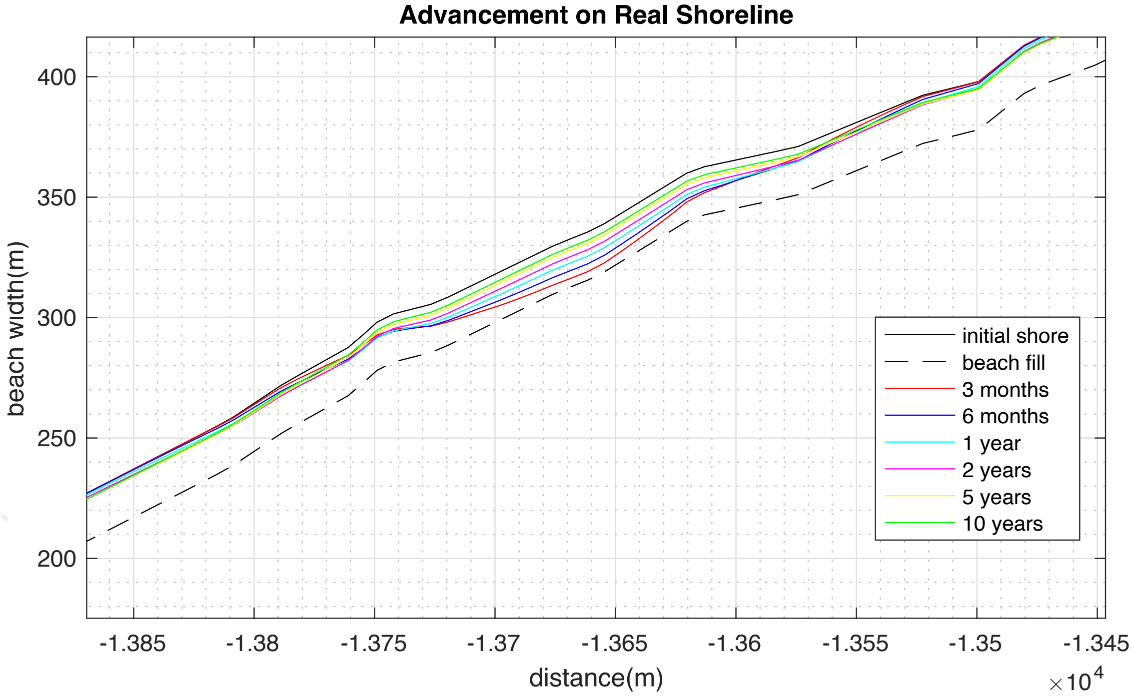

Figure 4.25. Beach nourihment advancedment on closer look at real shoreline.

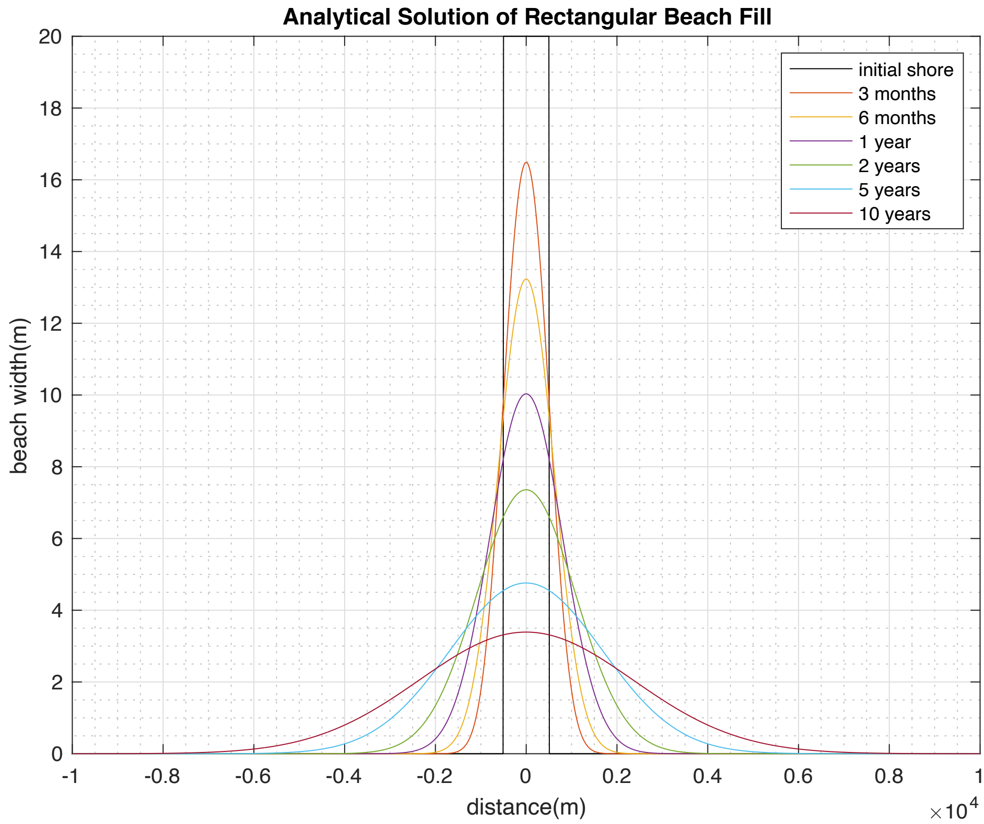

Figure 4.26. Analytical model of a rectangular beach fill of 1000m’s.

5. CONCLUSION AND RECOMMENDATIONS

The erosion problem in Alanya is examined, and the mechanisms behind it are explored, leading to the design of a suitable beach nourishment strategy. Although protective structures with hard materials can offer some protection, their primary goal is to safeguard upland areas, often at the expense of the natural balance of the beach. The concept of beach nourishment is introduced as a means of maintaining beach integrity while preserving its natural attributes for social, economic, and recreational purposes. The study's area, methodology, and measurements are detailed, including field surveys, wave analysis, and modeling techniques.

It is considered that there are three drivers to shoreline change in the case of Alanya; the longshore transport due to breaking waves, longshore transport due to wave setup and river discharge change in the area. After the analyses are done, it shows that as hypothesis suggested, the primary that is the most effective shoreline change factor is from breaking of the oblique waves. So, the wave setup induced transport is the secondary driver. As for the rivers, the effect of rivers is similar to each others' in terms of yearly sediment discharge. Gümüş River has the least effect on the shoreline change of the bay since it has negligible discharge. The construction of the Dim Dam on the river significantly reduced the sediment discharge and after the observation of the unsteady river discharge through different periods of year, an erosive effect of the river might be taken into consideration.

An initial beach nourishment proposal of 1 km length was done suitable for the wave climate and natural characteristics of the beach after the evaluation of field survey and sediment analyses. The fill material is decided to be borrowed from a quarry with a mean sediment diameter of 2.47mm. The beach fill is designed to have a net shoreline advancement of 20m immediately after cross-shore evolution take place and is reached its equilibrium beach profile. With these specifications, the beach nourishment is within the budget of Municipality of Alanya.

The planform evolution of the bay with consideration of the rivers and the beach nourishment is modeled using analytical solutions of the shoreline shapes in Alanya. The river data is used as an instantaneous point source. Because of the instability of the discharges, continuous discharge is not considered to be suitable. The analytical models were tested for 3 months, 6 months, 1 years, 2 years, 5 years and 10 years, considering the lifetime of the nourishment as approximately 10 years.

The rectangular beach fill displayed a more rapid recession of the nourished shoreline compared to other nourishment projects done in the past, the half-life of the project is between 1 to 2 years. This is due to the relationship of the beach nourishment length with its lifetime. From the analytical formula of the rectangular beach fill, the time needed for the nourished shore to reach its half width is proportional to the nourishment length, so greater scope of beach fill projects has higher change of success.

The nourishment project is not the only option to mitigate the erosion problem in Alanya. It is observed that the beach area is highly controlled by the tourism facilities. Practices like gathering sand at the end of summer season to upland to protect it from storms and relaying again are done in some parts. Not only this aggravates the erosion problem since the natural characteristic of the shore is changed by human hands, it is also costly and time consuming. Breaking of the rocks to provide sandy beach also alters the natural harmony of the beach and it might also aggravate the erosion problem.

The rivers supply sediments to bay and are an important factor on the shoreline change. The monitoring of the river basins, discharges and sediment capacity of the rivers should be done better to eliminate the possibility of rivers acting as erosion drivers. Especially with the Dim river, the discharge released from the dam should be stabilized to prevent river discharge becoming an erosion factor and most importantly ensure safety of the humans swimming near the river mouth area.

Concluding, a beach nourishment project in Alanya is feasible both economically and in engineering aspect. But due to the complex mechanisms of the bay, monitoring must be improved and practices that change the balance of the beach should be avoided.

REFERENCES

Aksel, M. and M. Dikici, 2019, *Alanya Keykubat Plajı Kıyı Erozyonun İncelenmesi Projesi Raporu*, Alanya Alaaddin Keykubat Üniversitesi İnşaat Mühendisliği Bölümü, Antalya.

Coastal Engineering Manual, 2002, U.S. Army Corps of Engineers, Washington, D.C. Accessed on April 23, 2023.

Dean, R.G., 1987, "Coastal Sediment Processes: Toward Engineering Solutions", in *Proceedings of Coastal Sediments '87*, New Orleans, Louisiana, Vol. 1, pp. 1–24.

Dean, R.G. and R.A. Dalrymple, 2004, *Coastal Processes with Engineering Applications*, Cambridge University Press, Cambridge.

Dean, R.G. and C.H. Yoo, 1992, "Beach Nourishment Performance Predictions", *Journal of Waterway, Port, Coastal, Ocean Engineering*, Vol. 118, No. 6, pp. 567-587.

Ergin, A., I. Güler, A. Yalciner, C. Baykal, S. Artagan and I. Şafak, 2006, "A One-Line Numerical Model for Wind Wave Induced Shoreline Changes", *7th International Congress on Advances in Civil Engineering*, Istanbul.

Evans, C. and J.R.C. Hsu, 1989, "Parabolic Bay Shapes and Applications", *Proceedings of the Instution of Civil Engineers,* London, Vol. 87, No. 4, pp. 557-570.

González, M. and R. Medina, 2001, "On the Application of Static Equilibrium Bay Formulations to Natural and Man-Made Beaches", *Coastal Engineering*, Vol. 43, No. 3-4, pp. 209-225.

Hanson, H. and M. Larson, 1987, "Comparison of Analytic and Numerical Solutions of the One-Line Model of Shoreline Change", *Proceedings of Coastal Sediments '87*, New Orleans, Louisiana, pp. 500–514.

Hanson, H. and N.C. Kraus, 1989, "GENESIS - Generalized Model for Simulating Shoreline Change, Vol. 1", Reference Manual and Users Guide, *Technical Report,* CERC-89-19, U.S. Army Corps of Engineers, Coastal Engineering Research Center, Waterway Experiment Station, Vicksburg, MS.

Hsu J.R.C. and R. Silvester, 1996, "Stabilizing Beaches Downcoast of Harbor Extensions", *Proceedings of Coastal Engineering 25*, Orlando, Florida, pp. 3986-3999.

Hsu, J.R.C., R. Silvester and Y.M. Xia, 1989, "Generalities on Static Equilibrium Bays", *Coastal Engineering*, Vol.12, No. 4, pp. 353- 369.

Hurst, M. D., A. Barkwith, M. A.Ellis, C. W.Thomas and A. B.Murray, 2015, "Exploring the Sensitivities of Crenulate Bay Shorelines to Wave Climates Using a New Vector-Based One-Line Model", *Journal of Geophysical Research: Earth Surface*, Vol. 120, No. 12, pp. 2586– 2608.

Komar, P. and D. Inman, 1970, "Longshore Sand Transport on Beaches", *Journal of Geophysical Research,* Vol. 75, No. 30, pp. 5914-5927.

Larson, M., H. Hanson and N.C. Kraus, 1997, "Analytical Solutions of One-Line Model for Shoreline Change near Coastal Structures", *Journal of Waterway, Port, Coastal, and Ocean Engineering*, Vol. 123, No. 4, pp.180-191.

Le Blond, P.H., 1972, "On the Formation of Spiral Beaches", *Proceedings of the 13th International Conference on Coastal Engineering*, Vancouver, B.C., Vol. 2, pp. 1331-1345.

Le Blond, P.H., 1979. "An Explanation of the Logarithmic Spiral Plan Shape of Headland Bay Beaches", *Journal of Sediment Research.*, Vol. 49, No. 4, pp. 1093-1100.

Le Mahaute, B. and M. Soldate, 1978, "Mathematical Modeling of Shoreline Evolution", Miscellaneous Report No. 77-10, U.S. Army Corps of Engineers, Coastal Engineering Research Center.

Longuet-Higgins, M.S., 1970, "Longshore Currents Generated by Obliquely Incident Sea Waves", *Journal of Geophysical Research*, Vol.75, No. 33, pp. 6778-6801.

Otay, E.N., 1994, *Long-Term Evolution of Nearshore Disposal Berms*, Ph.D. Thesis, University of Florida.

Otay, E.N., M. Aslan, O. Sevim, İ. Bilgün and O. Akagündüz, 2022, *Alanya Belediyesi, Alanya Sahili Erozyon Problemi: Analiz ve Modelleme Faz-2 Ara Rapor*.

Ozasa, H. and A.H. Brampton, 1980, "Mathematical Modelling of Beaches Backed by Seawalls", *Coastal Engineering*, Vol. 4, pp. 47-63.

Pelnard-Considere, R., 1956, "Essai de Théorie de L'evolution des Formes de Rivage en Plages de Sable et de Galets", *Journes de l'Hydraulique*, Vol. 4, No. 1, pp. 289-298.

Perlin, M. and R.G. Dean, 1983, "A Numerical Model to Simulate Sediment Transport in the Vicinity of Coastal Structures", Miscellaneous Report, No. 83-10, U.S. Army Corps of Engineers, Coastal Engineering Research Center.

Rasmeemasmuang, T. and S. Weesakul, 2009, "One-Line Model Using the Combination of Polar and Cartesian Coordinates for Crenulate Shaped Bay", *Proceedings of Coastal Dynamics 2009*, Tokyo, Japan, pp. 1-14.

Silvester, R. and S. Ko, 1972, "Use of Crenulate Shaped Bays to Stabilize Coasts", *Proceedings of 13th Conference of Coastal Engineering,* Vancouver, Canada, Vol.2, pp. 1347-1365.

SWAN Cycle III Version 40.72 User Manual, 2008, SWAN Team, Delft University of Technology, Netherlands. Accessed on December 2, 2022.

Tao,H.C., T.W. Hsu and C.M. Fan, 2022, "Developments of Dynamic Shoreline Planform of Crenulate-Shaped Bay by a Novel Evolution Formulation", *Water,* Vol.14, No.21, p. 3504.

Weesakul, S., T. Rasmeemasmuang, S. Tasaduak and C. Thaicharoen, 2010, “Numerical Modeling of Crenulate Bay Shapes”, *Coastal Engineering*, Vol. 57, No. 2, pp. 184-193.

Wind, H.G., 1994, “An Analytical Model of Crenulate Shaped Beaches”, *Coastal Engineering*, Vol. 23, No. 3–4, pp. 243-253.

Work, P.A. and R.G. Dean, 1995, “Assessment and Prediction of Beach-Nourishment Evolution”, *Journal of Waterway, Port, Coastal, and Ocean Engineering,* Vol. 121, No. 3, pp. 182-189.

Yu, A., 2004, “Discrete Element Method—An Effective Method for Particle Scale Research of Particulate Matter”, *Engineering Computations,* Vol. 21, No. 2-3-4, pp. 205-214.

APPENDIX A: SUMMARY OF SIEVE ANALYSIS FOR SEDIMENT CHARACTERISTICS

The sieve analysis summary of every sample taken in the site is shown below.

Table A. 1. Summary of sieve analysis for sediment characteristics.

Sample No.	Description	Depth	Type of Sand	X	Y	D50 (mm)	%F
S01	Diver sample	-11m	Fine Sand	418590.2	4039791.9	0.20	3.1%
S02	Diver sample	-16m	Fine Sand	418214.9	4039904.5	0.18	3.4%
S03	Diver sample	-15m	Fine Sand	418529.2	4039500.2	0.21	8.0%
S04	Diver sample	-20.5m	Fine Sand	412705.3	4044677.2	0.16	8.2%
S05	Diver sample	-20m	Fine Sand	409164.3	4045529.5	0.24	9.5%
S06	Diver sample	-15.8m	Fine Sand	409003.3	4045836.4	0.24	3.4%
S07	Diver sample	-15m	Fine Sand	409024.2	4045836.2	0.20	3.5%
S08	Diver sample	-18m	Fine Sand	409006.8	4046021.4	0.65	2.3%
S09	Diver sample	-16m	Fine Sand	408033.0	4046810.5	0.41	1.7%
S10	Diver sample	-20m	Fine Sand	407244.9	4047212.9	0.18	7.1%
S11	Diver sample	-20m	Fine Sand	408195.4	4046499.8	0.19	2.5%
S12	Diver sample	-14m	Fine Sand	408202.4	4046592.2	0.20	3.4%
S13	Diver sample	-11m	Fine Sand	408406.0	4046793.5	0.34	1.7%
S14	Diver sample	-20m	Fine Sand	408786.3	4045918.3	0.20	4.9%
S15	Diver sample	-15m	Fine Sand	408808.9	4045942.1	0.49	3.3%
S16	Diver sample	-10m	Fine Sand	408971.2	4046166.5	0.56	1.6%
S17	Diver sample	-6.5m	Sand	409009.3	4046258.1	0.27	0.2%
N1	Dock+1m	+1m	Sand	410290.6	4045467.8	0.90	0.0%
N2	Dock-0m	0m	Sand	410318.3	4045448.0	0.78	0.0%

Table A. 1. Summary of sieve analysis for sediment characteristics. (cont.)

N27	K14-1m	-1m	Medium Sand	413310.3	4045381.5	0.39	0.2%
N28	K14-2m	-2m	Medium Sand	413269.5	4045344.2	0.33	0.0%
N29	K14-5m	-5m	Medium Sand	413198.3	4045272.1	0.20	2.9%
N30	K14-5m(Oba)	-5m	Medium Sand	413196.5	4045245.6	0.31	1.6%
N31	K14-10m	-10m	Fine Sand	412992.8	4045063.6	0.16	5.7%
N32	K20+2m	+2m	Medium Sand	414318.7	4044699.4	0.66	0.3%
N33	K20+1m	+1m	Fine Pebble	414309.9	4044689.6	1.80	0.0%
N34	K20B-0m	0m	Fine Pebble	414305.2	4044684.5	1.79	0.0%
N35	K20-1m	-1m	Pebble	414303.1	4044681.5	6.47	0.0%
N36	K20B-2m	-2m	Pebble	414263.6	4044639.0	13.25	0.1%
N37	K20-5m	-5m	Fine Sand	414190.1	4044557.7	0.25	0.7%
N38	K20-10m	-10m	Fine Sand	414087.5	4044445.5	0.21	13.2%
N39	K26+2m	+2m	Coarse Sand	415200.2	4043956.4	0.96	0.1%
N40	K26+1m	+1m	Pebble	415186.1	4043941.0	13.58	0.0%
N41	K26-0m	0m	Pebble	415182.5	4043937.8	4.34	0.0%
N42	K26-1m	-1m	Coarse Pebble	415178.6	4043932.8	9.53	0.0%
N43	K26-2m	-2m	Coarse Pebble+Cobble	415158.7	4043913.4	48.49	0.0%
N44	K26-5m	-5m	Fine Sand	415071.7	4043822.6	0.30	1.3%
N45	K26-5m(Dim)	-5m	Fine Sand	415068.3	4043798.7	0.35	0.8%
N46	K26-10m	-10m	Fine Sand	414941.2	4043686.4	0.18	8.4%
N47	Dim-0.5m	-0.5m	Coarse Sand+Pebble	415308.5	4043818.2	1.15	0.0%
N48	Dim-3.5m	-3.5m	Sand	415212.3	4043624.6	0.35	0.2%
N49	K31+2m	+2m	Coarse Sand	415847.2	4043209.2	0.68	0.1%

Table A. 1. Summary of sieve analysis for sediment characteristics. (cont.)

N50	K31+1m	+1m	Pebble	415836.7	4043200.2	0.21	0.0%
N51	K31-0m	0m	Coarse Sand	415834.4	4043198.2	0.68	0.0%
N52	K31-2m	-2m	Pebble	415803.8	4043174.5	17.87	0.0%
N53	K31-5m	-5m	Sand	415745.8	4043120.1	0.39	0.2%
N54	K31-10m	-10m	Sand	415625.6	4043014.1	0.18	8.3%
N55	Kleopatra	+2m	Coarse Sand	409173.0	4046332.9	1.01	0.0%
N56	June-1	-10m	Sand	410298.3	4045284.7	0.16	20.8%
N57	June-2	-10m	Sand	410415.2	4045282.8	0.16	17.7%
N58	June-3	-10m	Sand	410558.9	4045277.0	0.16	22.2%
N59	Quarry 1	-	Mixed material	-	-	13.94	0.8%
N60	Quarry 2	-	15-25mm	-	-	16.59	0.3%
N61	Quarry 3	-	7-15mm	-	-	8.00	0.2%
N62	Quarry 4	-	0-7mm	-	-	2.47	2.4%
N63	Quarry 5	-	0-7mm	-	-	1.32	2.3%

APPENDIX B: WAVE AND WIND HISTOGRAMS

Wind and wave histograms for Alanya region are shown below.

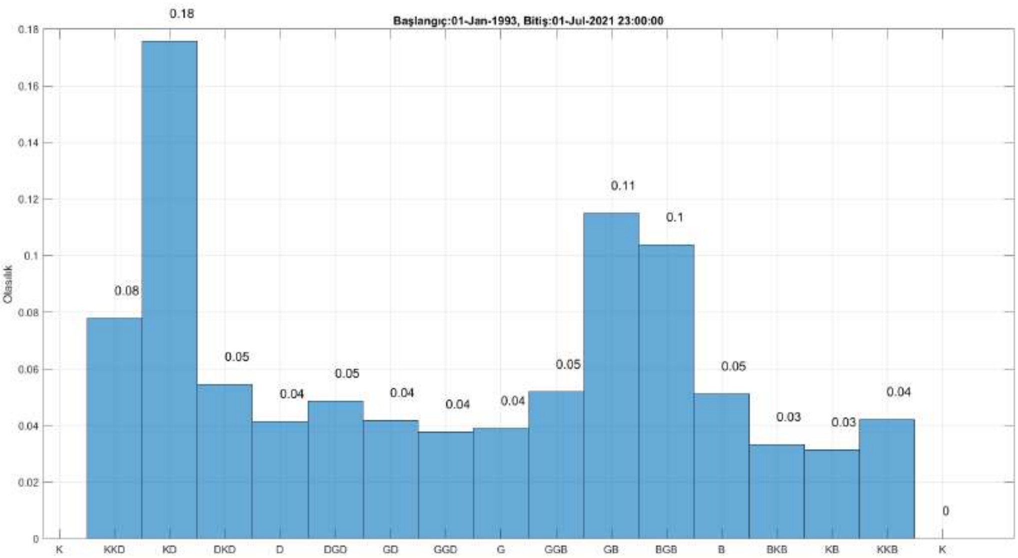

Figure B. 1. Wind direction histogram for Alanya.

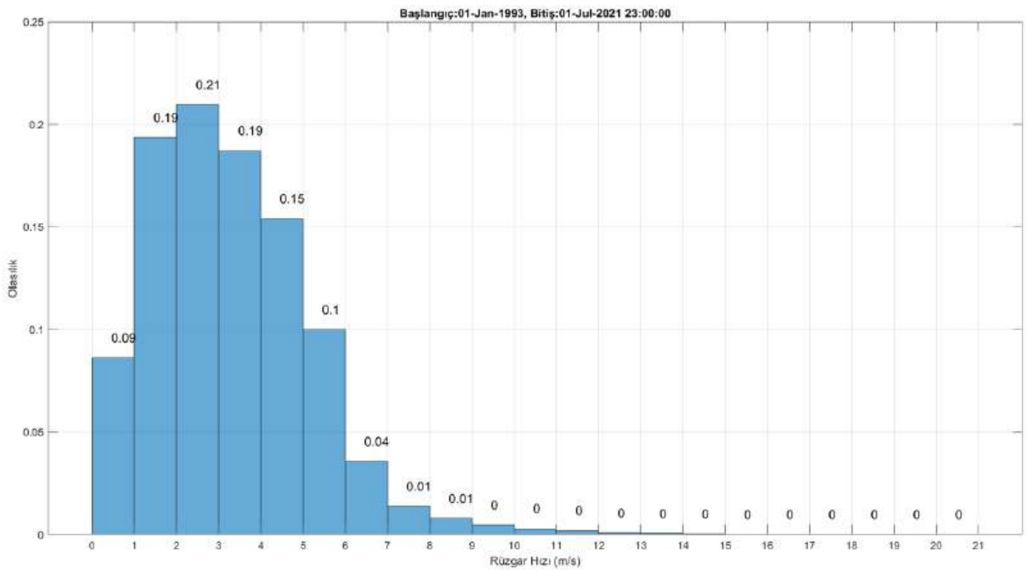

Figure B. 2. Wind speed histogram for Alanya.

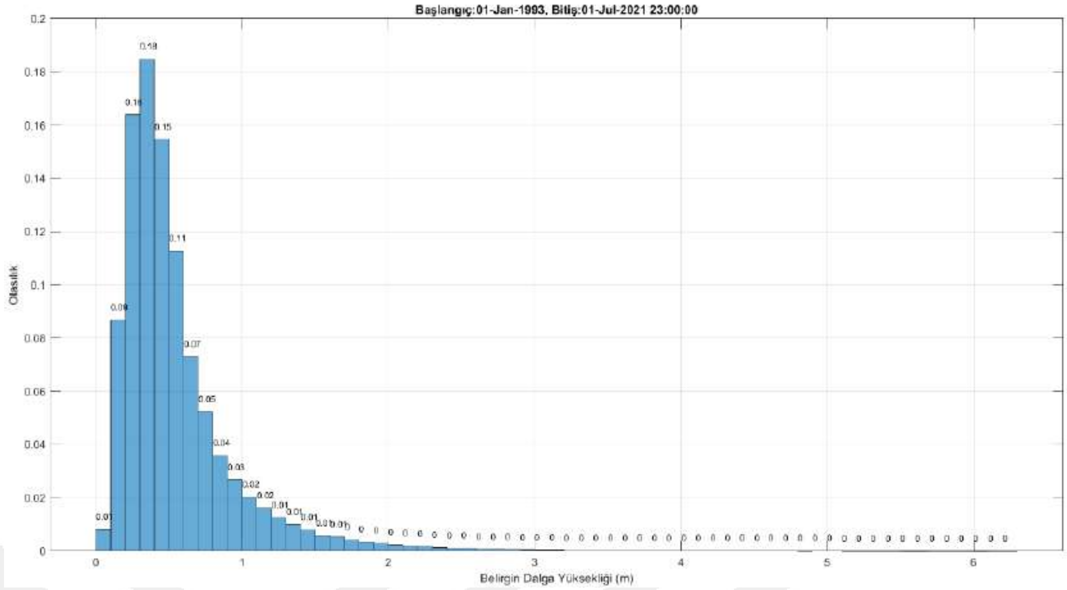

Figure B. 3. Significant wave height histogram for Alanya.

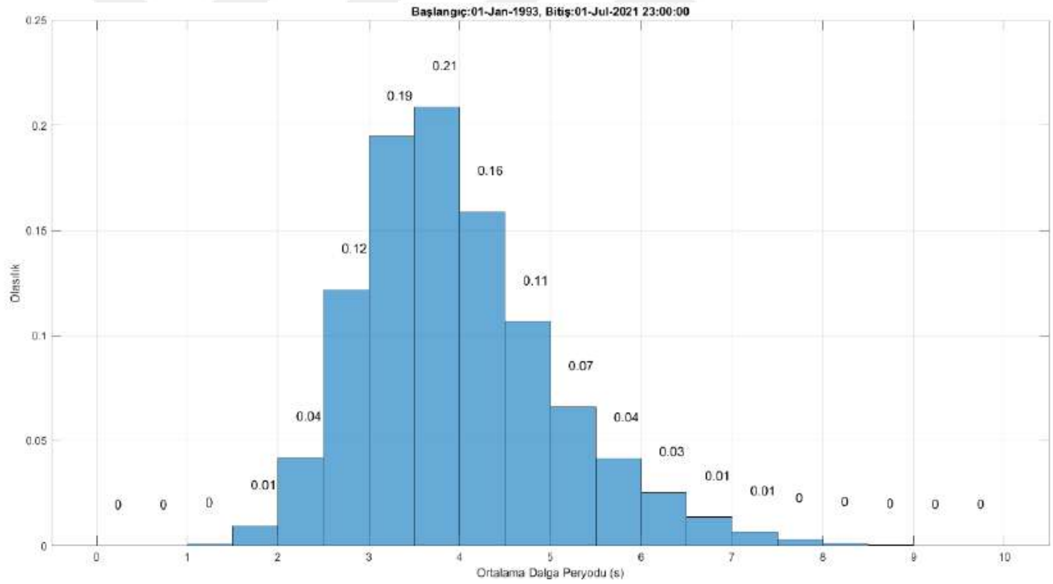

Figure B. 4. Mean wave period histogram for Alanya.

Table A. 1. Summary of sieve analysis for sediment characteristics. (cont.)

N3	Dock-1m	-1m	Sand	410354.4	4045428.7	1.21	0.0%
N4	Dock-2m	-2m	Sand	410398.8	4045410.1	1.96	0.0%
N5	Dock-5m	-5m	Sand	410424.2	4045394.2	1.09	0.3%
N6	Dock-10m	-10m	Sand	410560.8	4045317.0	0.19	2.3%
N7	Pier Middle	-4m	Sand	410591.7	4045848.4	0.15	13.6%
N8	Pier Entrance	-6m	Sand	410750.1	4045846.7	0.16	24.9%
N9	K02+2m	+2m	Medium Sand	411017.6	4046262.2	0.39	0.4%
N10	K02+1m	+1m	Medium Sand	411020.4	4046252.1	0.48	0.6%
N11	K02-0m	0m	Coarse Sand	411021.4	4046249.0	0.77	0.0%
N12	K02-1m	-1m	Fine Sand	411024.4	4046239.5	0.21	0.6%
N13	K02-2m	-2m	Fine Sand	411033.3	4046178.6	0.20	0.7%
N14	K02-5m	-5m	Fine Sand	411081.0	4045975.7	0.17	4.6%
N15	K02-5m(HD)	-5m	Fine Sand	411093.7	4045951.7	0.16	6.1%
N16	K02-10m	-10m	Fine Sand	411158.4	4045656.7	0.17	28.5%
N17	K09+2m	+2m	Sand+Pebble	412467.6	4045971.5	0.52	0.9%
N18	K09+1m	+1m	Sand+Pebble	412458.3	4045952.5	0.47	0.1%
N19	K09-0m	0m	Fine Pebble	412457.1	4045950.3	1.48	0.0%
N20	K09-2m	-2m	Coarse Sand	412433.7	4045897.4	0.66	0.0%
N21	K09-5m	-5m	Fine Sand	412376.7	4045775.2	0.25	0.6%
N22	K09-5m(GD)	-5m	Fine Sand	412375.9	4045752.2	0.26	1.0%
N23	K09-10m	-10m	Fine Sand	412212.7	4045423.9	0.16	15.8%
N24	K14+2m	+2m	Medium Sand	413340.0	4045415.8	0.50	0.4%
N25	K14+1m	+1m	Medium Sand	413318.3	4045393.9	0.48	0.0%
N26	K14-0m	0m	Coarse Sand+Pebble	413315.0	4045390.4	1.83	0.0%

APPENDIX C: CTD MEASUREMENTS

CTD measurements of temperature, salinity, density and sound velocity for all points.

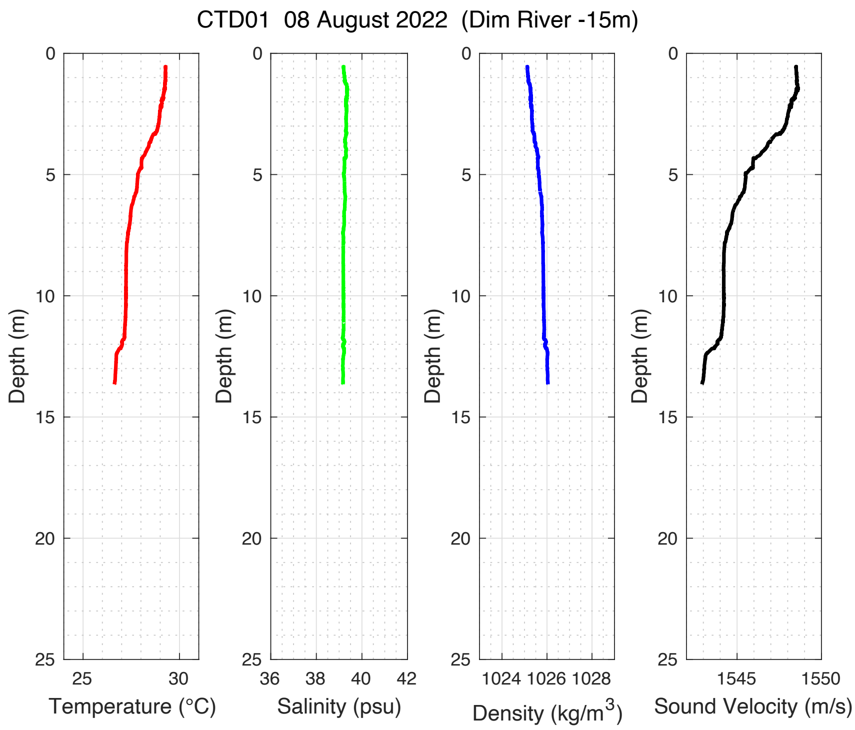

Figure C. 1. CTD measurements at Dim River -15m measured in August 8th.

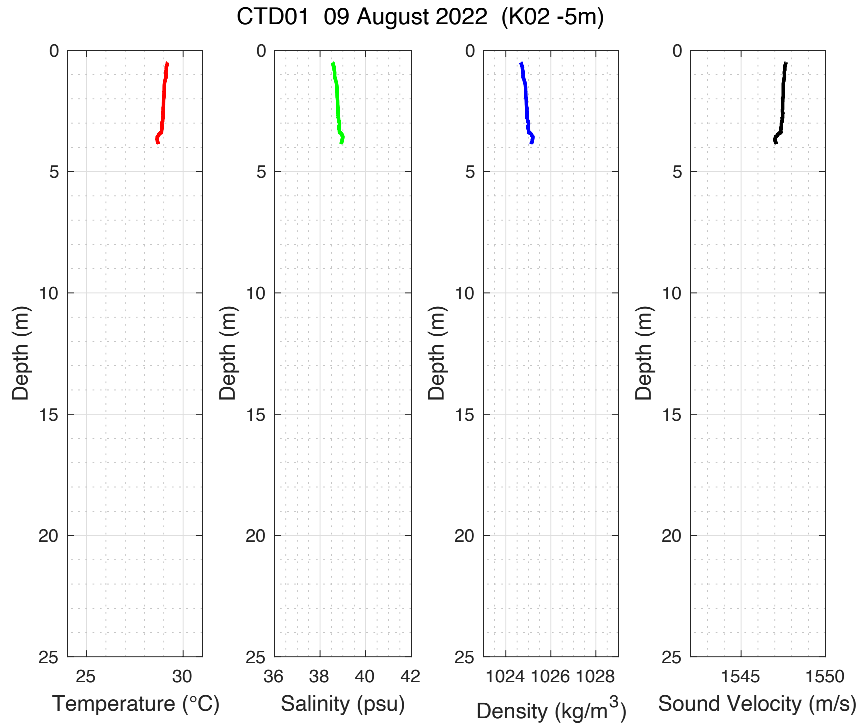

Figure C. 2. CTD measurements at K02 -2m measured in August 9th.

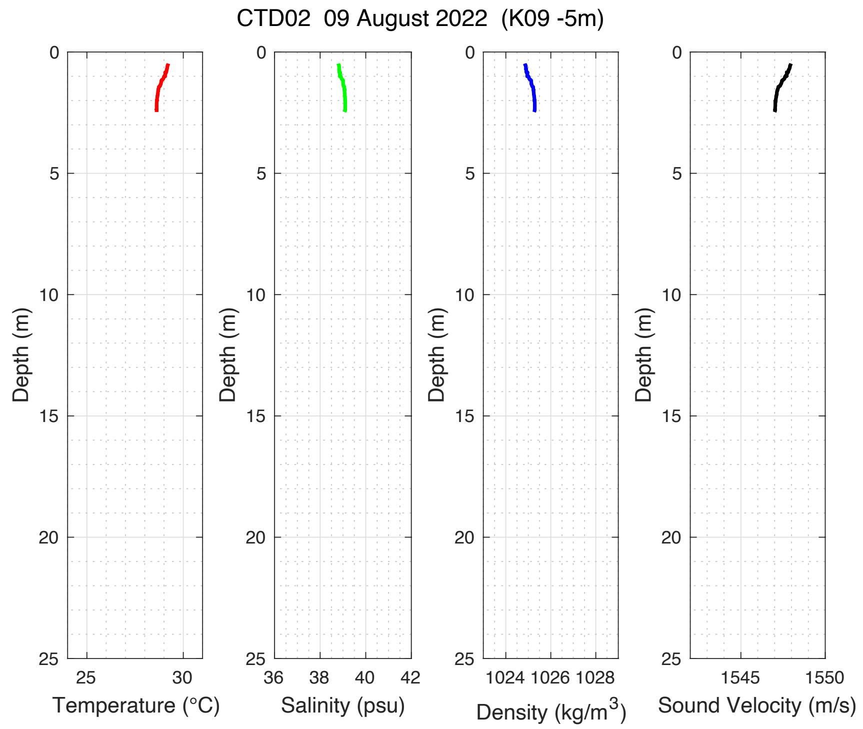

Figure C. 3. CTD measurements at K09 -5m measured in August 9th.

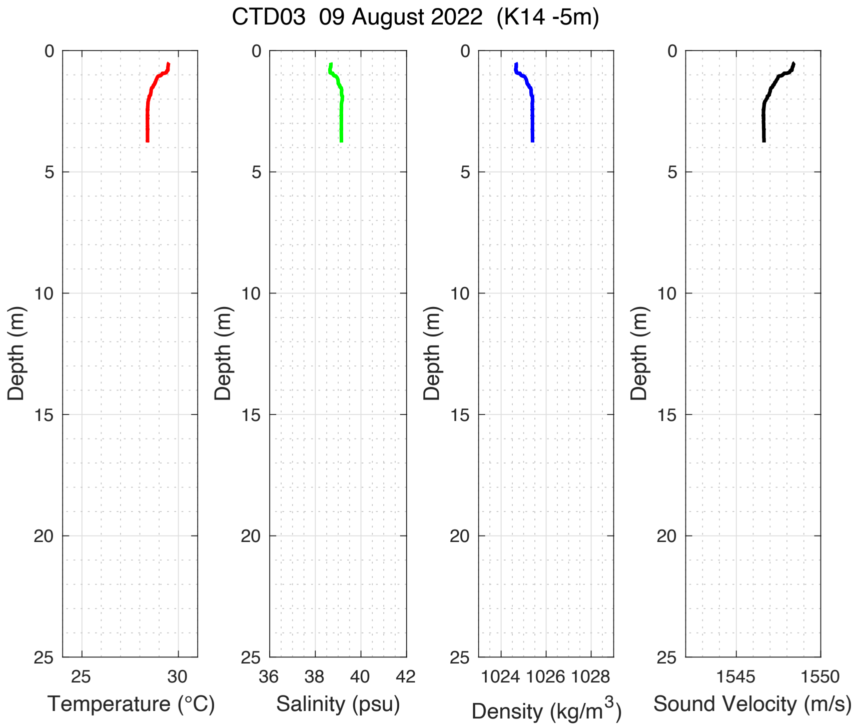

Figure C. 4. CTD measurements at K14 -5m measured in August 9th.

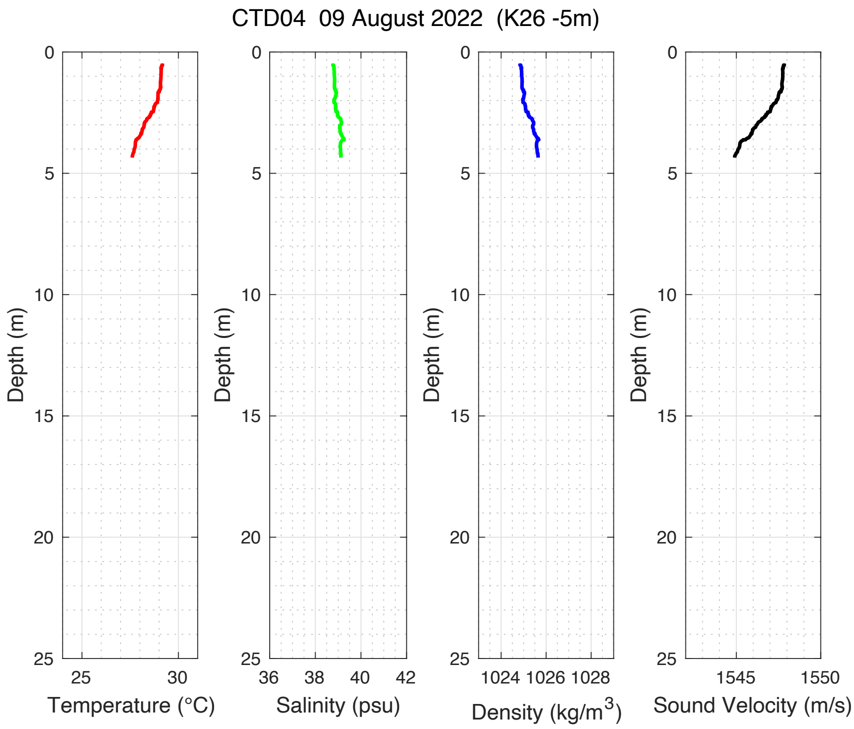

Figure C. 5. CTD measurements at K26 -5m measured in August 9th.

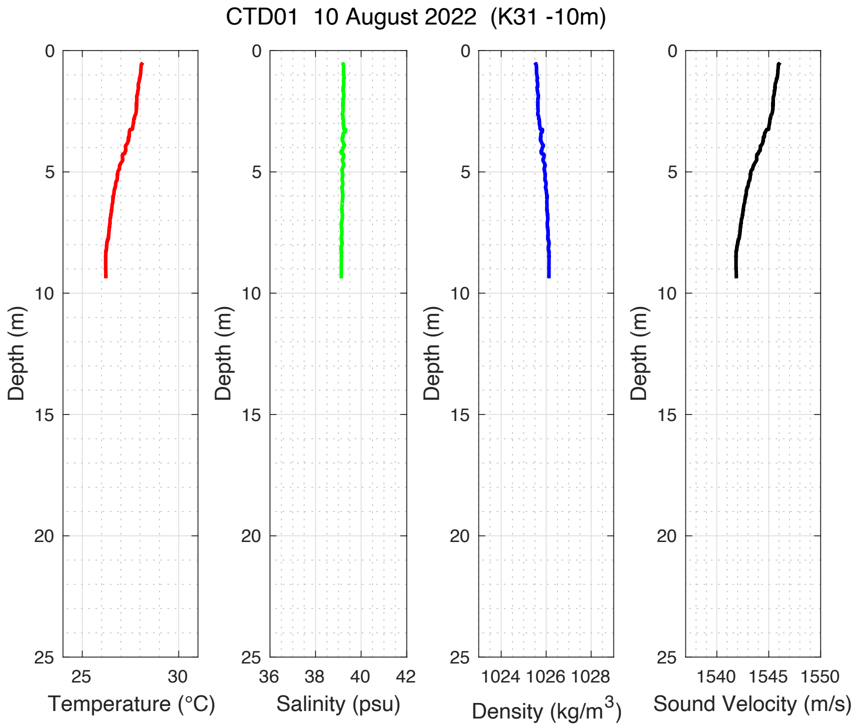

Figure C. 6. CTD measurements at K31 -10m measured in August 10th.

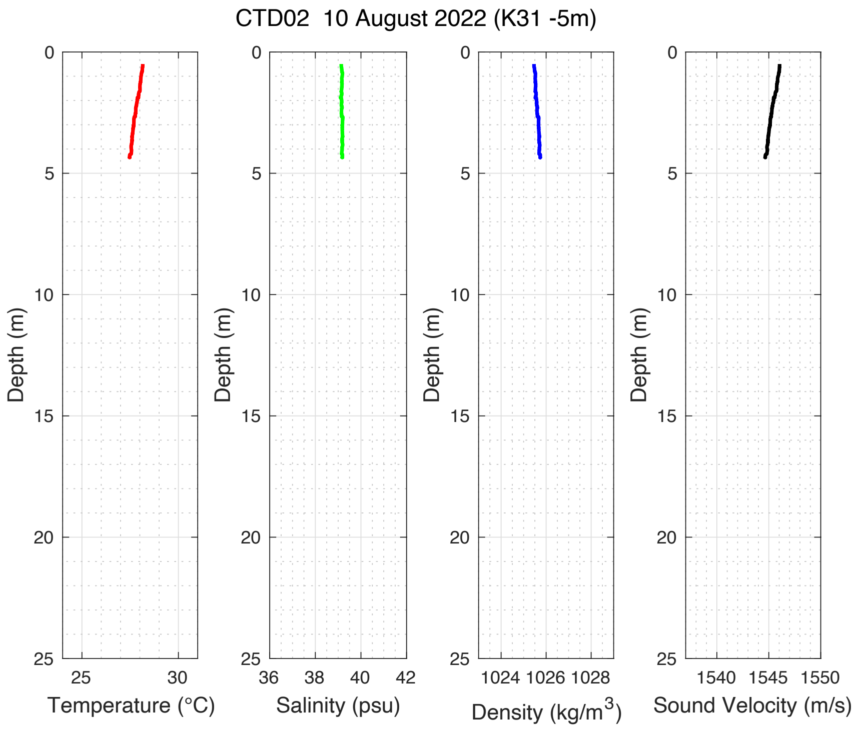

Figure C. 7. CTD measurements at K31 -5m measured in August 10th.

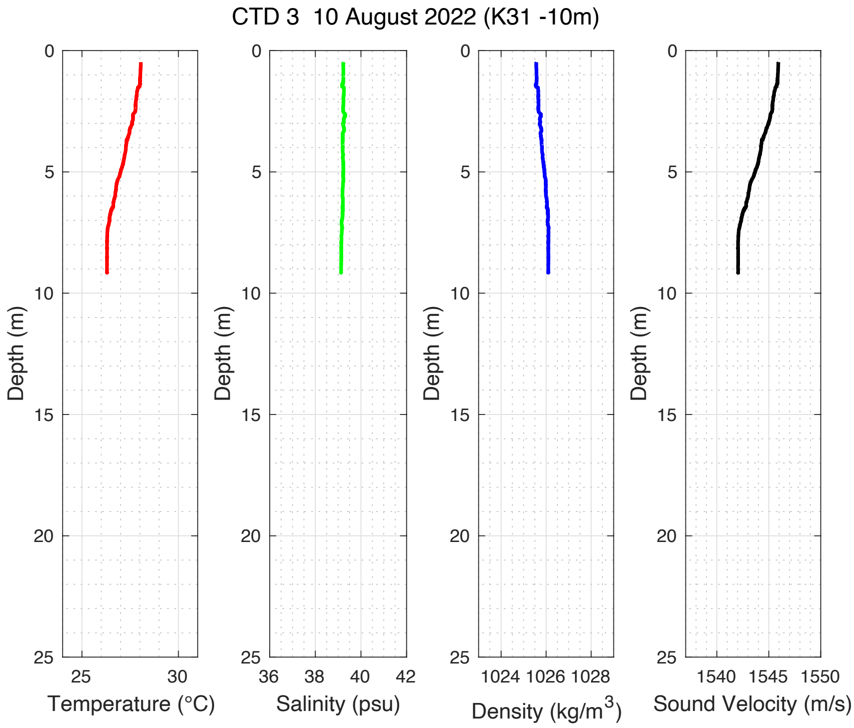

Figure C. 8. CTD measurements at K31 -10m measured in August 10th.

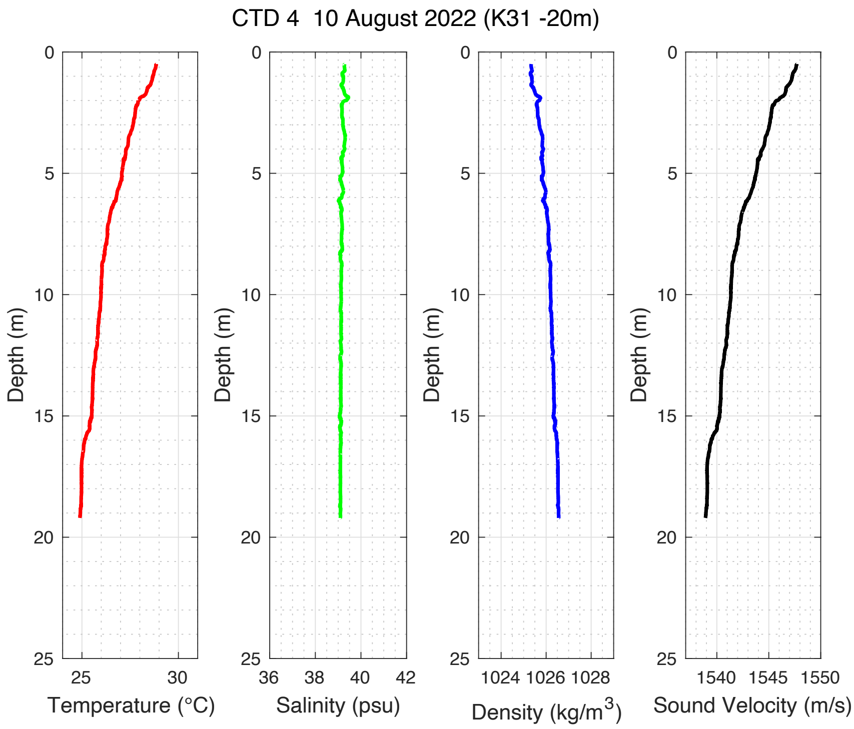

Figure C. 9. CTD measurements at K31 -20m measured in August 10th.

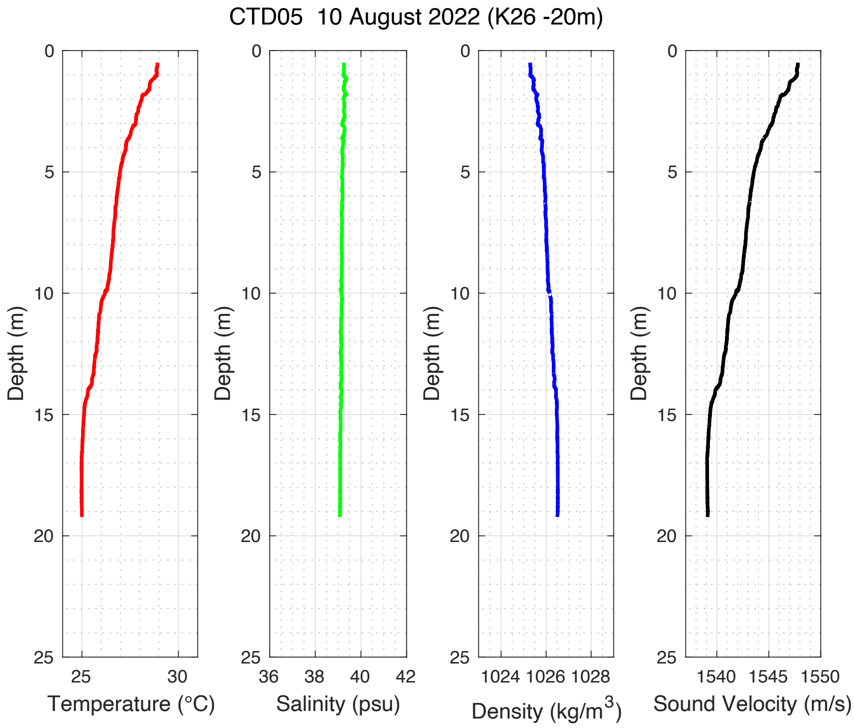

Figure C. 10. CTD measurements at K26 -20m measured in August 10th.

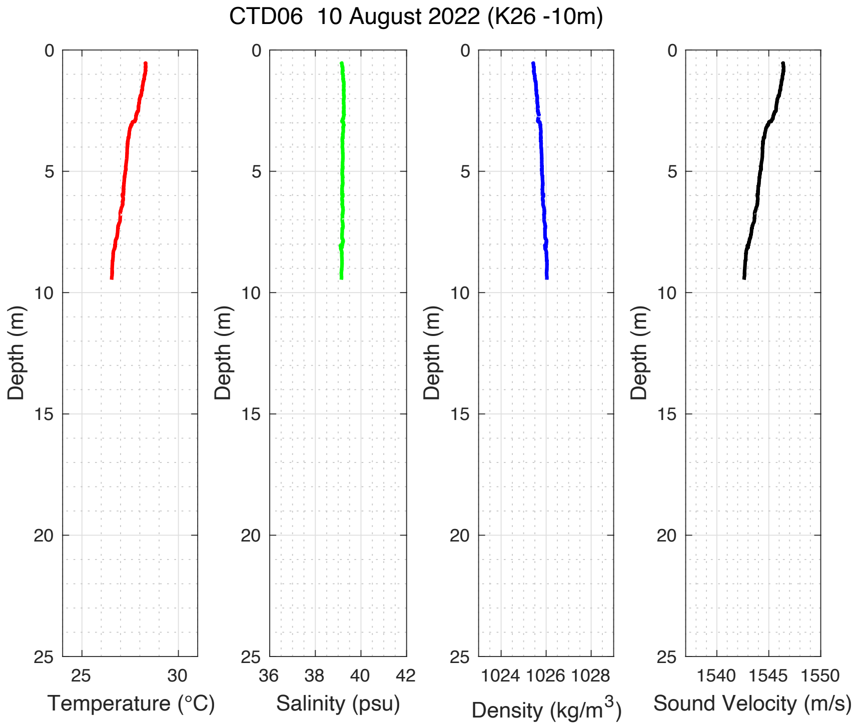

Figure C. 11. CTD measurements at K26 -10m measured in August 10th.

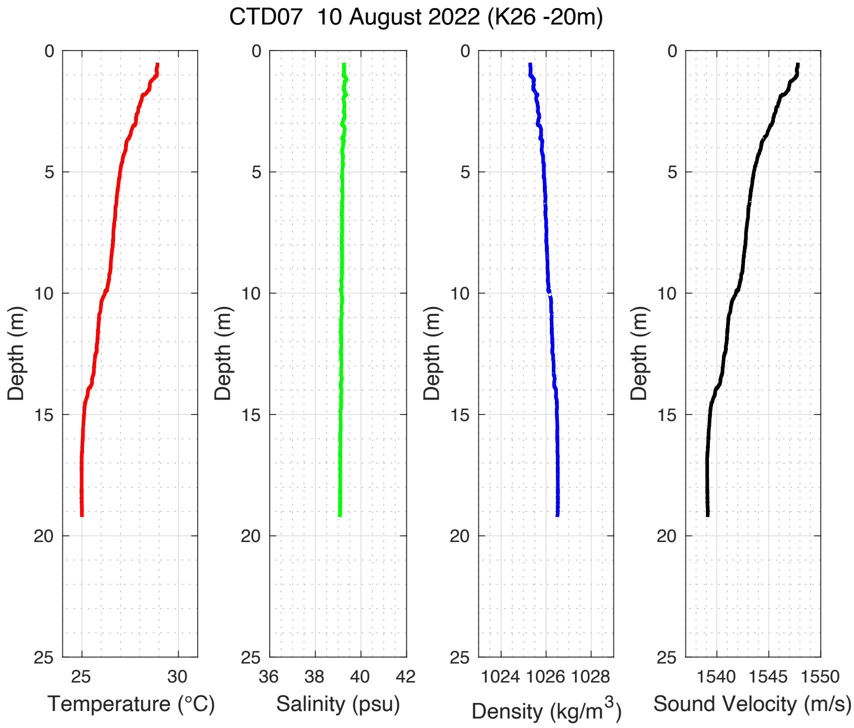

Figure C. 12. CTD measurements at K26 -20m measured in August 10th.

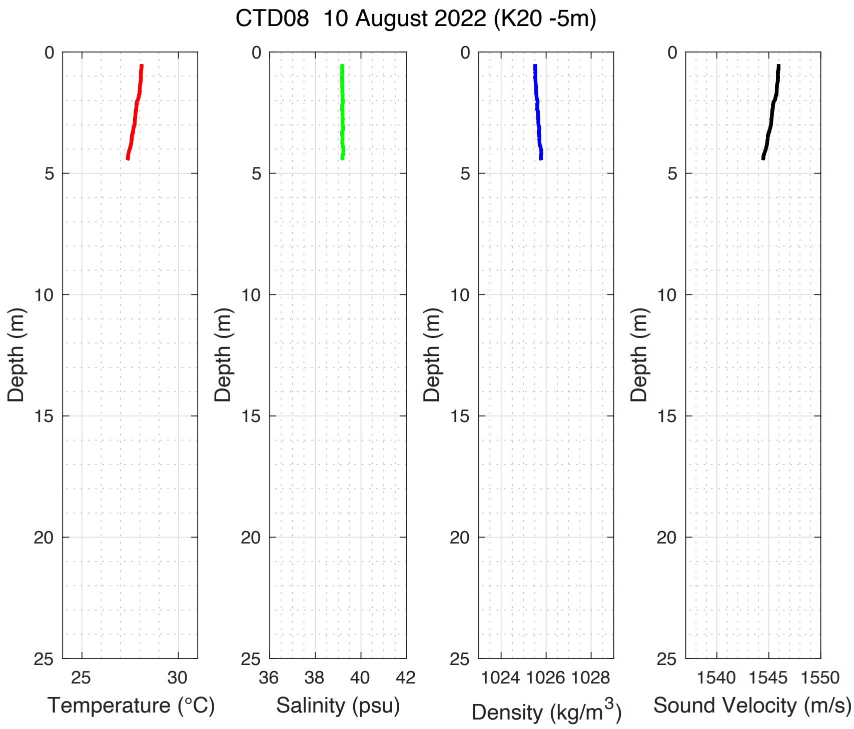

Figure C. 13. CTD measurements at K20 -5m measured in August 10th.

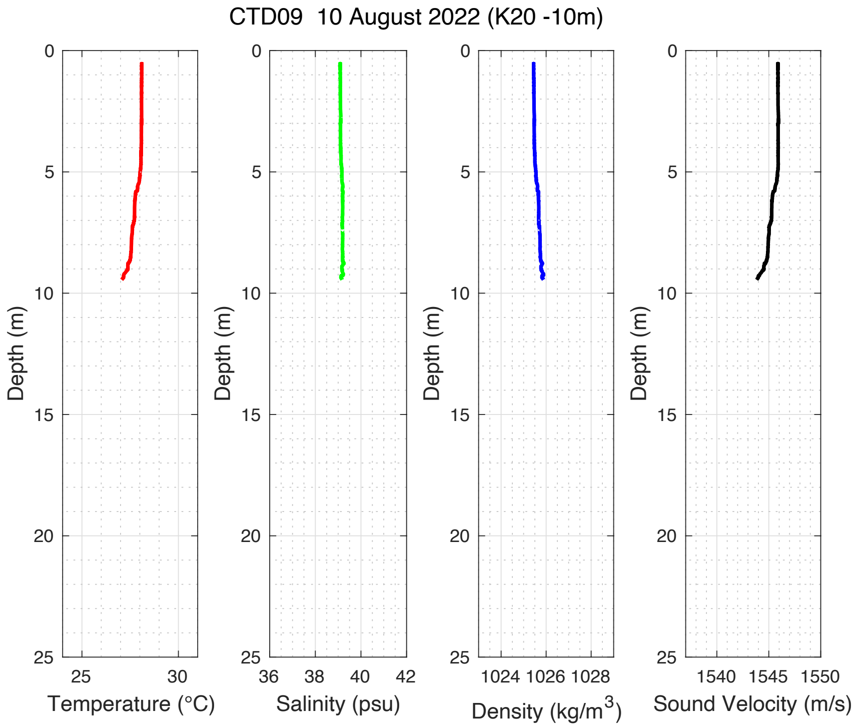

Figure C. 14. CTD measurements at K20 -10m measured in August 10th.

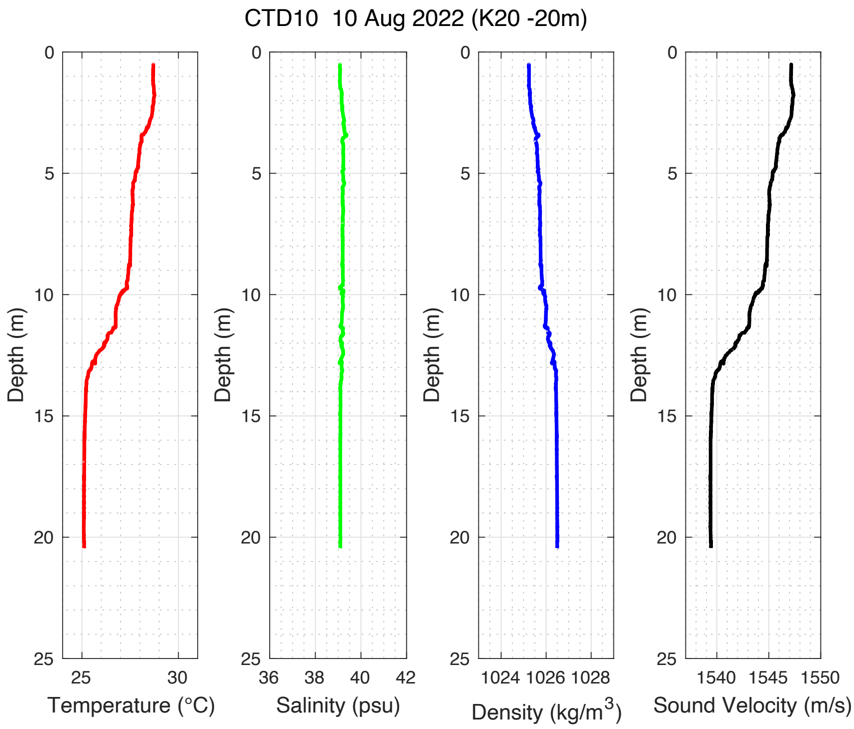

Figure C. 15. CTD measurements at K20 -20m measured in August 10th.

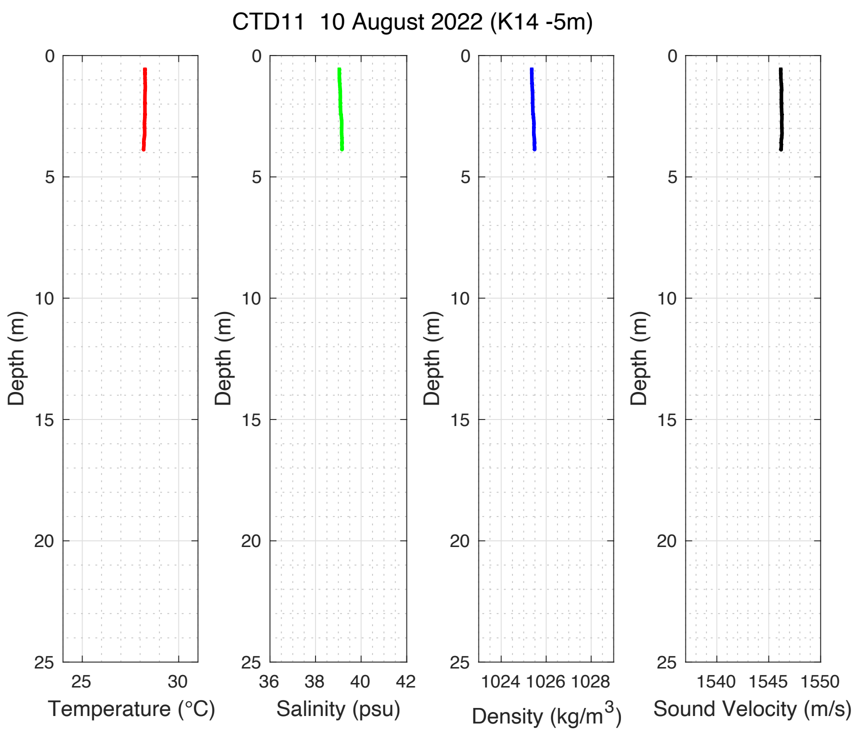

Figure C. 16. CTD measurements at K14 -5m measured in August 10th.

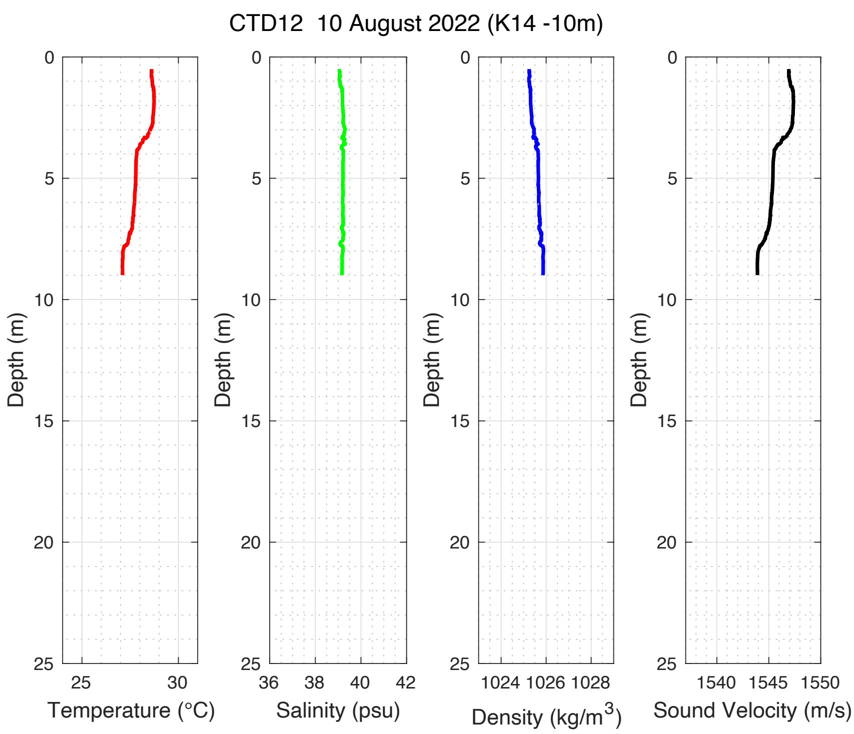

Figure C. 17. CTD measurements at K14 -10m measured in August 10th.

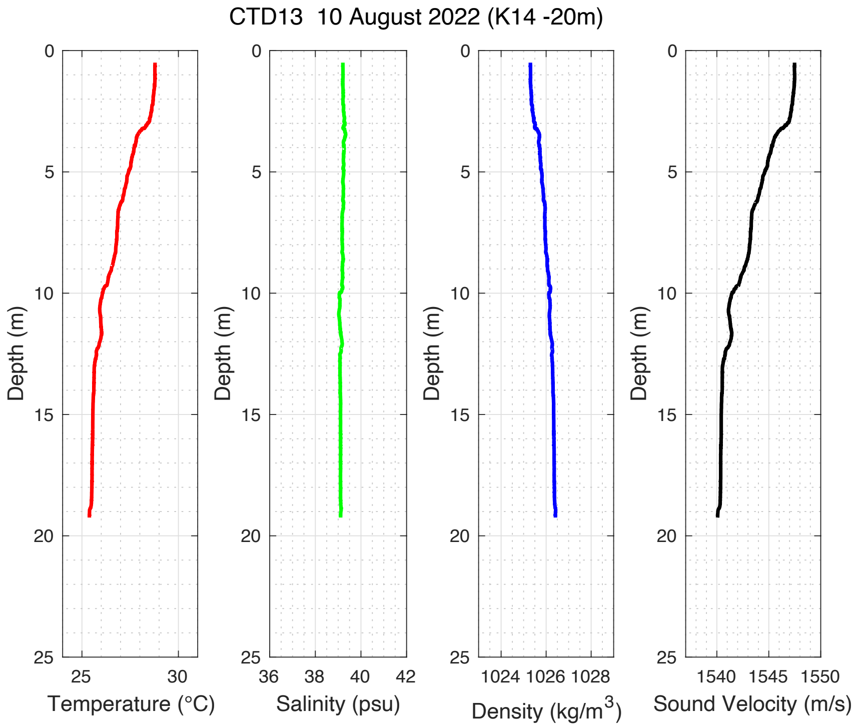

Figure C. 18. CTD measurements at K14 -20m measured in August 10th.

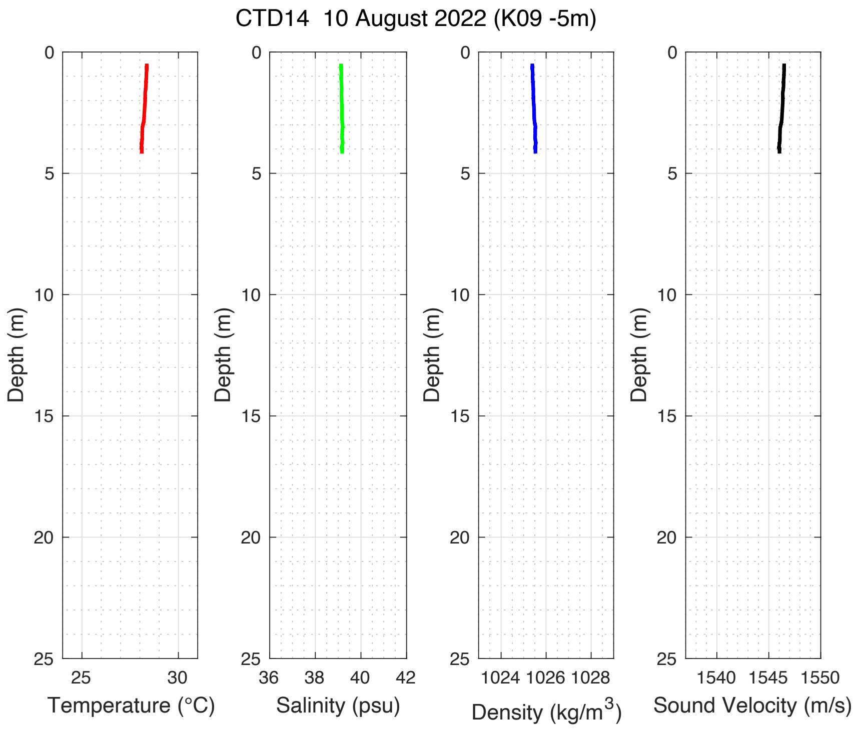

Figure C. 19. CTD measurements at K09 -5m measured in August 10th.

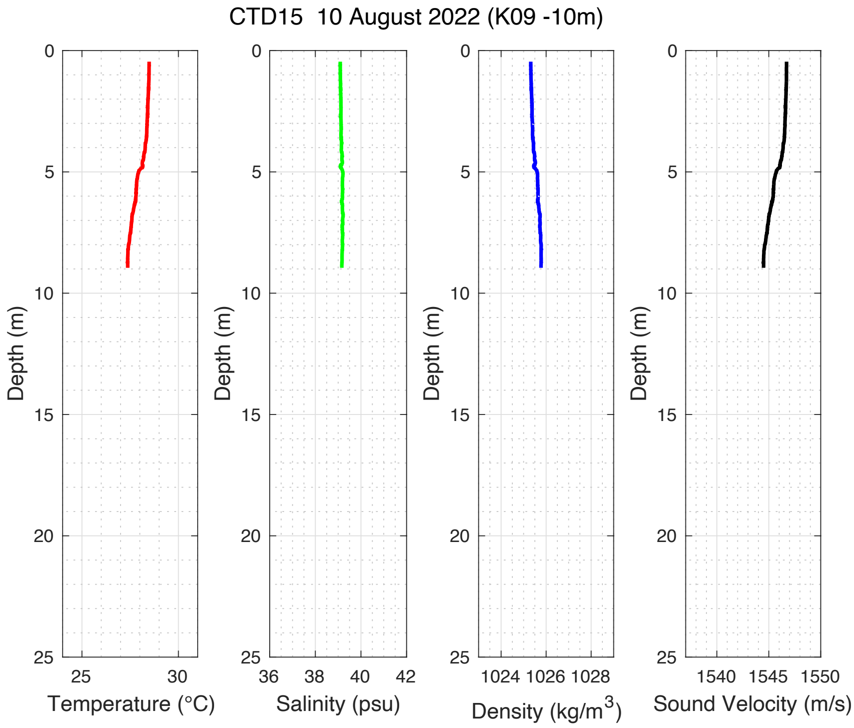

Figure C. 20. CTD measurements at K09 -10m measured in August 10th.

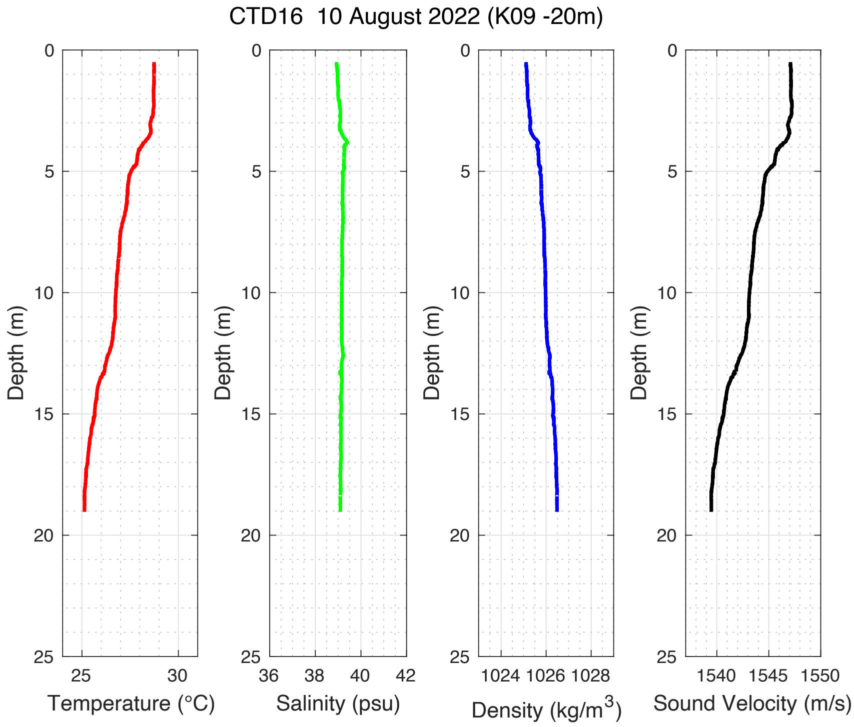

Figure C. 21. CTD measurements at K09 -20m measured in August 10th.

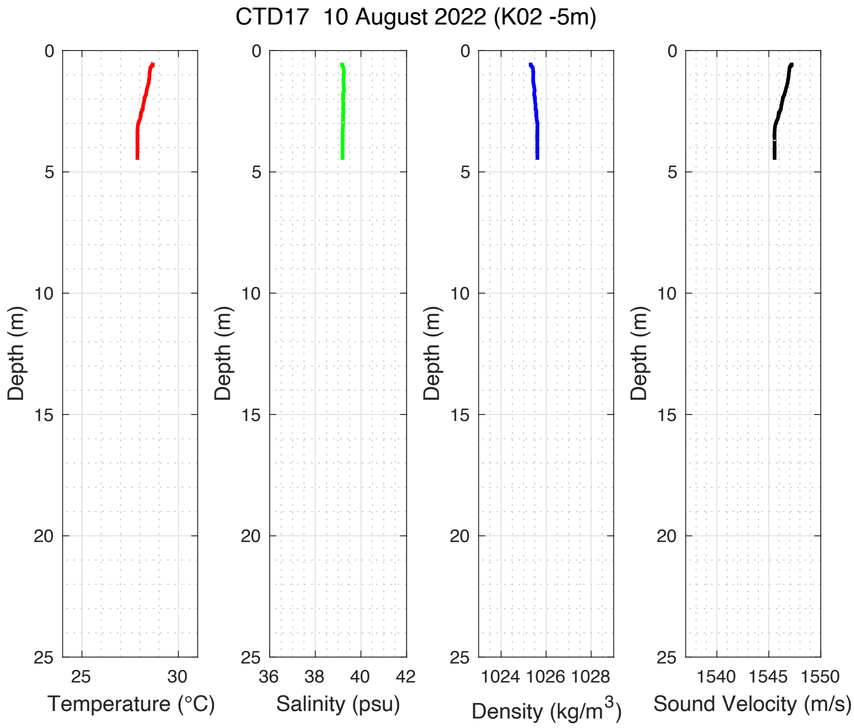

Figure C. 22. CTD measurements at K02 -5m measured in August 10th.

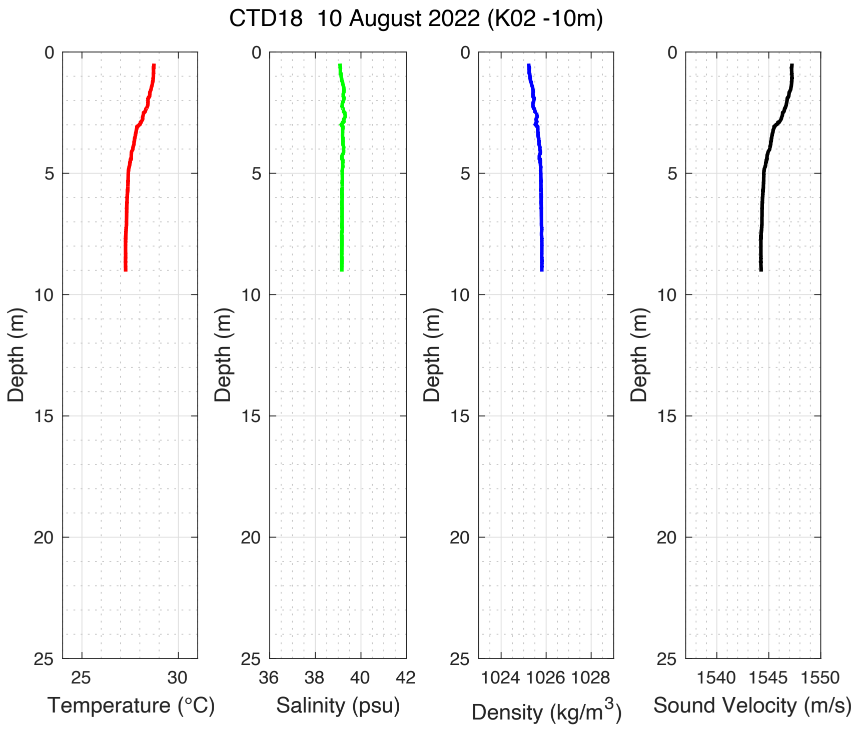

Figure C. 23. CTD measurements at K02 -10m measured in August 10th.

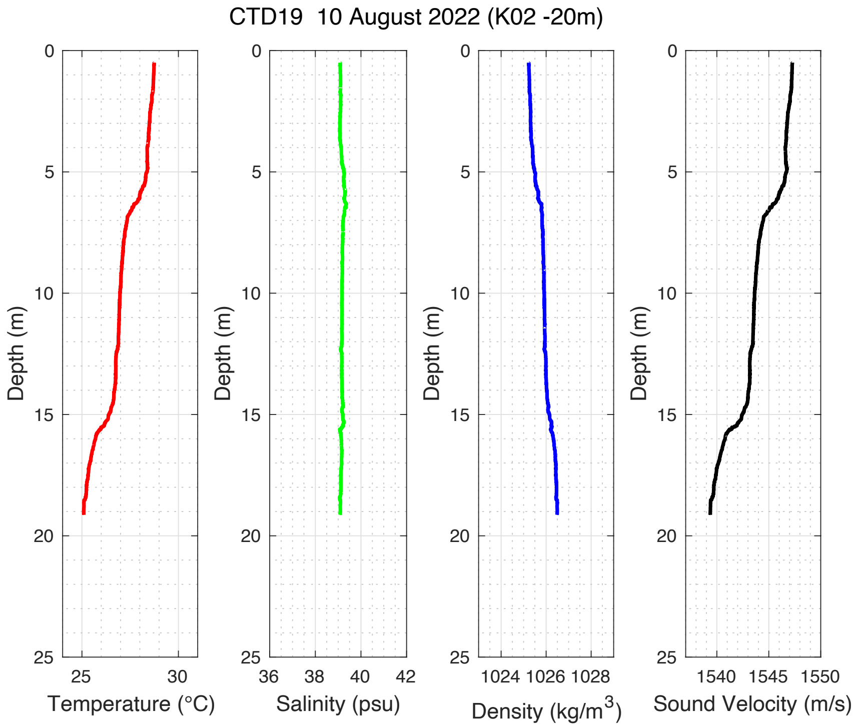

Figure C. 24. CTD measurements at K02 -20m measured in August 10th.

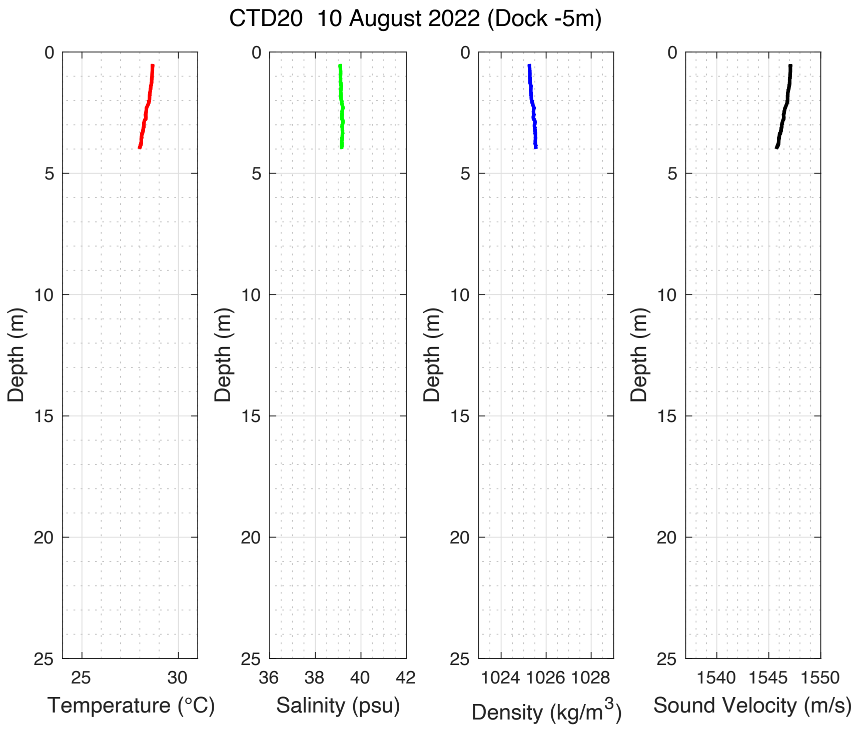

Figure C. 25. CTD measurements at Dock -5m measured in August 10th.

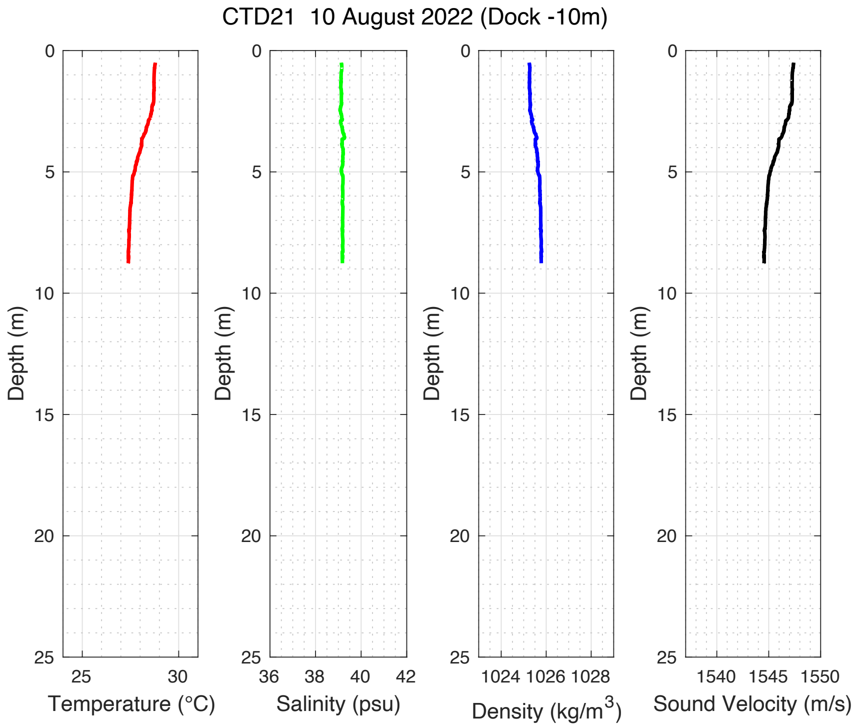

Figure C. 26. CTD measurements at Dock -10m measured in August 10th.

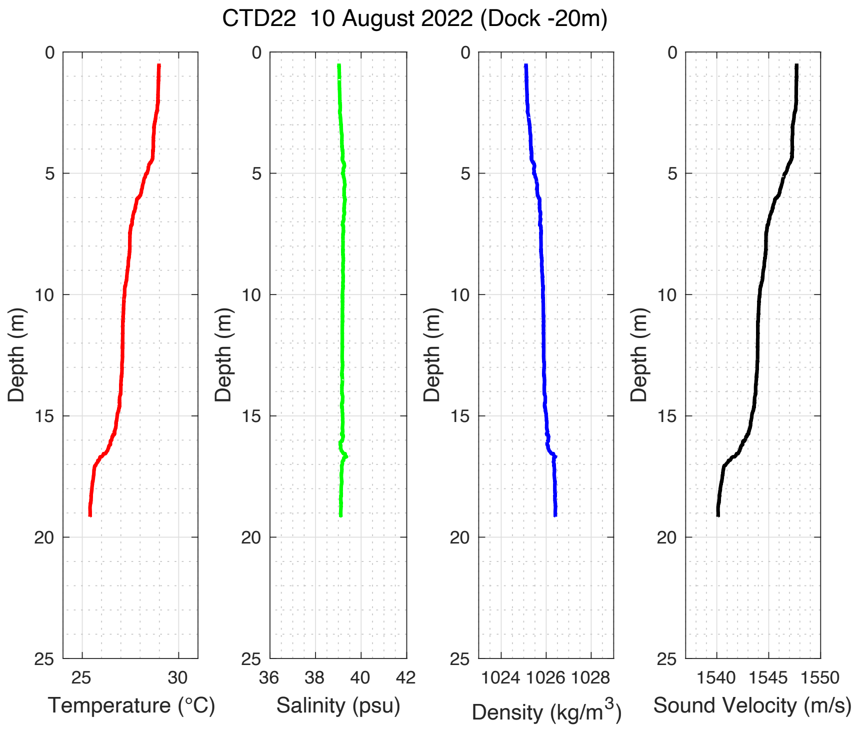

Figure C. 27. CTD measurements at Dock -20m measured in August 10th.

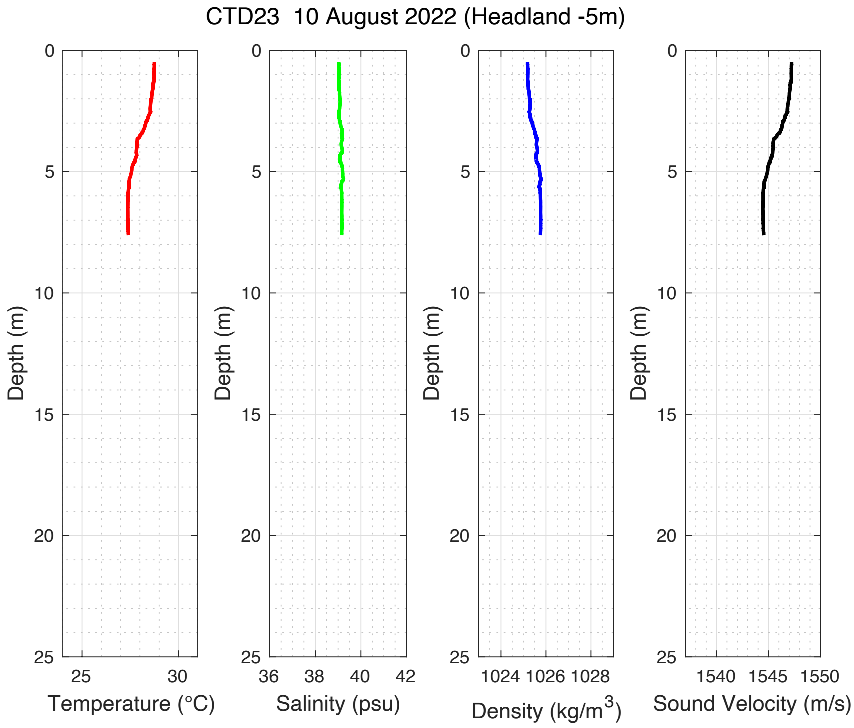

Figure C. 28. CTD measurements at Headland -5m measured in August 10th.

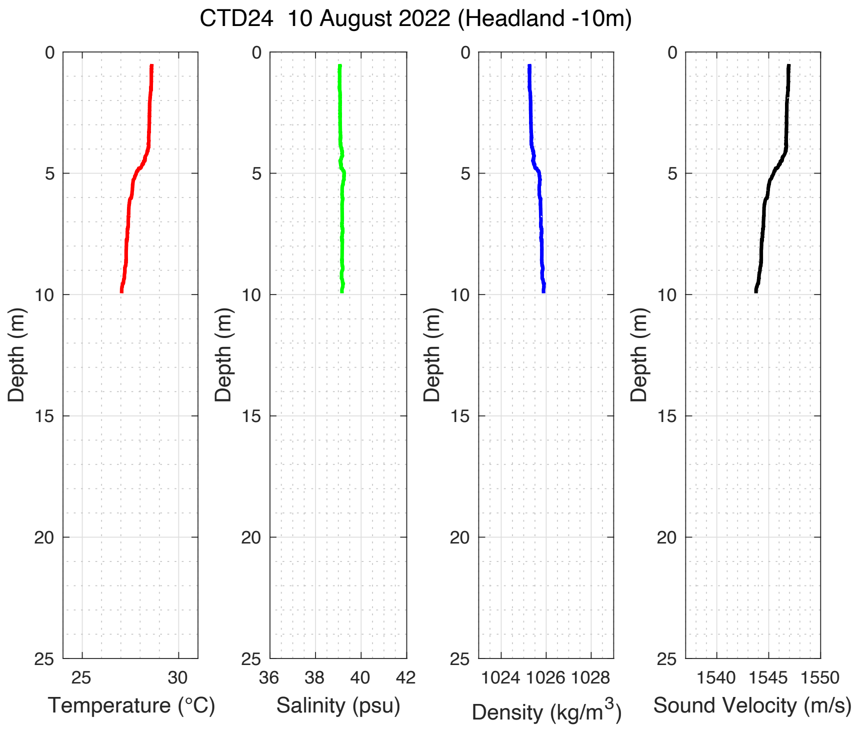

Figure C. 29. CTD measurements at Headland -10m measured in August 10th.

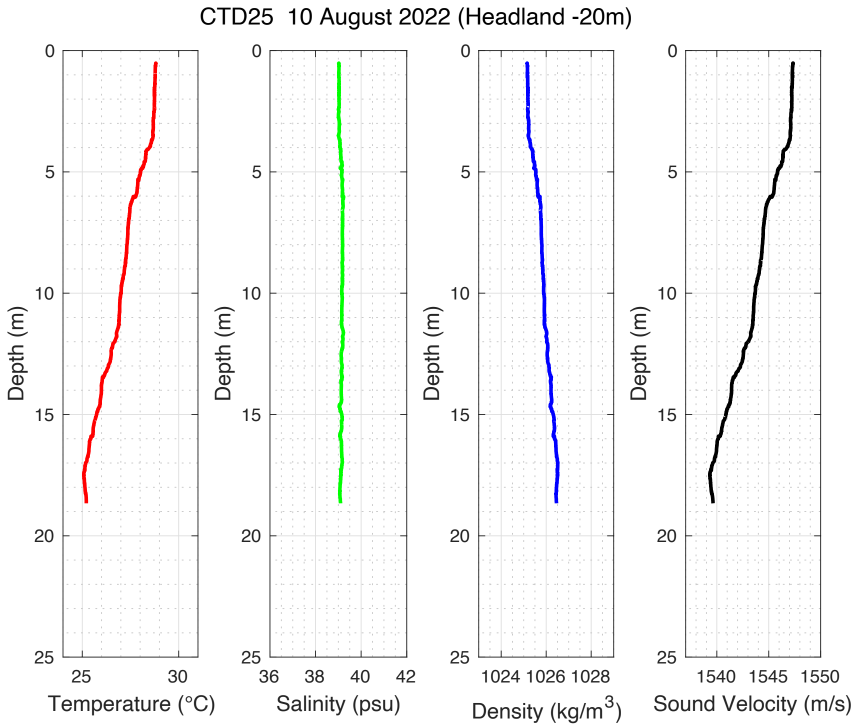

Figure C. 30. CTD measurements at Headland -20m measured in August 10th.

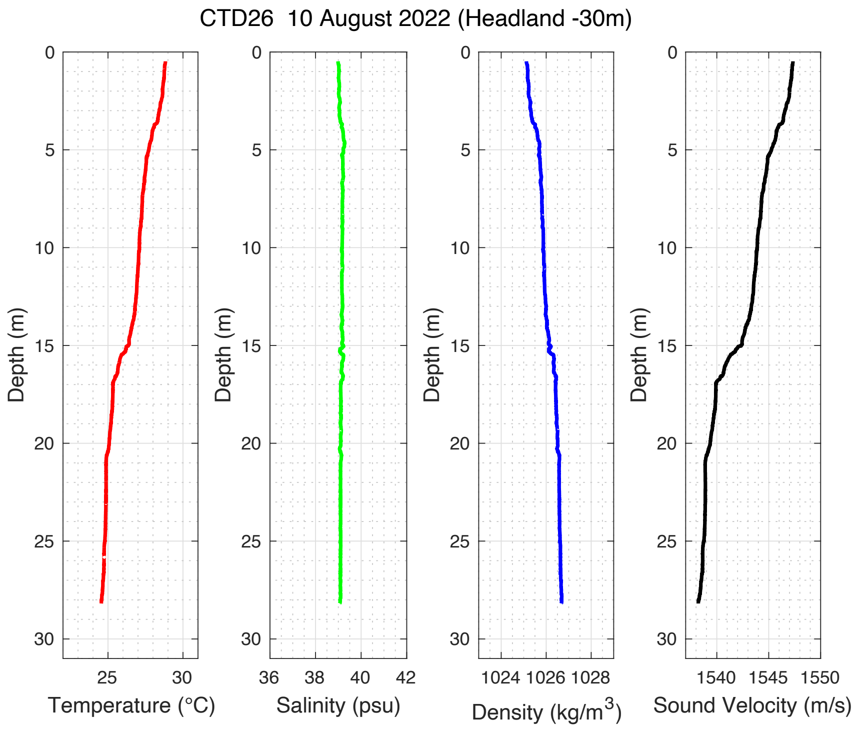

Figure C. 31. CTD measurements at Headlnd -30m measured in August 10th.

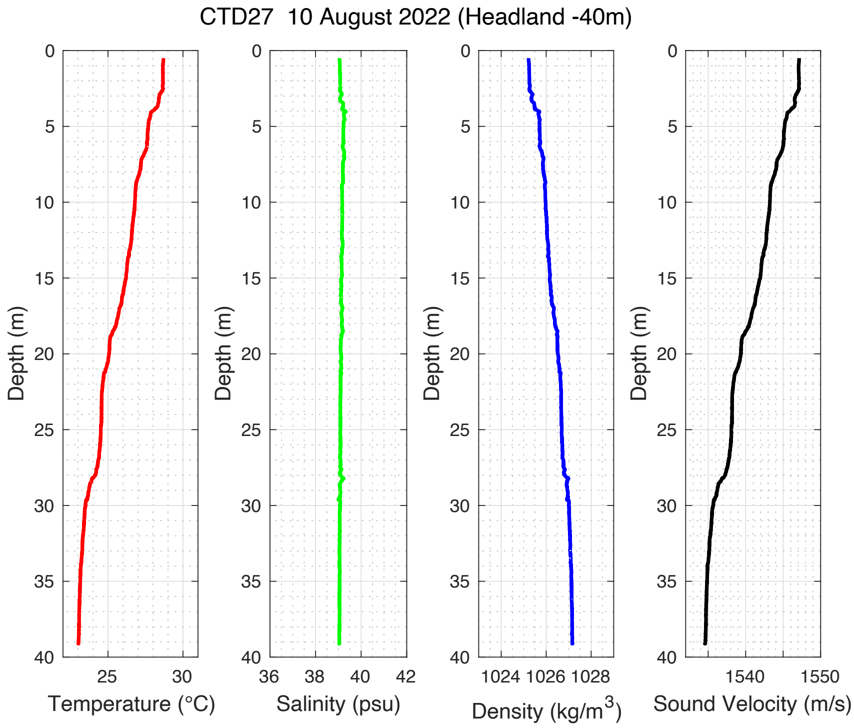

Figure C. 32. CTD measurements at Headland -40m measured in August 10th.

APPENDIX D: SEDIMENT GRADING GRAPHS

Sediment grading graphs for samples taken from the beach after sieve analysis.

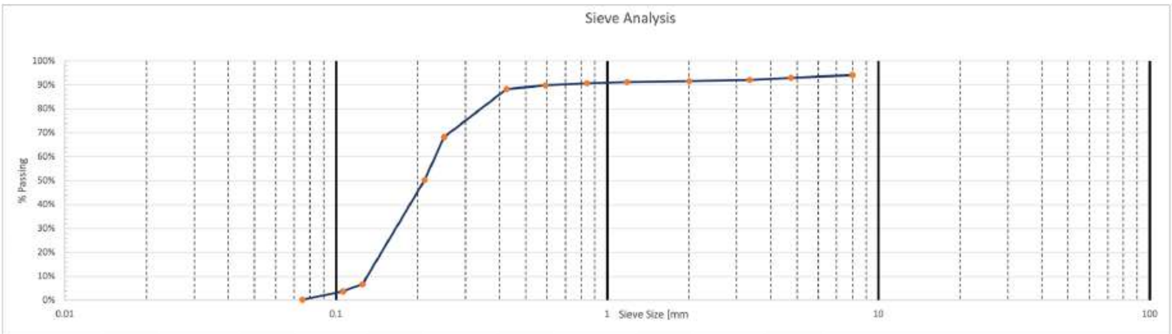

Figure D. 1. Sediment grading graph for diver sample S01.

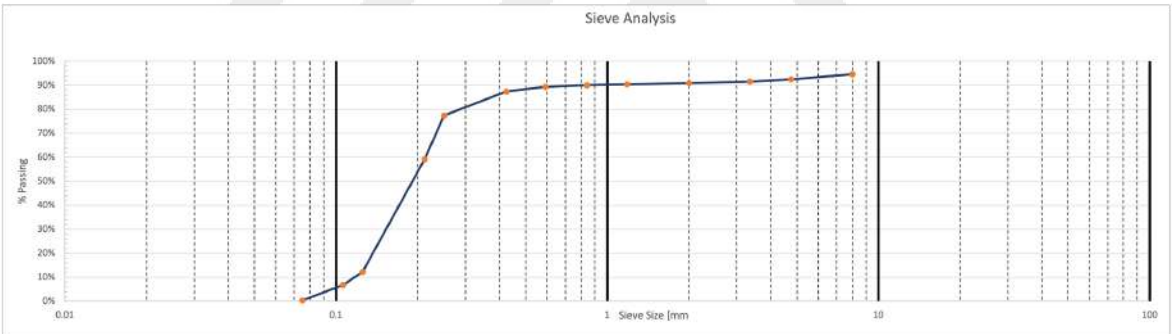

Figure D. 2. Sediment grading graph for diver sample S02.

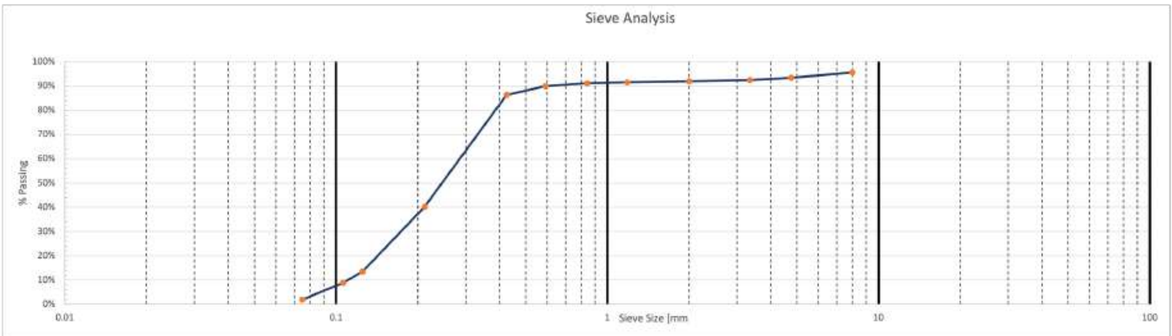

Figure D. 3. Sediment grading graph for diver sample S03.

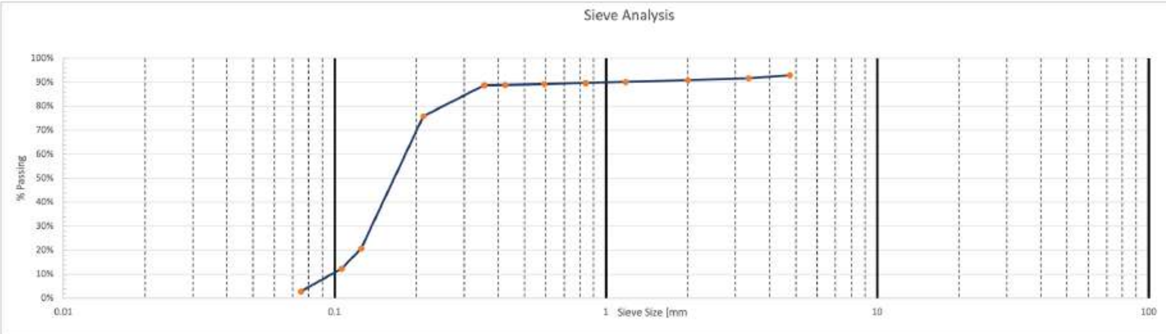

Figure D. 4. Sediment grading graph for diver sample S04.

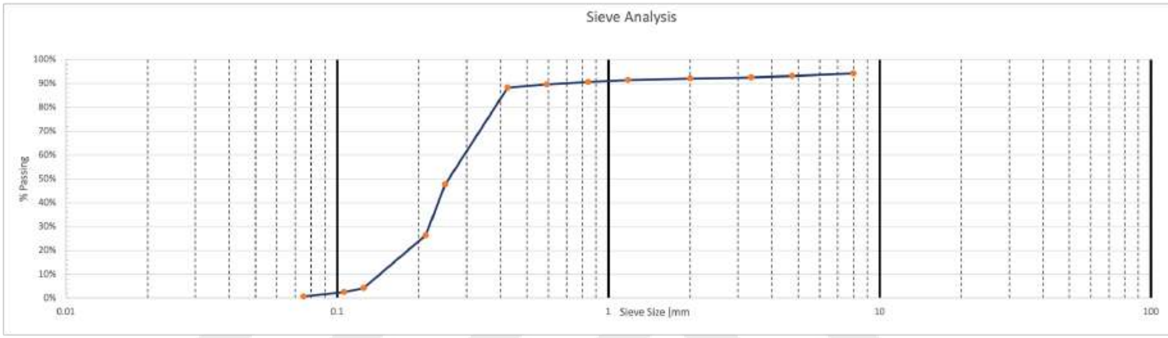

Figure D. 5. Sediment grading graph for diver sample S05.

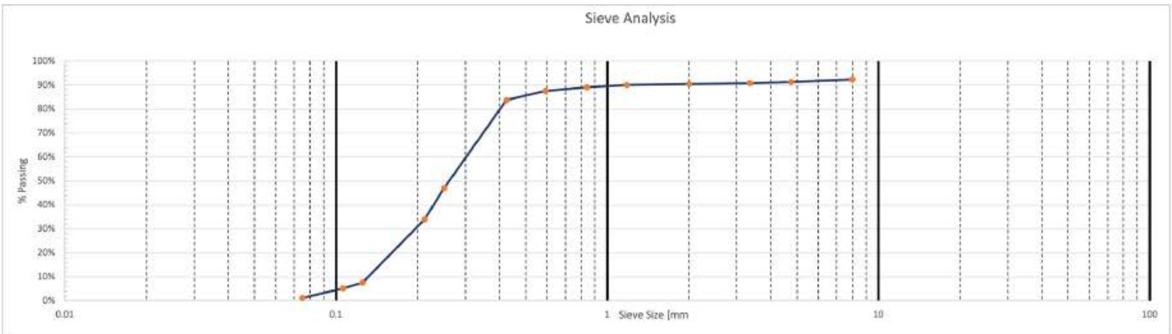

Figure D. 6. Sediment grading graph for diver sample S06.

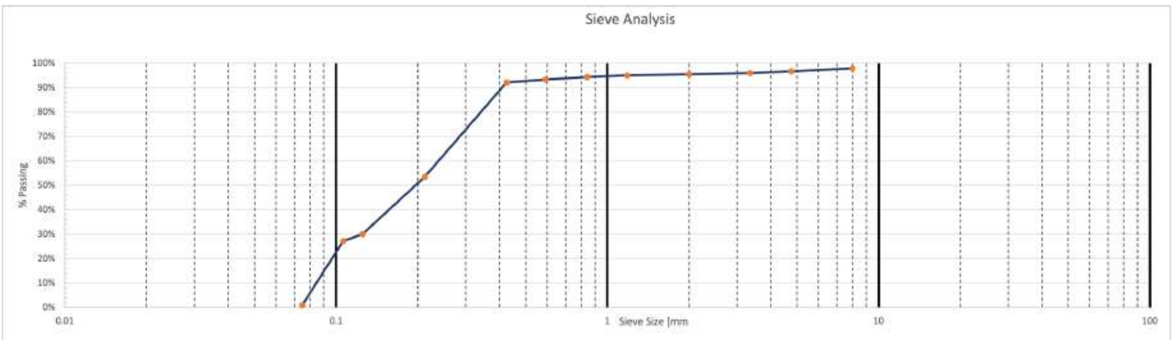

Figure D. 7. Sediment grading graph for diver sample S07.

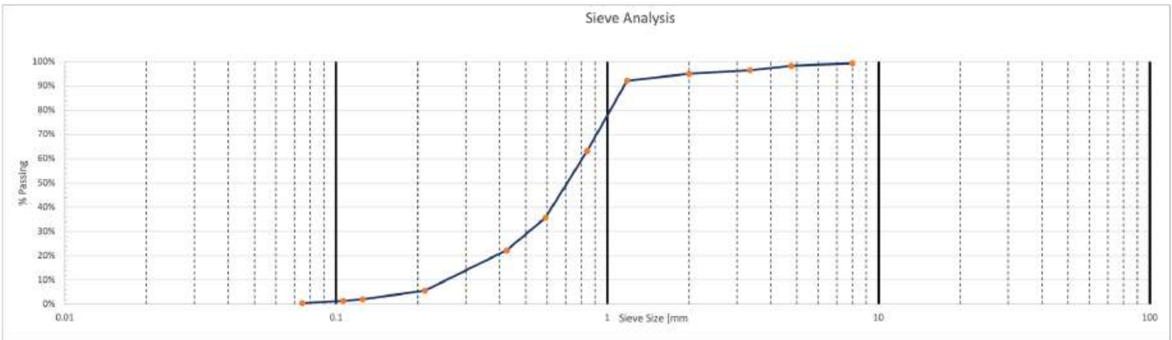

Figure D. 8. Sediment grading graph for diver sample S08.

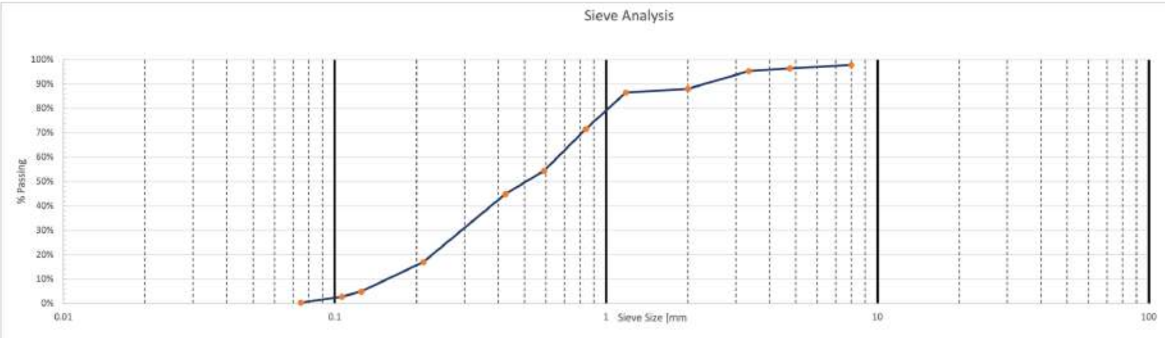

Figure D. 9. Sediment grading graph for diver sample S09.

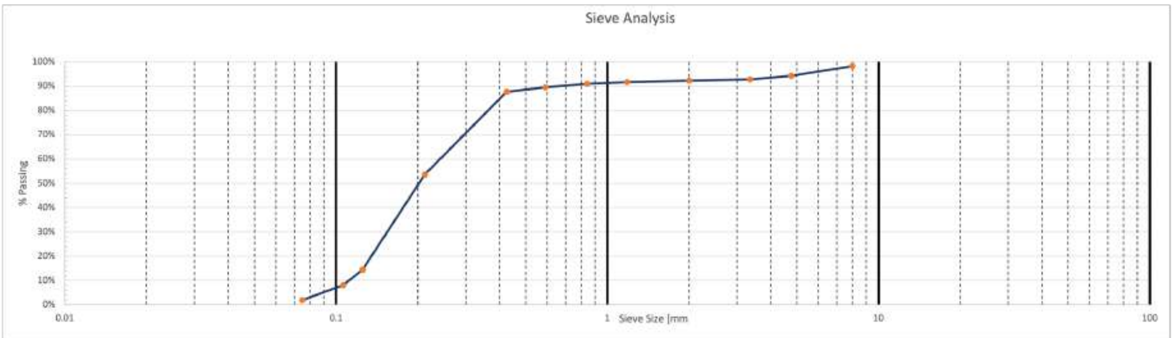

Figure D. 10. Sediment grading graph for diver sample S10.

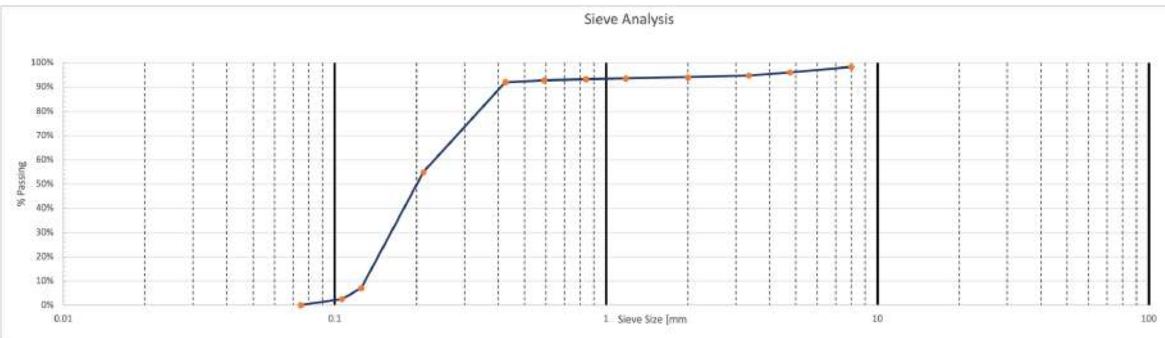

Figure D. 11. Sediment grading graph for diver sample S11.

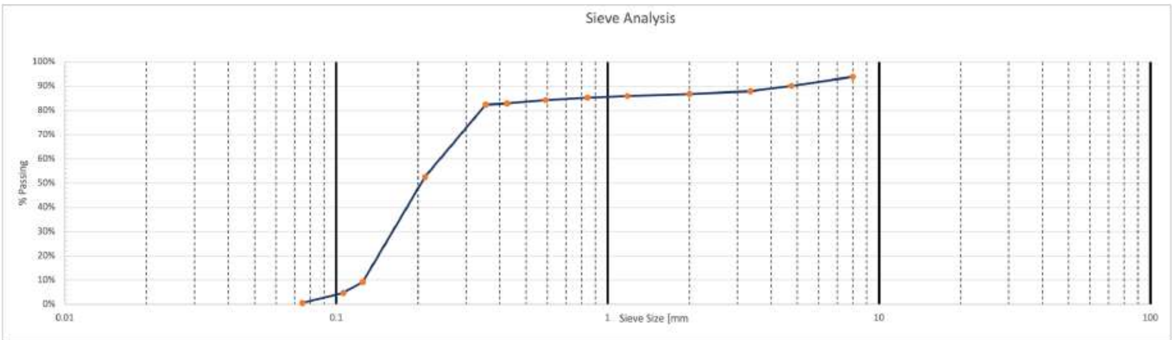

Figure D. 12. Sediment grading graph for diver sample S12.

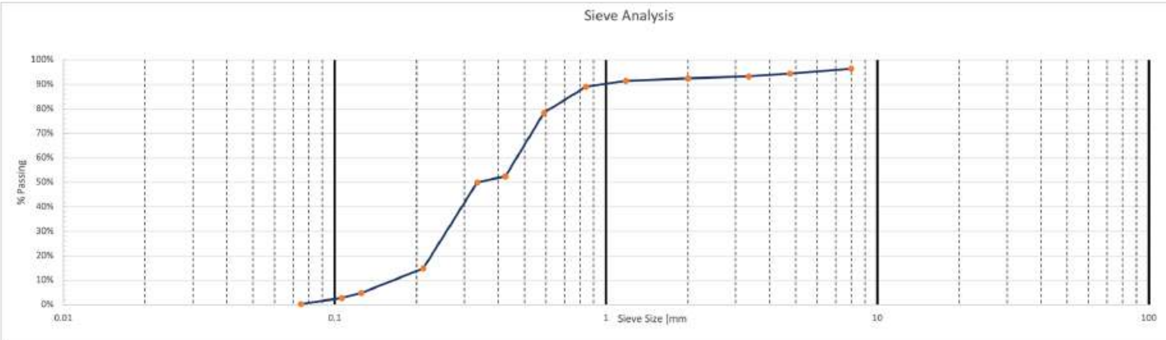

Figure D. 13. Sediment grading graph for diver sample S13.

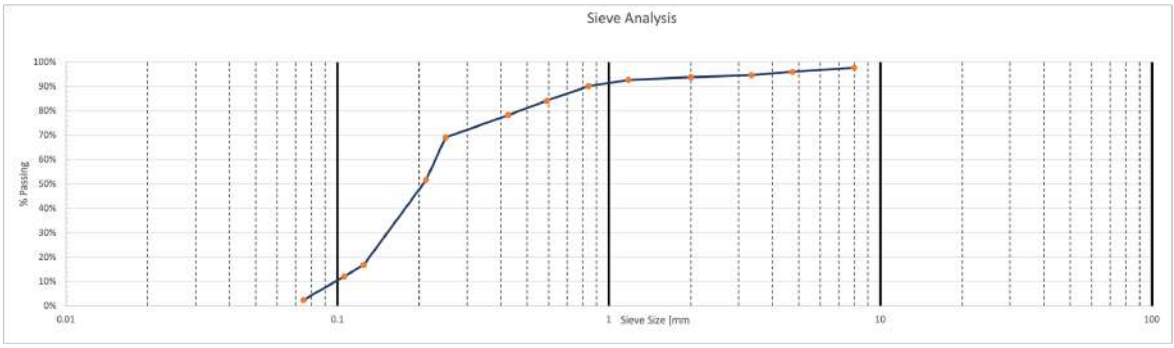

Figure D. 14. Sediment grading graph for diver sample S14.

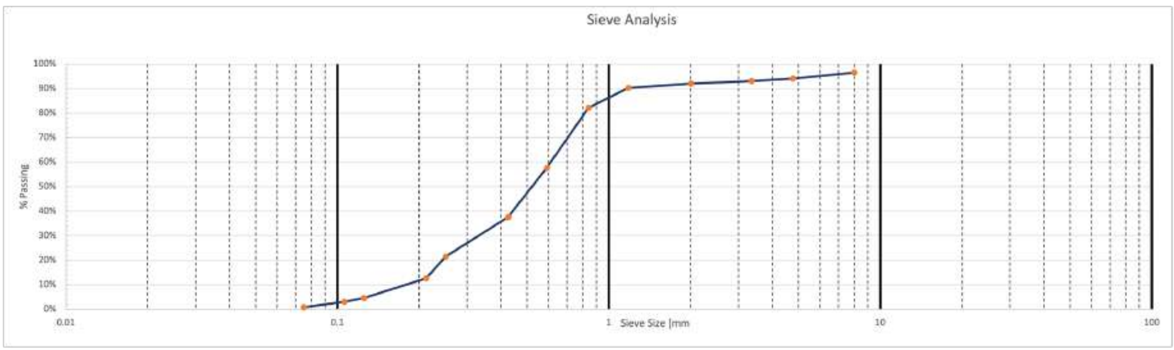

Figure D. 15. Sediment grading graph for diver sample S15.

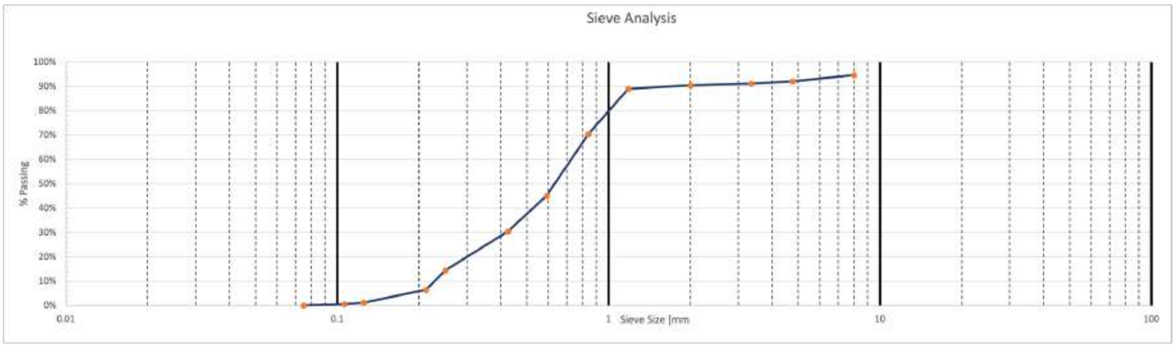

Figure D. 16. Sediment grading graph for diver sample S16.

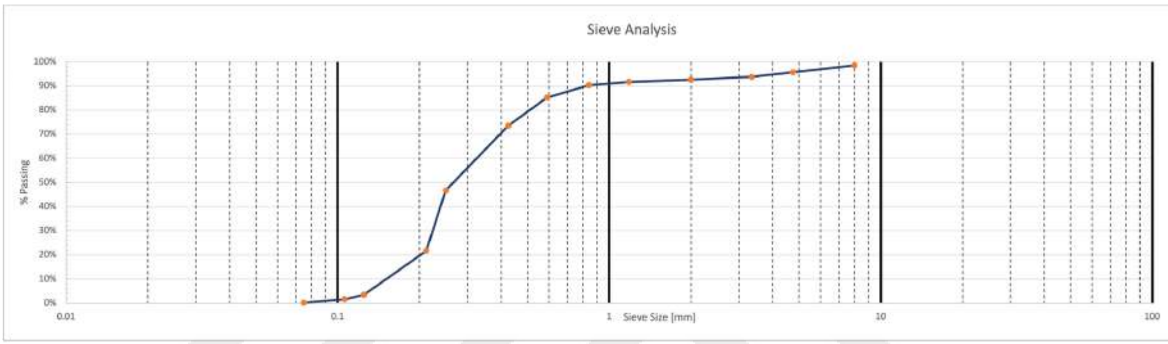

Figure D. 17. Sediment grading graph for diver sample S17.

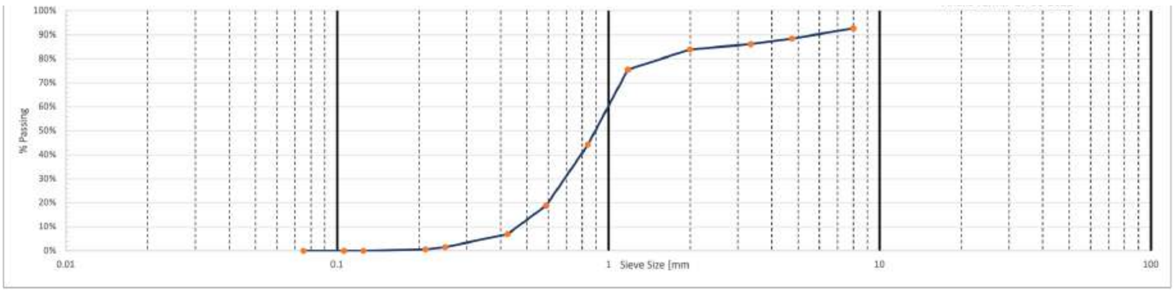

Figure D. 18. Sediment grading graph for Dock +1m sample.

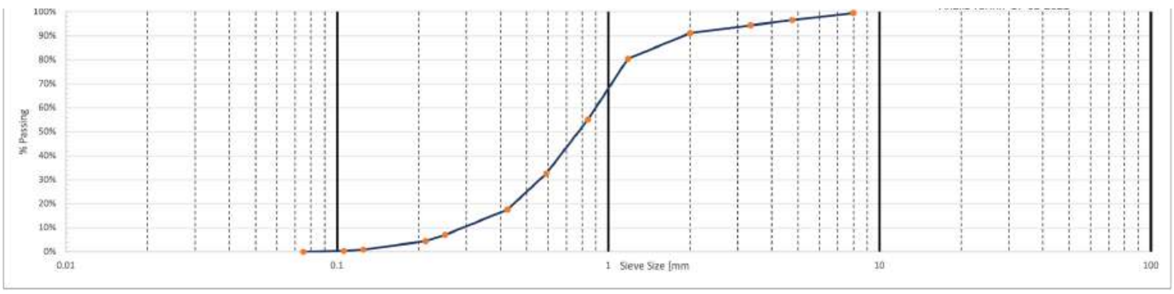

Figure D. 19. Sediment grading graph for Dock 0m sample.

Figure D. 20. Sediment grading graph for Dock -1m sample.

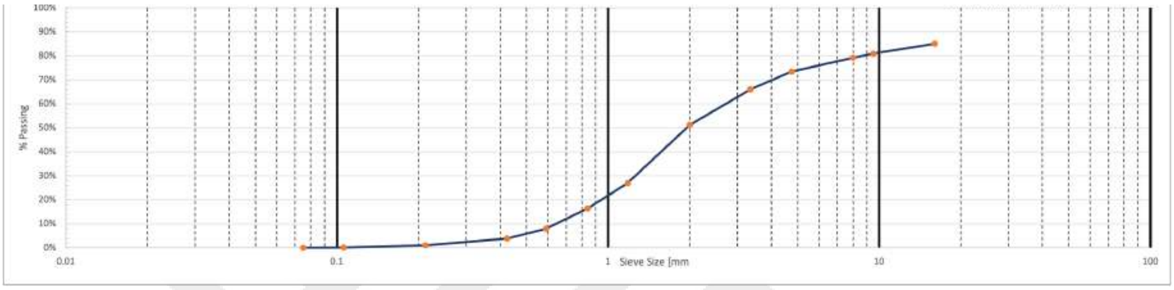

Figure D. 21. Sediment grading graph for Dock -2m sample.

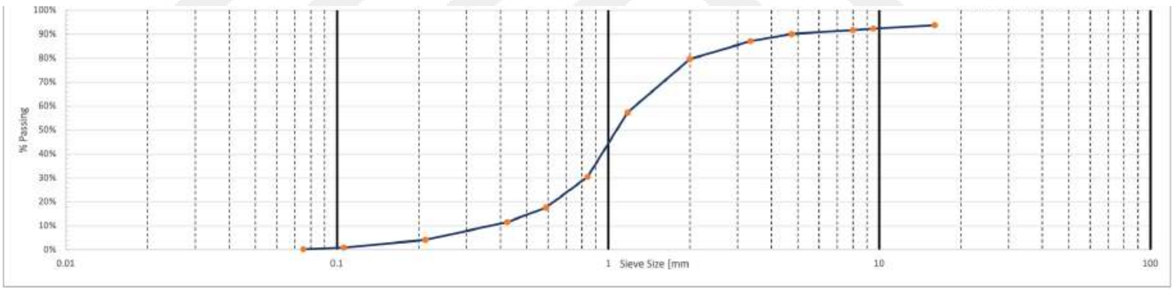

Figure D. 22. Sediment grading graph for Dock -5m sample.

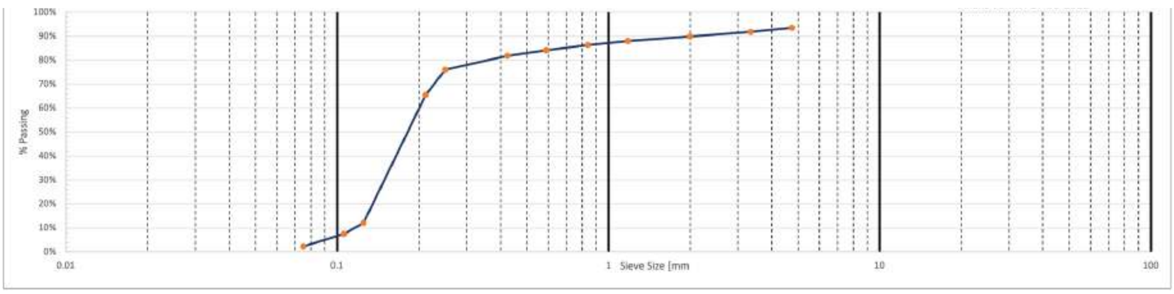

Figure D. 23. Sediment grading graph for Dock -10m sample.

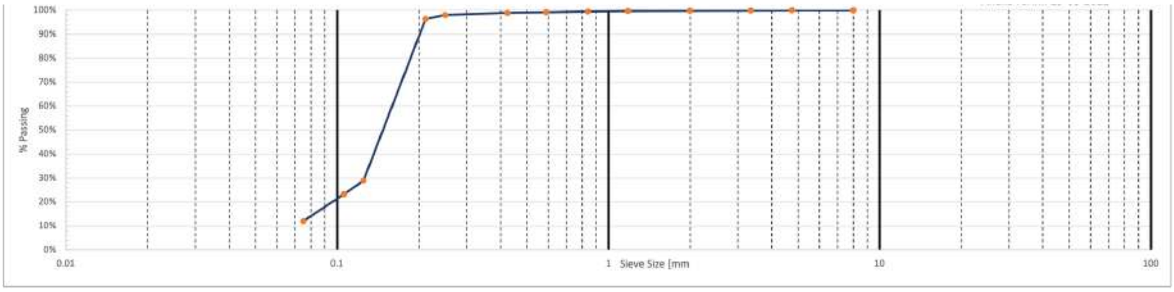

Figure D. 24. Sediment grading graph for Port Middle sample.

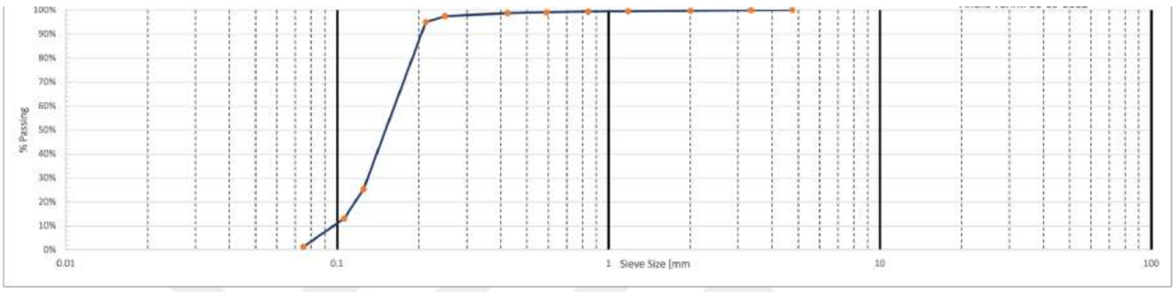

Figure D. 25. Sediment grading graph for Port Entrance sample.

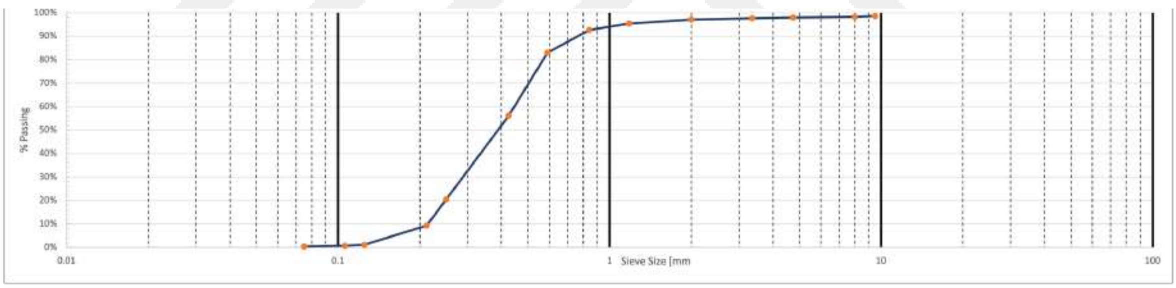

Figure D. 26. Sediment grading graph for K02 +2m sample.

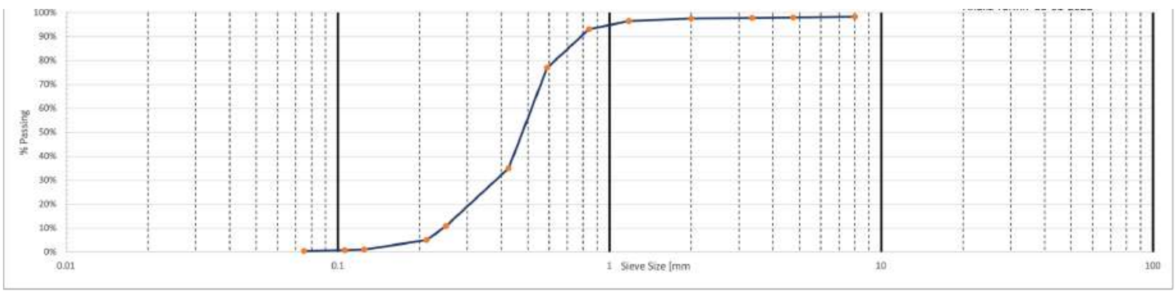

Figure D. 27. Sediment grading graph for K02 +1m sample.

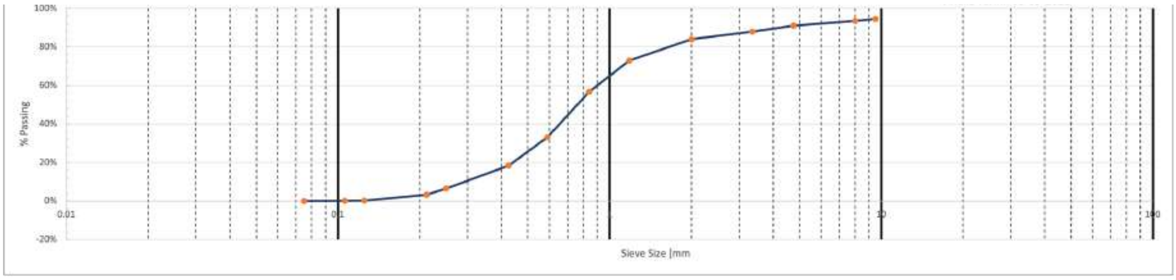

Figure D. 28. Sediment grading graph for K02 0m sample.

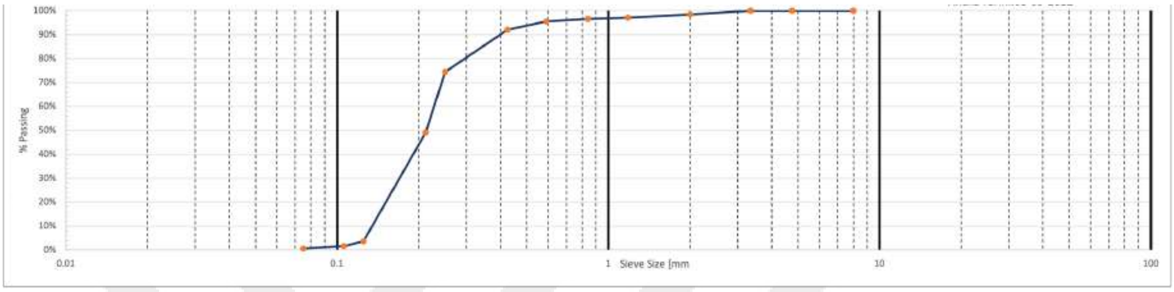

Figure D. 29. Sediment grading graph for K02 -1m sample.

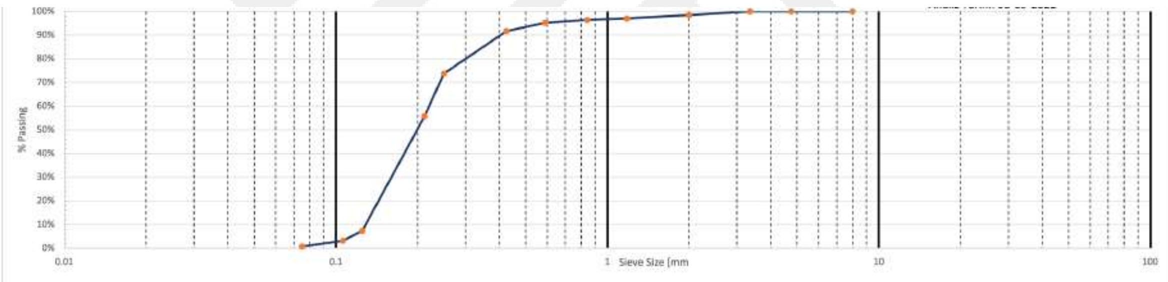

Figure D. 30. Sediment grading graph for K02 -2m sample.

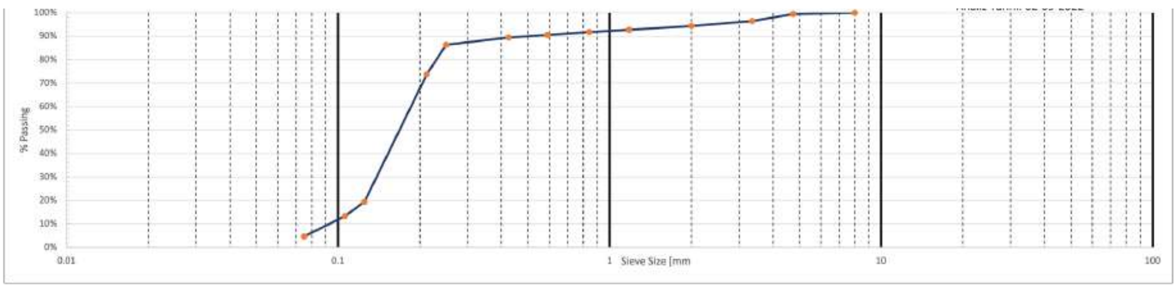

Figure D. 31. Sediment grading graph for K02 -5m sample.

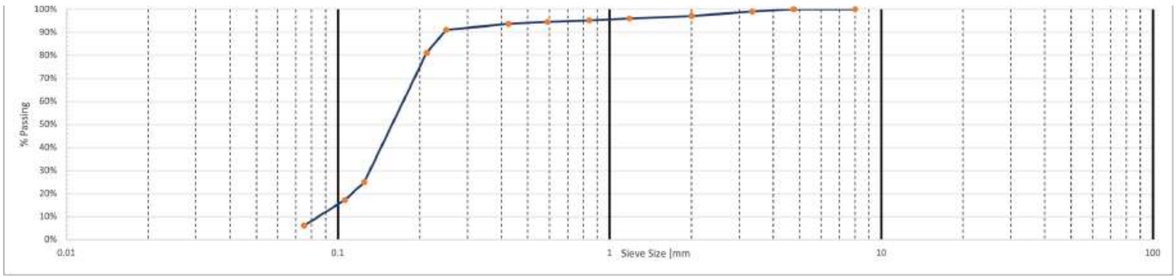

Figure D. 32. Sediment grading graph for K02 -5m(Hacet River) sample.

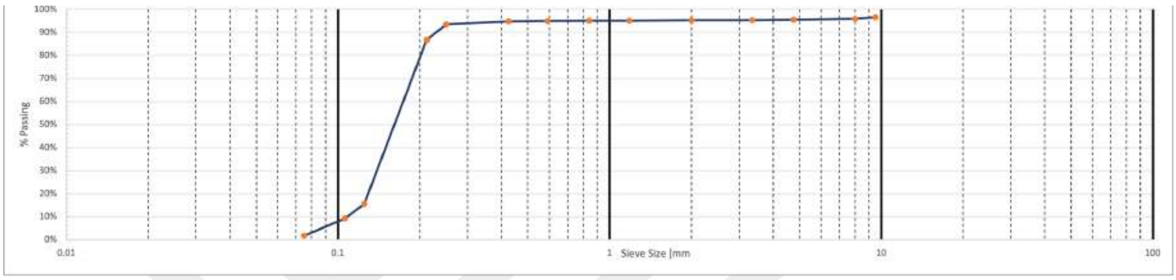

Figure D. 33. Sediment grading graph for K02 -10m sample.

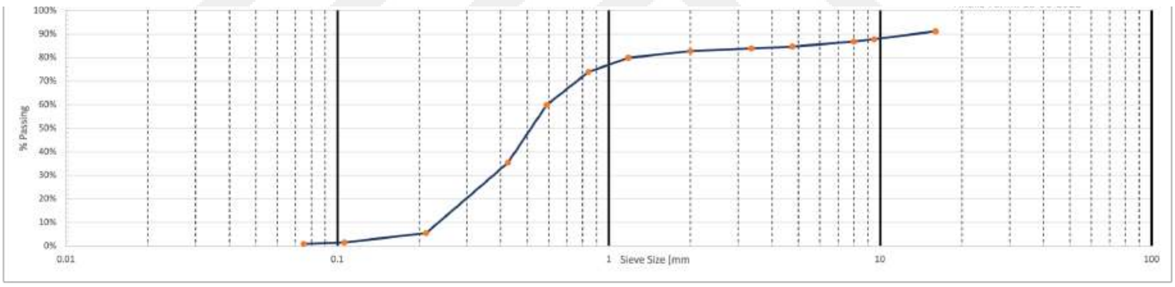

Figure D. 34. Sediment grading graph for K09 +2m sample.

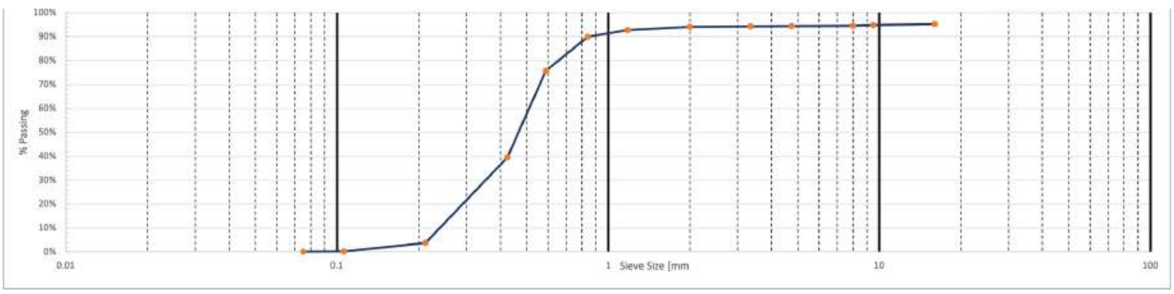

Figure D. 35. Sediment grading graph for K09 +1m sample.

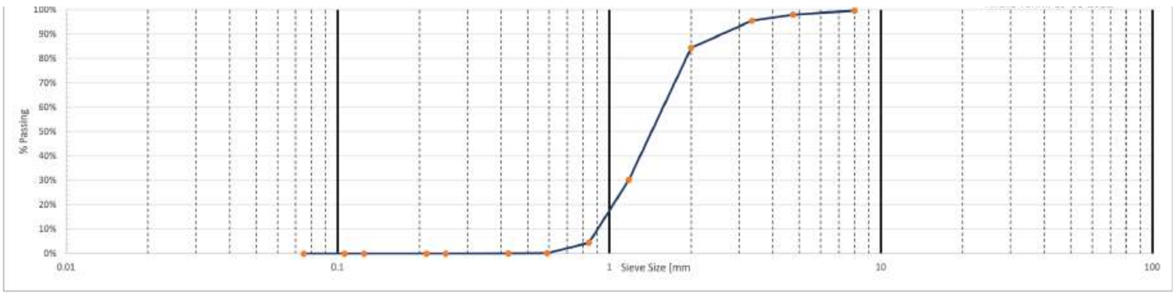

Figure D. 36. Sediment grading graph for K09 0m sample.

Figure D. 37. Sediment grading graph for K09 -2m sample.

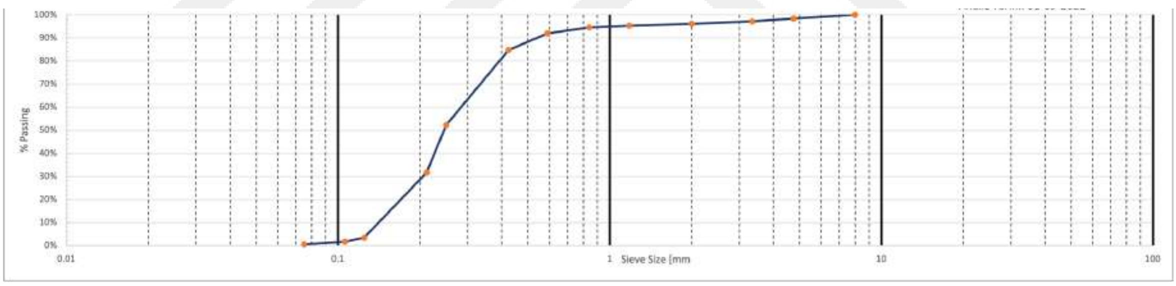

Figure D. 38. Sediment grading graph for K09 -5m sample.

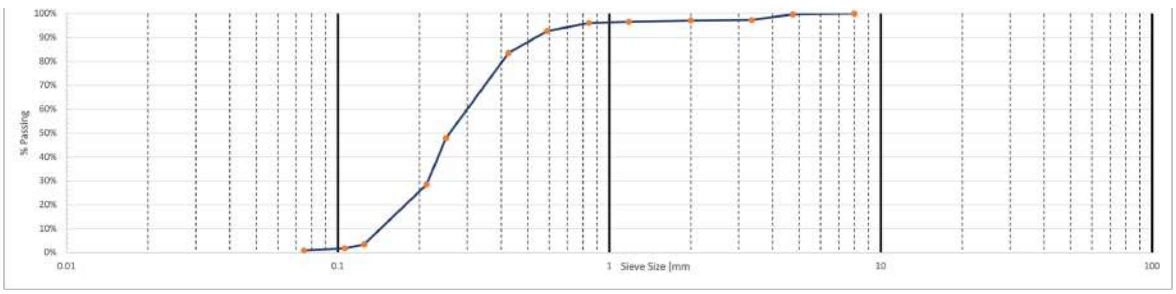

Figure D. 39. Sediment grading graph for K09 -5m(Gümüş River) sample.

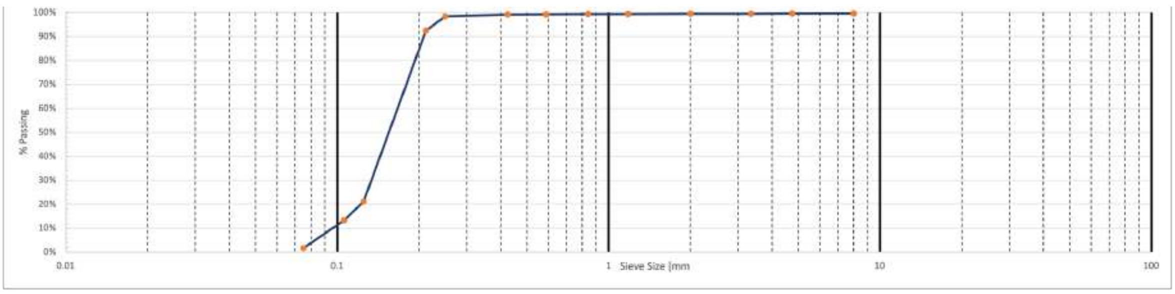

Figure D. 40. Sediment grading graph for K09 -10m sample.

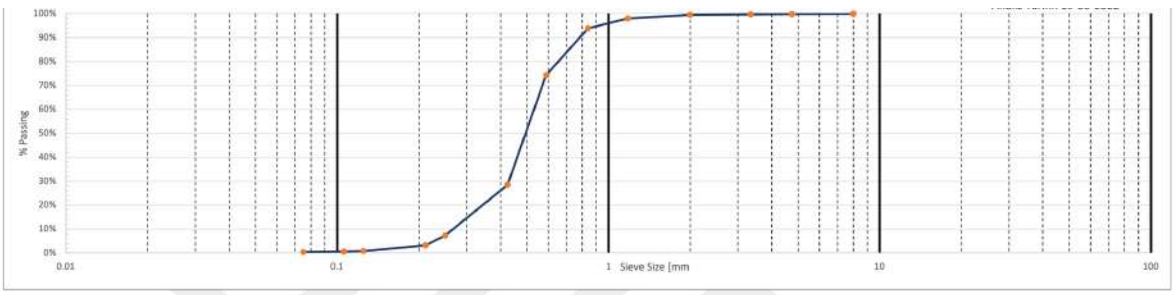

Figure D. 41. Sediment grading graph for K14 +2m sample.

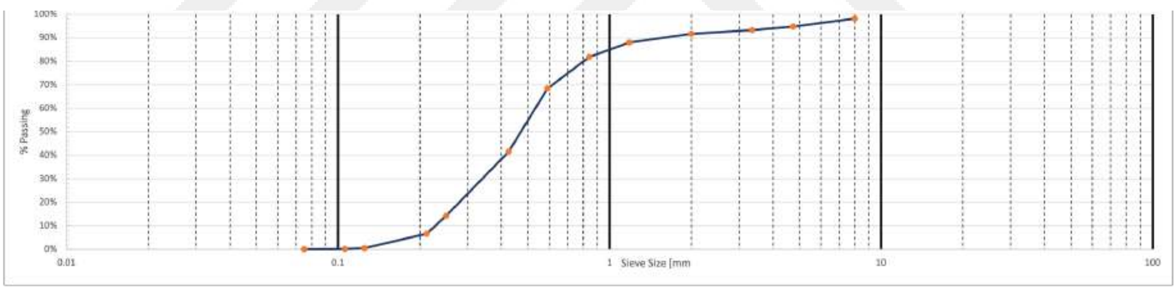

Figure D. 42. Sediment grading graph for K14 +1m sample.

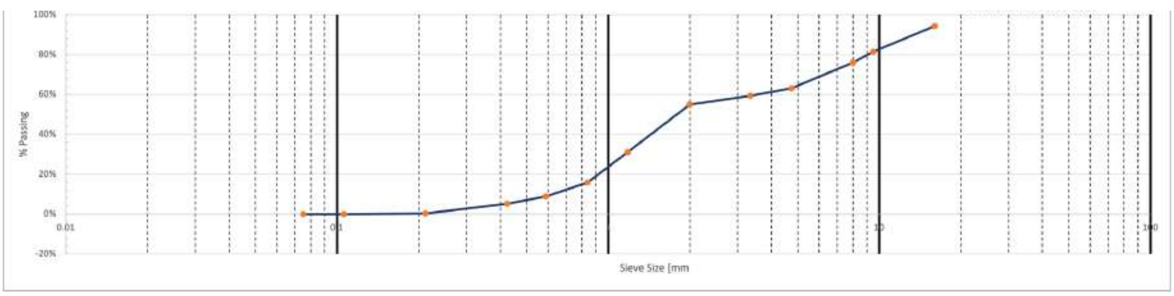

Figure D. 43. Sediment grading graph for K14 0m sample.

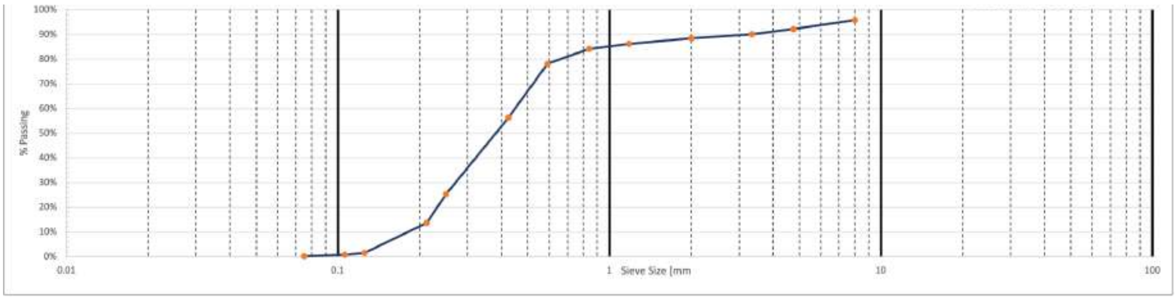

Figure D. 44. Sediment grading graph for K14 -1m sample.

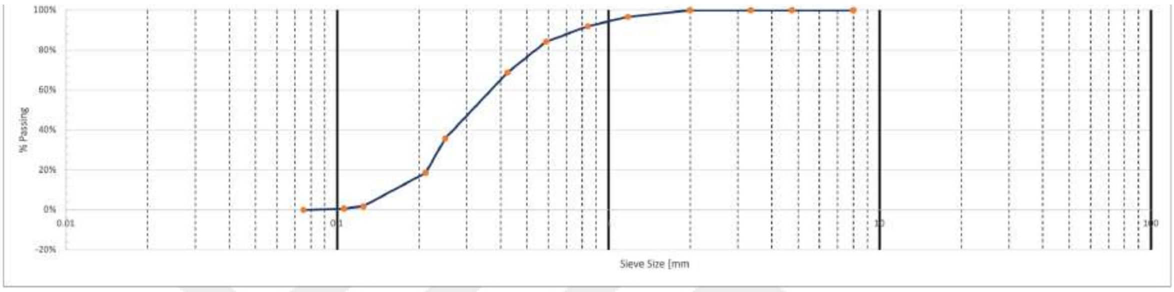

Figure D. 45. Sediment grading graph for K14 -2m sample.

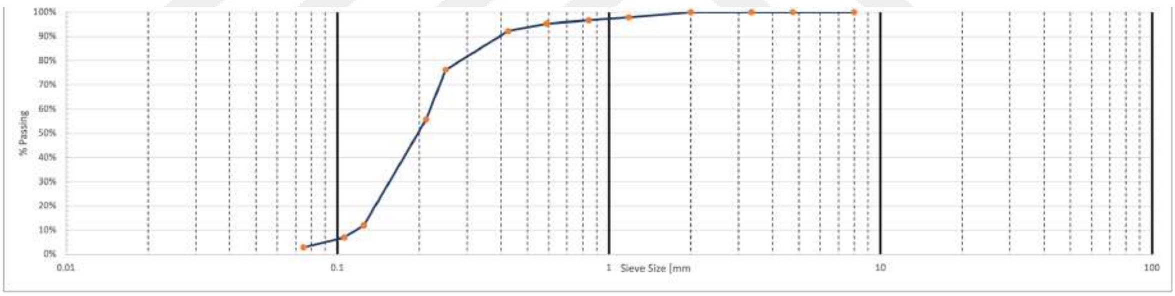

Figure D. 46. Sediment grading graph for K14 -5m sample.

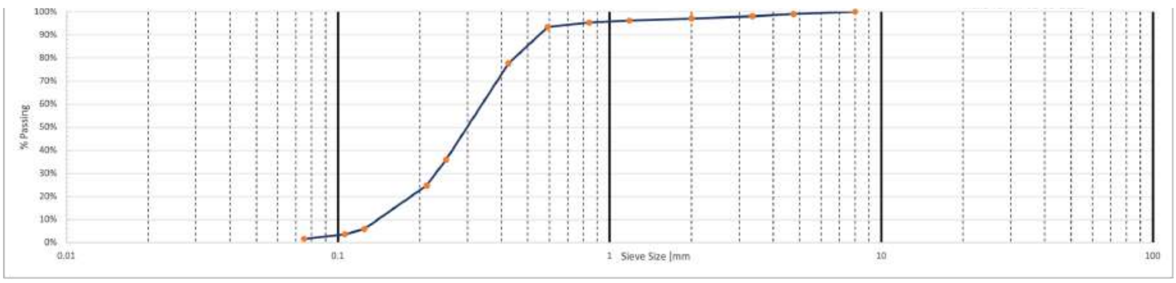

Figure D. 47. Sediment grading graph for K14 -5m(Oba River) sample.

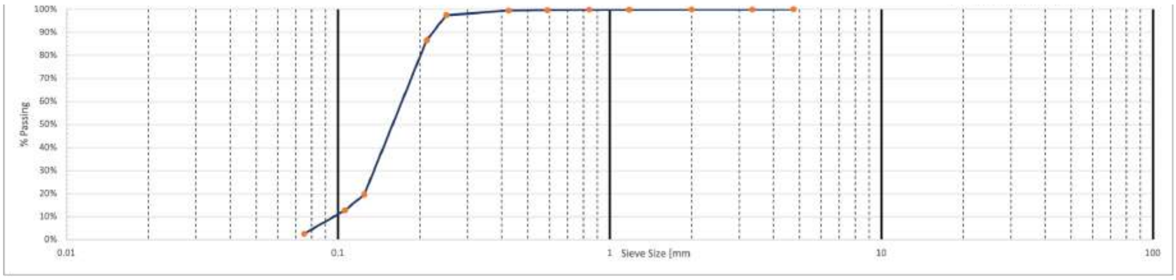

Figure D. 48. Sediment grading graph for K14 -10m sample.

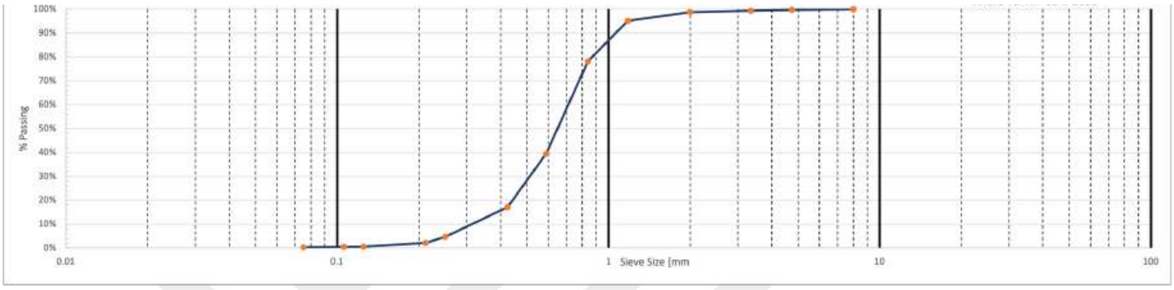

Figure D. 49. Sediment grading graph for K20 +2m sample.

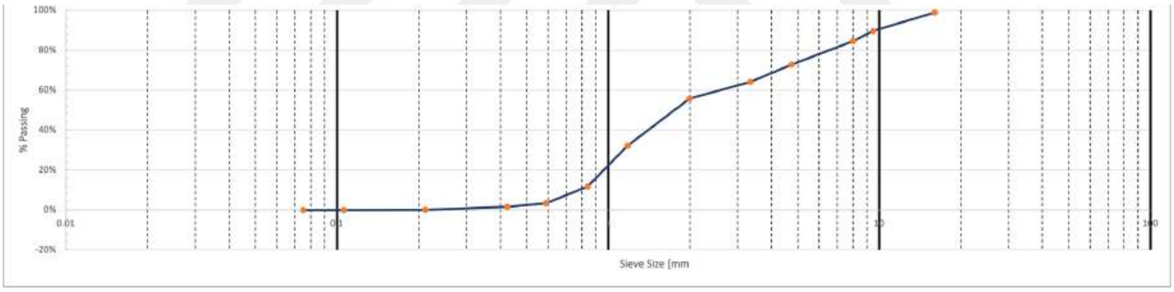

Figure D. 50. Sediment grading graph for K20 +1m sample.

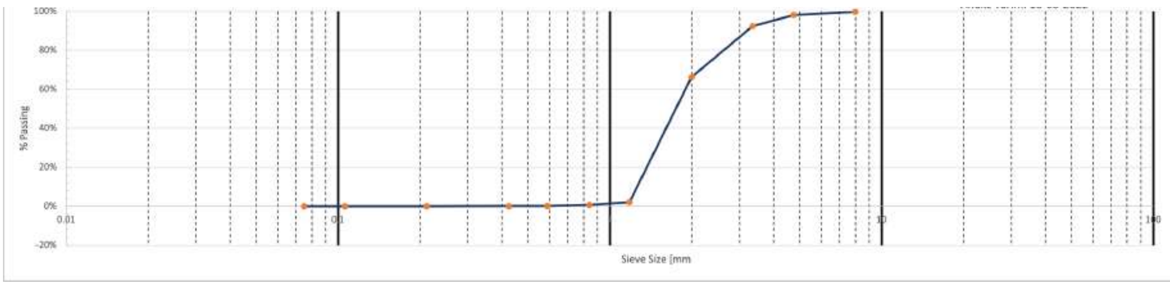

Figure D. 51. Sediment grading graph for K20 0m sample.

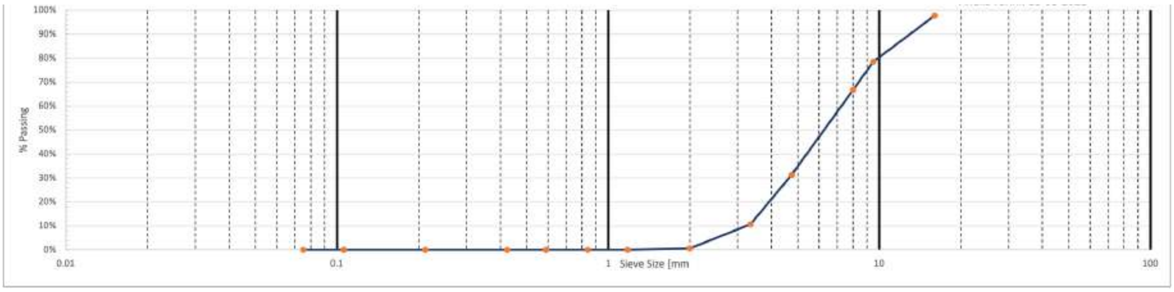

Figure D. 52. Sediment grading graph for K20 -1m sample.

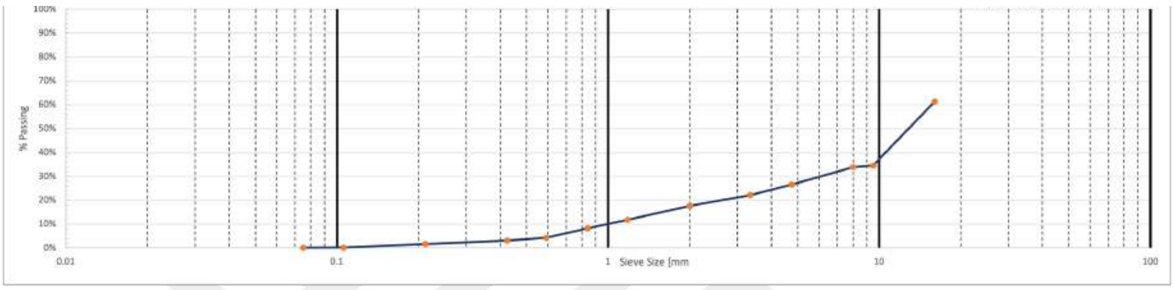

Figure D. 53. Sediment grading graph for K20 -2m sample.

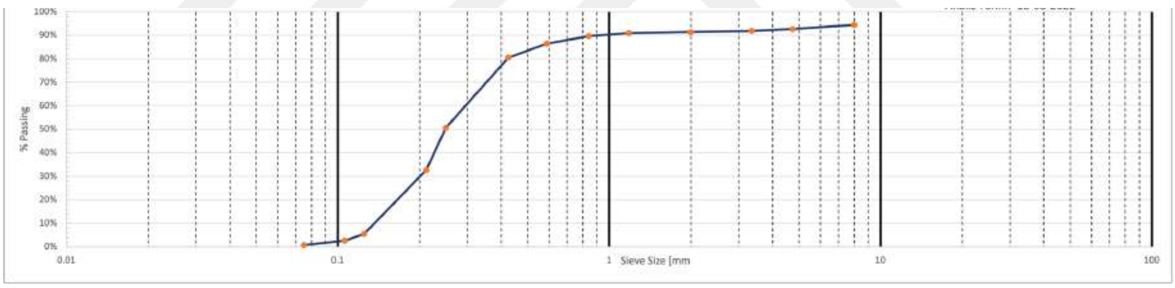

Figure D. 54. Sediment grading graph for K20 -5m sample.

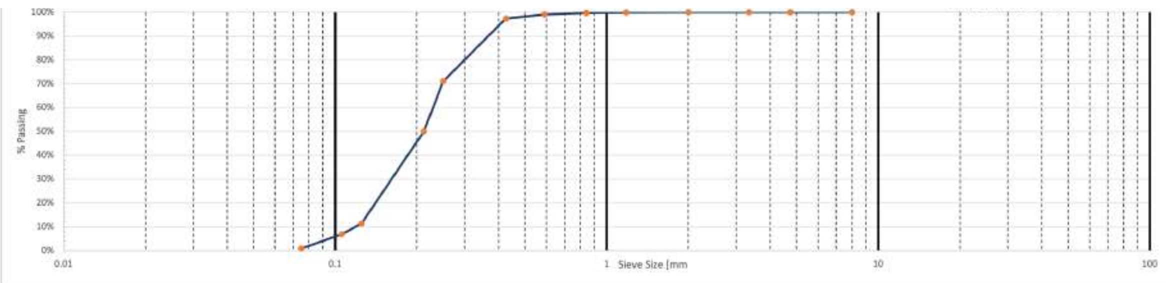

Figure D. 55. Sediment grading graph for K20 -10m sample.

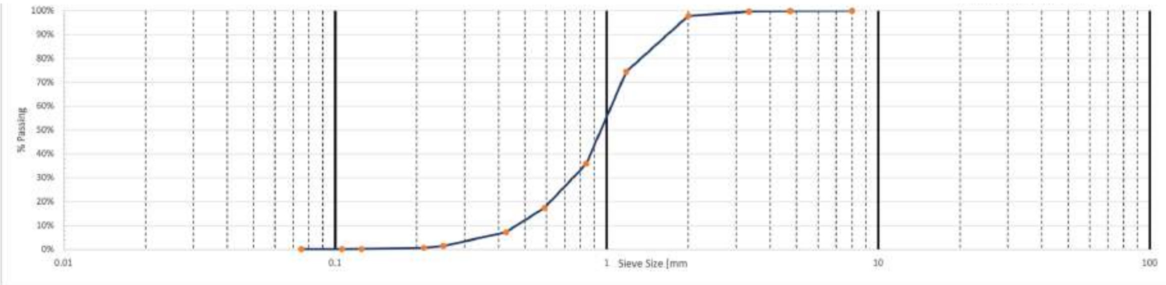

Figure D. 56. Sediment grading graph for K26 +2m sample.

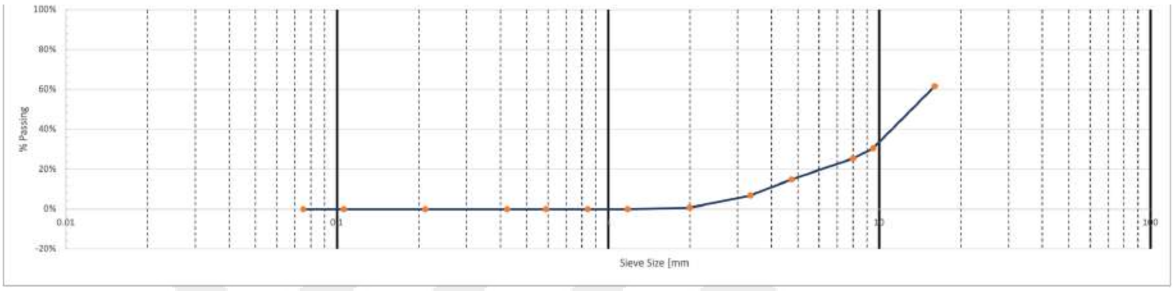

Figure D. 57. Sediment grading graph for K26 +1m sample.

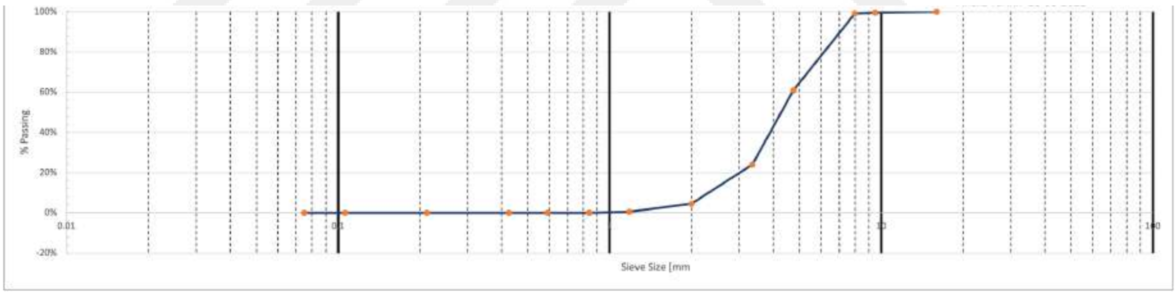

Figure D. 58. Sediment grading graph for K26 0m sample.

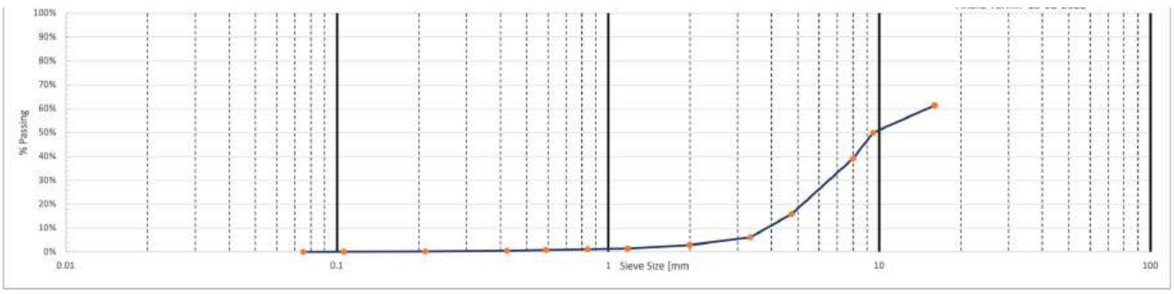

Figure D. 59. Sediment grading graph for K26 -1m sample.

Figure D. 60. Sediment grading graph for K26 -2m sample.

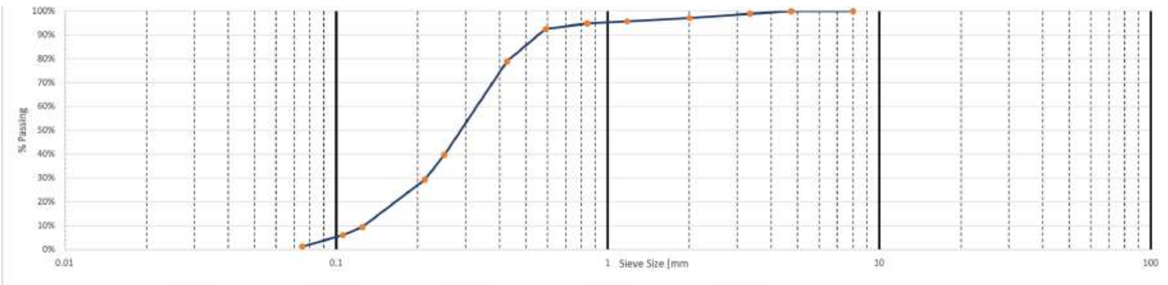

Figure D. 61. Sediment grading graph for K26 -5m sample.

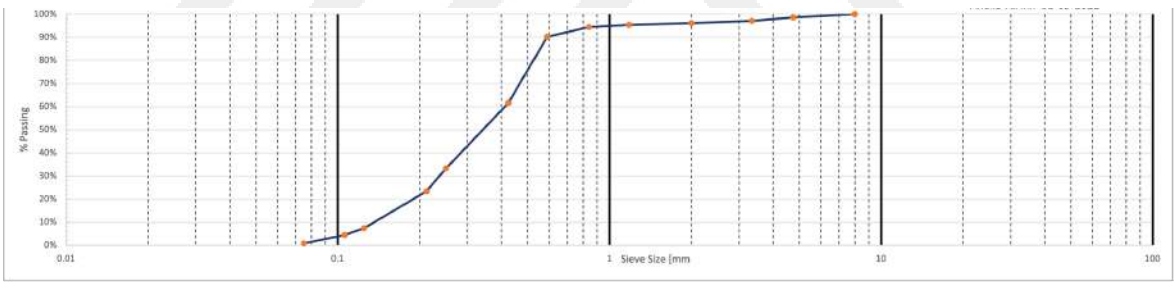

Figure D. 62. Sediment grading graph for K26 -5m(Dim River) sample.

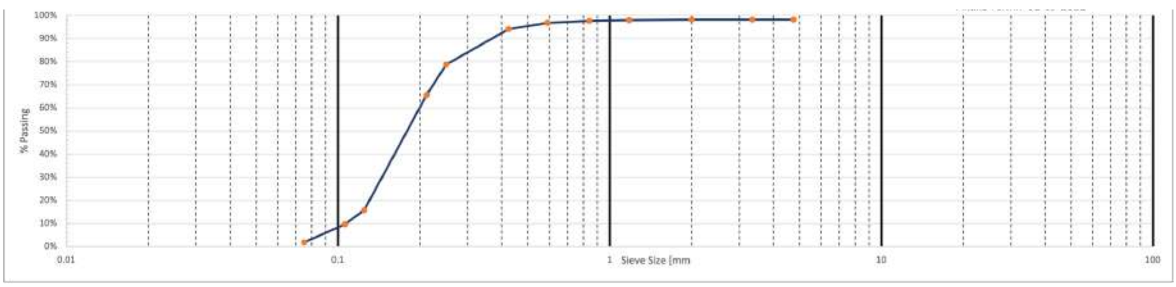

Figure D. 63. Sediment grading graph for K26 -10m sample.

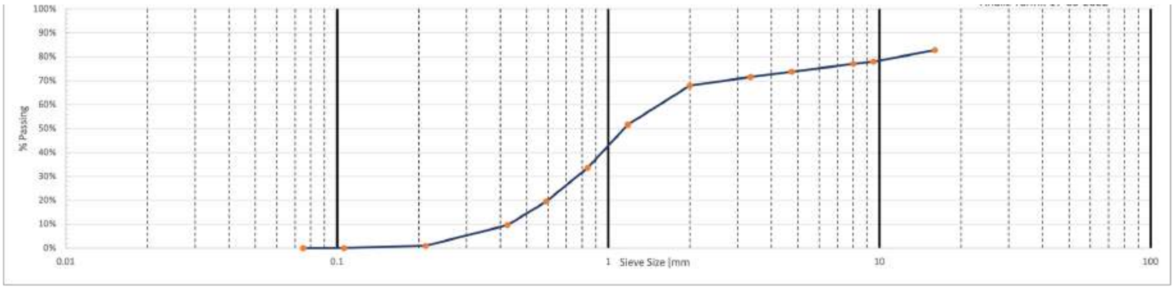

Figure D. 64. Sediment grading graph for Dim River -0.5m sample.

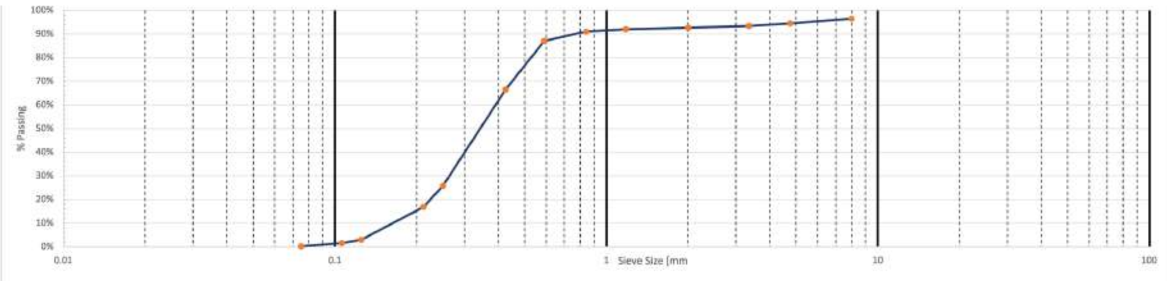

Figure D. 65. Sediment grading graph for Dim River -3.5m sample.

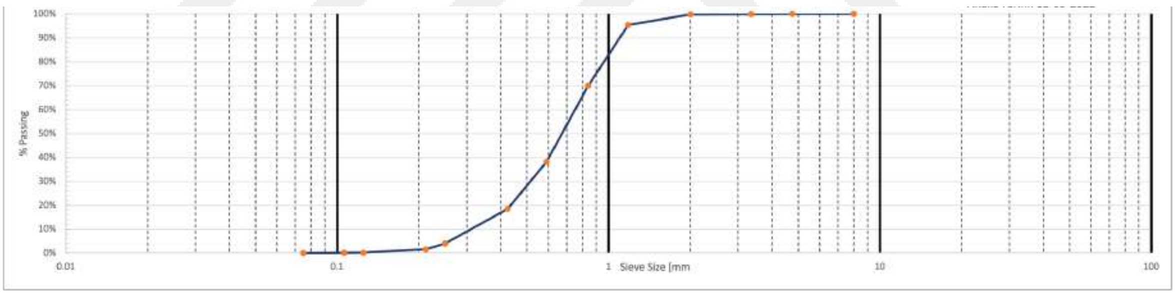

Figure D. 66. Sediment grading graph for K31 +2m sample.

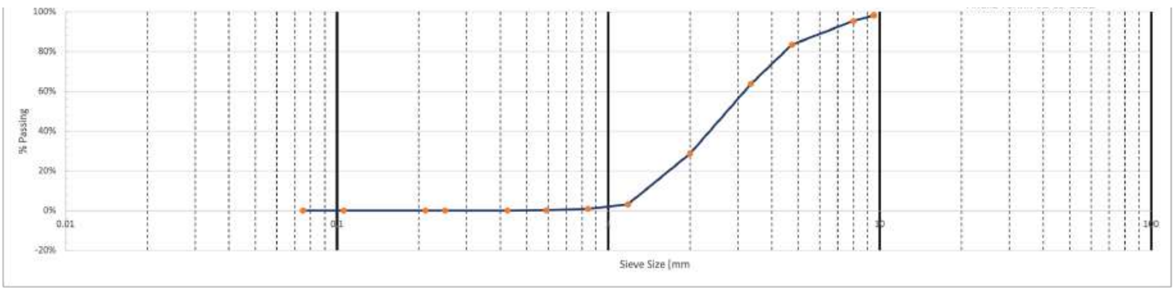

Figure D. 67. Sediment grading graph for K31 +1m sample.

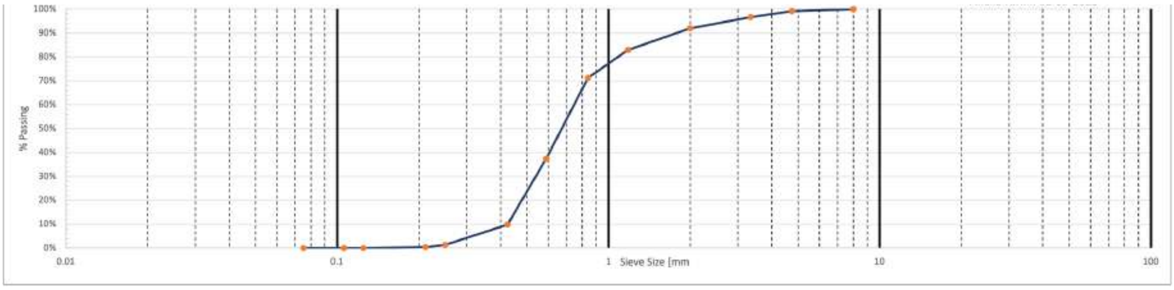

Figure D. 68. Sediment grading graph for K31 0m sample.

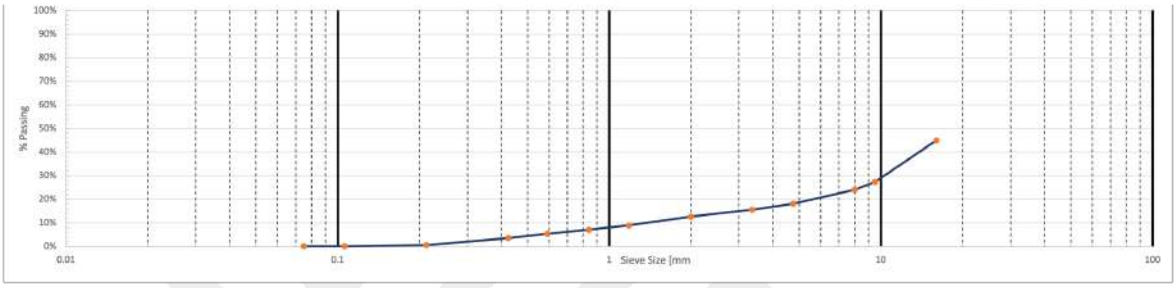

Figure D. 69. Sediment grading graph for K31 -2m sample.

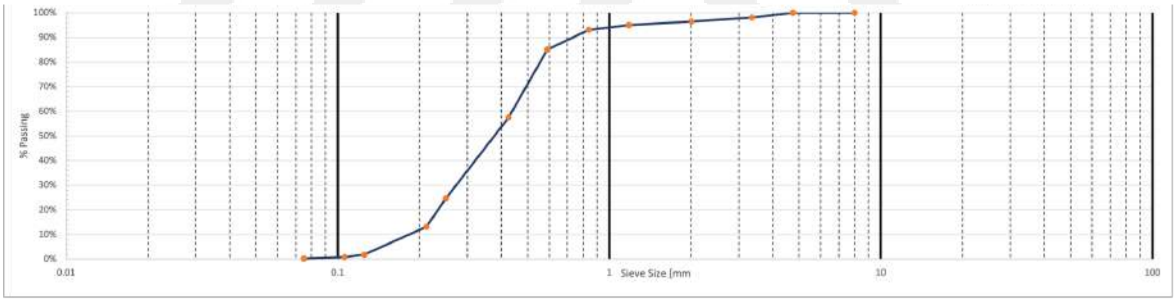

Figure D. 70. Sediment grading graph for K31 -5m sample.

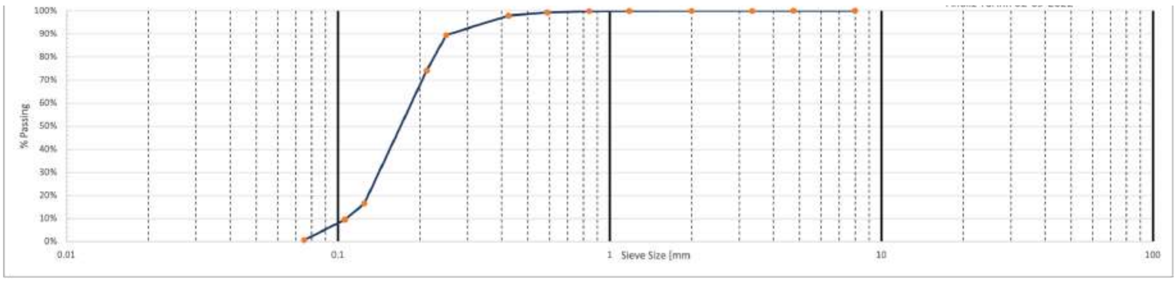

Figure D. 71. Sediment grading graph for K31 -10m sample.

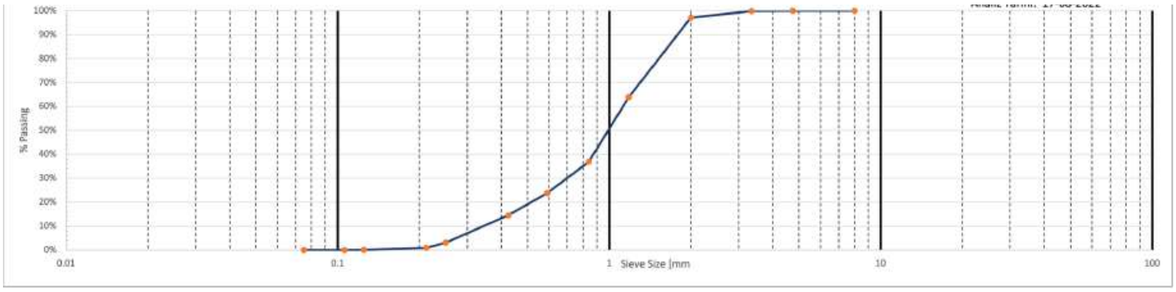

Figure D. 72. Sediment grading graph for Kleopatra Beach sample.

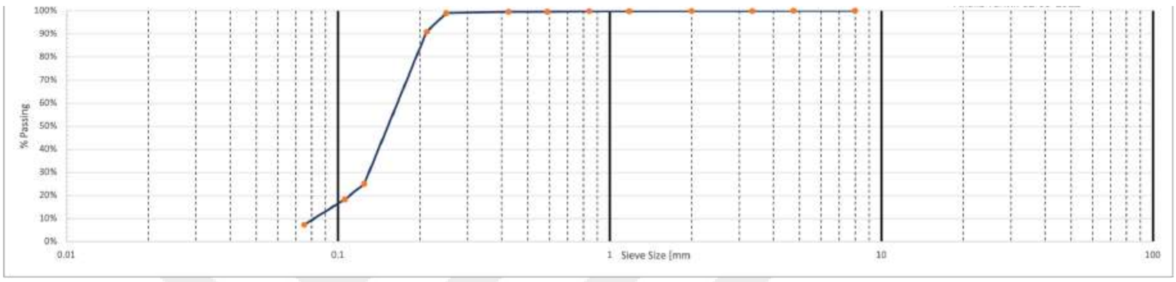

Figure D. 73. Sediment grading graph for sample taken in June 1st.

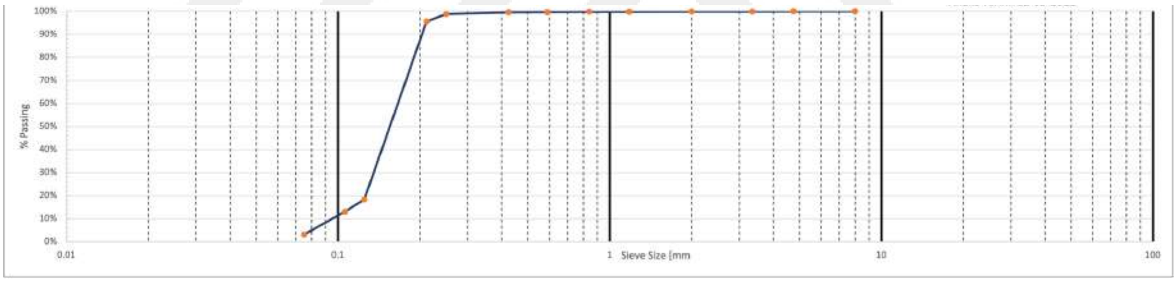

Figure D. 74. Sediment grading graph for sample taken in June 2nd.

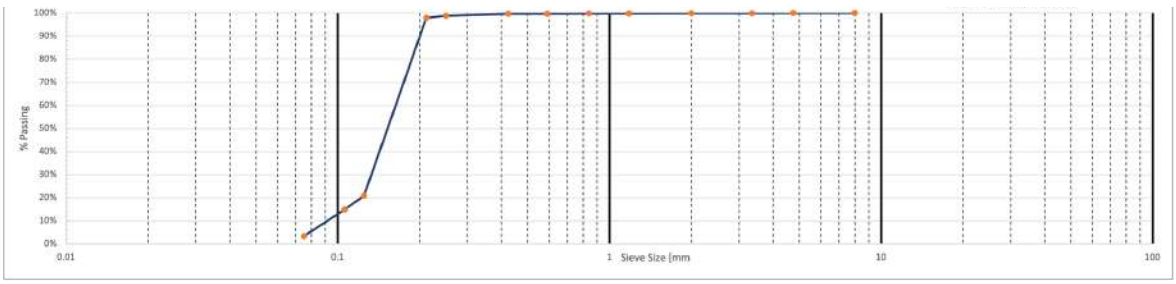

Figure D. 75. Sediment grading graph for sample taken in June 3rd.

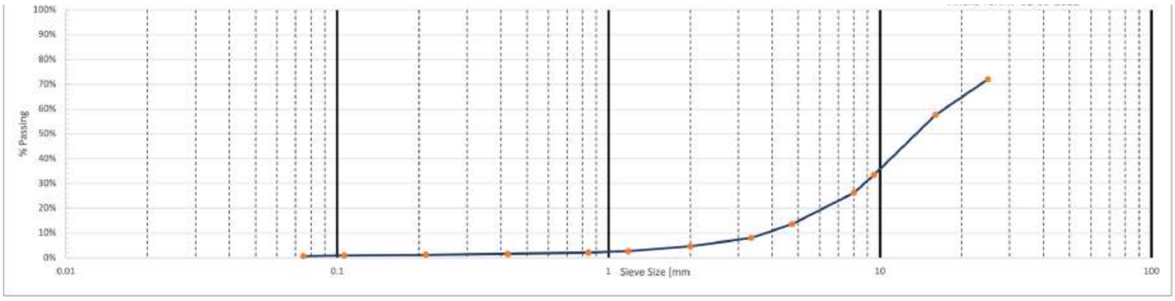

Figure D. 76. Sediment grading graph for quarry sample 1.

Figure D. 77. Sediment grading graph for quarry sample 2.

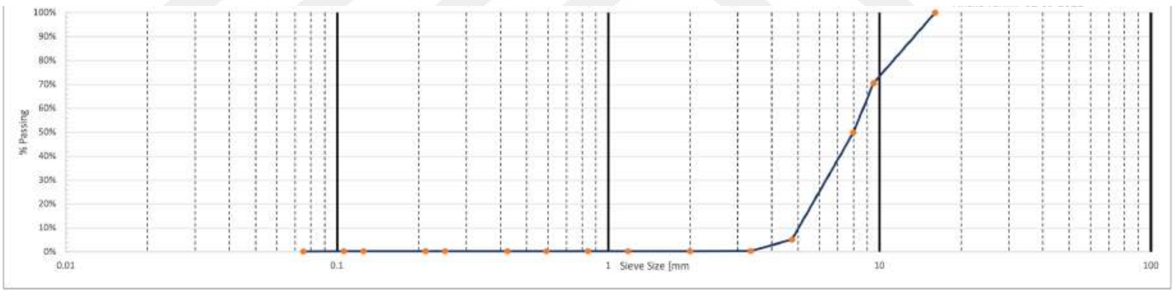

Figure D. 78. Sediment grading graph for quarry sample 3.

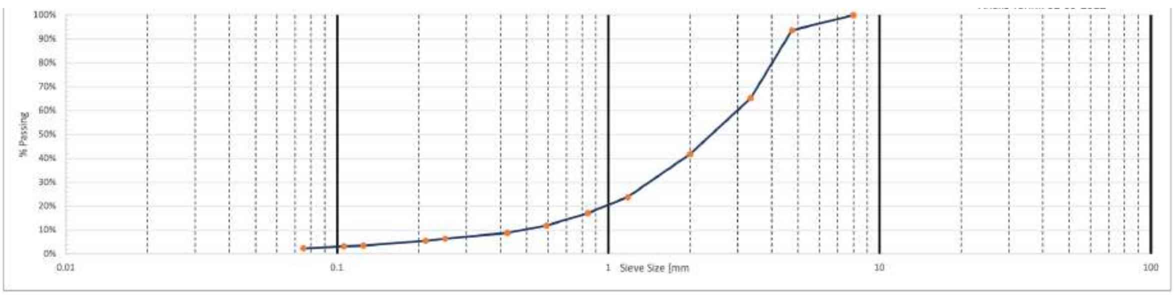

Figure D. 79. Sediment grading graph for quarry sample 4.

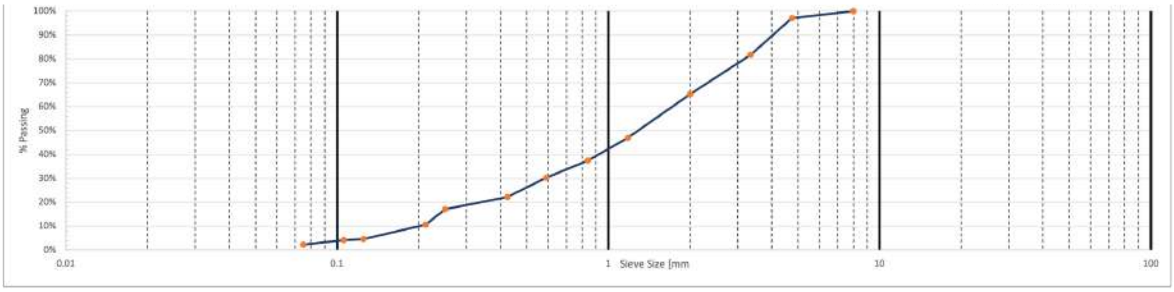

Figure D. 80. Sediment grading graph for Quarry sample 5.